

A project funded by the United Nations Development Programme/Global Environment Facility (UNDP/GEF) and executed by the United Nations Office for Project Services (UNOPS)

**Special Study on Sediment Discharge  
and Its Consequences (SedSS)**

**Technical Report Number 14**

MONITORING AND EXPLANATION  
OF SEDIMENT PLUMES IN  
LAKE TANGANYIKA

by  
A Bryant

1999

**Pollution Control and Other Measures to Protect Biodiversity in Lake Tanganyika  
(RAF/92/G32)**

**Lutte contre la pollution et autres mesures visant à protéger la biodiversité du Lac  
Tanganyika (RAF/92/G32)**

<p>Le Projet sur la diversité biologique du lac Tanganyika a été formulé pour aider les quatre Etats riverains (Burundi, Congo, Tanzanie et Zambie) à élaborer un système efficace et durable pour gérer et conserver la diversité biologique du lac Tanganyika dans un avenir prévisible. Il est financé par le GEF (Fonds pour l'environnement mondial) par le biais du Programme des Nations Unies pour le développement (PNUD)"</p>	<p>The Lake Tanganyika Biodiversity Project has been formulated to help the four riparian states (Burundi, Congo, Tanzania and Zambia) produce an effective and sustainable system for managing and conserving the biodiversity of Lake Tanganyika into the foreseeable future. It is funded by the Global Environmental Facility through the United Nations Development Programme.</p>
---	---

**Burundi: Institut National pour Environnement et Conservation de la Nature**

**D R Congo: Ministrie Environnement et Conservation de la Nature**

**Tanzania: Vice President's Office, Division of Environment**

**Zambia: Environmental Council of Zambia**

Enquiries about this publication, or requests for copies should be addressed to:

Project Field Co-ordinator  
Lake Tanganyika Biodiversity Project  
PO Box 5956  
Dar es Salaam, Tanzania

UK Co-ordinator,  
Lake Tanganyika Biodiversity Project  
Natural Resources Institute  
Central Avenue, Chatham, Kent, ME4 4TB, UK

# Abstract

Extensive deforestation and bad land use practises has lead to rapid erosion in much of the Lake Tanganyika catchment, resultant sediment is being transported by rivers into the lake and has been linked with a decrease in biodiversity. AVHRR and ATSR-2 satellite imagery has been utilised along with in-situ data in an analysis of Lake Tanganyika and it's sediment plume behaviour.

Remotely sensed imagery has clearly identified large near-surface sediment plumes emanating from the largest of the catchment's rivers; the Malagarasi, and a number of smaller plumes originating from other rivers in the watershed, and even other Rift Valley lakes. More suprising was the lack of near-surface plumes from the Ruzizi River which is estimated as one of the main contributors to the sediment yield of the lake. However in-situ data suggests that waters from this river and many others may at times be more dense than the lake waters and therefore create subsurface plumes that are undetectable via satellite imagery. It seems the huge buoyant plumes of the Malagarasi could possibly indicate a previous underestimation in the significance of this river as a sediment contributor to the lake.

Statistically significant relationships have been identified between reflectance and suspended matter concentrations indicating the potential of remote sensing for the provision of quantitative estimations of near-surface suspended matter concentration. AVHRR was found to be more suited to the needs of this project than ATSR-2, and with a greater temporal resolution should be better equipped for long term monitoring.

# Contents

GENERAL OBJECTIVE	1
BACKGROUND	2
SPECIFIC AIMS	20
METHODOLOGY	21
RESULTS	40
DISCUSSION	62
CONCLUSION	73
CRITICISMS/FURTHER WORK	75
BIBLIOGRAPHY	76

# List of Tables

<b>Table No.</b>	<b>Title</b>	<b>Page No.</b>
1	ATSR-2 and AVHRR spectral bands.	22
2	Date and nature of sampling trips on Lake Tanganyika	33
3	The order of the AVHRR & ATSR-2 images	40

# List of Figures

<b>Figure No.</b>	<b>Title</b>	<b>Page</b>
Title Page	Image taken from the International Decade for East African Lakes Web page: <a href="http://irc.geo.umn.edu/ideal">http://irc.geo.umn.edu/ideal</a>	
1.	The Geographical setting of Lake Tanganyika (LTBP Web Site, 1999)	3
2	Morphological map of Tanganyika basin, (Burgess, 1985).	5
3	Drainage pattern of lake Tanganyika, (Tiercelin et al. 1992).	7
4	Map of the Malagarasi Delta (Nyanza Project, 1999).	8
5	Rift axial margin drainage and littoral platform of Ruzizi, (Tiercelin et al.,1992).	9
6	Bathymetric map of the Bujumbura sub-basin showing the Bujumbura (Bu) and Baraka (Ba) central depressions and the Ruzizi channel system , (Tiercelin et al.,1992).	10
7	Total sediment transported from up stream ( $\times 1000 \text{ t km}^2$ ) during March 1996, Northern Lake Tanganyika (Drake et al., 1999).	12
8	Sediment Core data from Tiercelin & Mondegeur, scanned in from (Patterson & Mackin 1998).	13
9	Calculated near surface wind over lake Tanganyika region, March 1997. Isolines show orography in metres above mean sea level, (Huttula (Ed.) 1997).	14
10	Percentage reflectance of tap water and water with a suspended sediment concentration of 300mg/l, (Novo et al., 1989).	16
11	Scatterplots and best fit curves for the relationships between exoatmospheric reflectance and SSC, (Harrington et al., 1992).	17

12	A histogram stretched Raw ATSR-2 false colour image subset of the Lake Tanganyika area, 27/04/98.	23
13	A histogram stretched, reflectance and geo-corrected ATSR-2 false colour image of the Lake Tanganyika area, 27/04/98	24
14	A histogram stretched, reflectance, geo-corrected, and sun angle corrected ATSR-2 false colour image of the Lake Tanganyika area, 27/04/98.	25
15	A histogram stretched, reflectance, geo-corrected, sun angle corrected, and land masked ATSR-2 false colour image of the Lake Tanganyika area, 27/04/98.	26
16	Histogram of Q ratio image.	27
17	A histogram stretched, reflectance, geo-corrected, sun angle corrected, land and cloud masked ATSR-2 false colour image of the Lake Tanganyika area, 27/04/98.	28
18	A histogram stretched, reflectance, geo-corrected, sun angle corrected, land and cloud masked, and atmospherically corrected ATSR-2 colour image of the Lake Tanganyika area, 27/04/98.	30
19	A histogram stretched fully corrected image with rivers and lake outline vector files overlain.	31
20	False colour ATSR-2 image of the study with an overlay of the main rivers	32
21	Map of the Malagarasi Delta (Nyanza Project, 1999).	37
22	22nd March, 1997, ATSR-2 image.	41
23	22nd January, 1998, ATSR-2 image.	42
24	26th February, 1998, ATSR-2 image.	43
25	1st March, 1998, ATSR-2 image.	44

26	4th March, 1998, ATSR-2 image.	45
27	20th March, 1998, ATSR-2 image.	46
28	6th April, 1998, AVHRR (NOAA-14) image.	47
29	14th April, 1998, AVHRR (NOAA-14) image.	48
30	23rd April, 1998, AVHRR (NOAA-14), image.	49
31	24th April, 1998, ATSR-2 image.	50
32	27th April, 1998, ATSR-2 image	51
33	18th May, 1998, AVHRR (NOAA-14) image.	52
34	Seasonal average temperatures. Data source; Pollution Special Study team.	53
35	Conductivity data plot for all rivers. Data source; Pollution Special Study team.	54
36	Malagarasi conductivity data. Data source; Pollution Special Study team.	54
37	Average conductivity plot. Data from; Pollution Special Study team.	55
38	Density data plot for the lake and rivers. Calculated from Pollution Special Study data.	56
39	Malagarasi River density data, calculated from Pollution Special Study data.	56
40	Average lake and river density, calculated from Pollution Special Study data.	57
41	Average TSM concentration for each sample point during each temporal monitoring period.	58
42	Luiche River line sample of TSM.	59
43	Malagarasi River line sample of TSM.	59
44	Green Band reflectance and TSM concentration.	60

45	Red Band reflectance and TSM concentration.	60
46	NIR Band reflectance and TSM concentration.	61
47	Ntahangwa River SSC and discharge. Data from; Sedimentation Special Study team.	62
48	Ruzizi River SSC and discharge. Data from; Sedimentation Special Study team.	62
49	Calculated near-surface wind over lake Tanganyika region (for 04/03/97). Isolines show orography in metres above sea-level. And satellite imagery from 23rd, 24th, & 27th April, 1998.	64
50	Images of 22nd March, 1997; 1st March, 1998; and 20th March 1998.	65
51	Images of the Southern end of lake Tanganyika and the Lufubu River.	66
52	AVHRR image subsets of Lake Victoria and the northern end of Lake Malawi	66
53	AVHRR image of the Tanzanian Indian Ocean coastline, 06/04/98.	67
54	Southerly view out from the mouth of the Grande Ruzizi River, 22nd July, 1999.	69
55	Close-up view of the sinking sediment plume, 22nd July, 1999.	69
56	Close-up view of the sinking sediment plume, 22nd July, 1999.	69
57	Malagarasi River mouth (lakeward view), 3rd August, 1999.	70

# Abbreviations

<b>ATSR-2</b>	Along Track Scanning Radiometer
<b>AVHRR</b>	Advanced Very High Resolution Radiometer
<b>ERS-2</b>	European Remote Sensing Satellite - 2
<b>ESA</b>	European Space Agency
<b>LARST</b>	Local Application of Remote Sensing Techniques, system developed by NRI.
<b>LTBP</b>	Lake Tanganyika Biodiversity Project
<b>NERC</b>	Natural Environment Research Council
<b>NIR</b>	Near Infra-Red
<b>NOM</b>	NOAA Operations Manager
<b>NOAA</b>	National Oceanic and Atmospheric Administration
<b>NRI</b>	Natural Resources Institute, University of Greenwich
<b>NYANZA PROJECT</b>	The Nyanza Project is a six week summer program of training and independent research on Lake Tanganyika run by the University of Arizona.
<b>SSC</b>	Suspended Sediment Concentration (specifically soil particles between certain sizes, does not include other particles such as biota, see TSM)
<b>TAFIRI</b>	Tanzanian Fisheries Resource Institute
<b>TSM</b>	Total Suspended Matter (includes other suspended particles than sediment, and is more representative of water leaving reflectance)

# Acknowledgements

Firstly I'd like to thank Dr. Martin Wooster and Dr. Nick Drake for initiating my interest in the lake and supervising the whole project, providing continuous support and enthusiasm throughout. And to NERC for fully funding my postgraduate studies and fieldwork to Africa.

The fieldwork was largely made possible by the generosity and hard work of Dr Kelly West of the LTBP who sacrificed much time and energy in the organisation of my trip to Burundi and Tanzania, and to Mamert Maboneza and James Bahati who provided additional logistical support.

I am also in debt to those who gave advice and guidance on the direction of my project; Dr Piere-Denis Plisnier, Prof. Andy Cohen, Dr, Kiram Lezzar, Graeme Patterson, to Olivier Drieu for providing additional locational support and guidance, and to Jerod Clabaugh for lending me clothes while my luggage was in Nairobi. To Tharcisse Songore, Gabriel Hakizimana, and Deonatus Chitamwebwa, for providing valuable river and lake data.

Finally thanks to Jean-Marie Tumba, Robert Wakafumbe, Mark Woodworth and Ildephonse Nahishakiye for providing transport to field sites both on and off the lake, and to Nick Mattieu and the Nyanza Project students for their kind help and hospitality whilst in Kigoma.

# General Objective

To assess the possibility and identify procedures for the detection, explanation, and monitoring of possible near-surface sediment plumes in Lake Tanganyika, through the use of satellite remote sensing imagery, contemporary image processing techniques, and field data analysis.

# Background

## *Physical Setting*

Lake Tanganyika is the largest of the Rift Valley Lakes in Africa and is the second largest freshwater body in the world containing almost one sixth of the world's freshwater. The Lake occupies the narrow trough of the western branch of the rift system between 3°30' and 8°50'S, and the mean elevation is 773m above sea level. Tanganyika is 650km long, has a mean width of 50km, and has a maximum depth of nearly 1.5km. The geographical setting of the lake can be seen over the page in Figure 1.

## *The Ecological setting*

Lake Tanganyika has the richest biota of any lake on Earth (Worthington & Lowe-McConnell 1994), and is at least 9-12 million years old with some three hundred fish species, of which two thirds are endemic. The lake is also special in having an open lake pelagic fish fauna of endemic clupeids (2 species) and their centropomid predators thus forming a simple community compared to the very complex littoral communities living on the rocky shores that surround most of the lake. Furthermore there is a deep benthic and bathypelagic fish fauna living below 40m and down to the oxygen limit, of which very little is known about the specific biology of the eighty or so species living here (Worthington & Lowe-McConnell 1994).

Populations of some of the endemic fish are naturally low, however six species occupying the open waters of the lake occur in vast numbers and are an important source of food and income for the local population.

**Figure 1.** The Geographical setting of Lake Tanganyika (Lake Tanganyika Fisheries Research Web Site, 1999. <http://titan.glo.be/eric.coenen/index.html>)

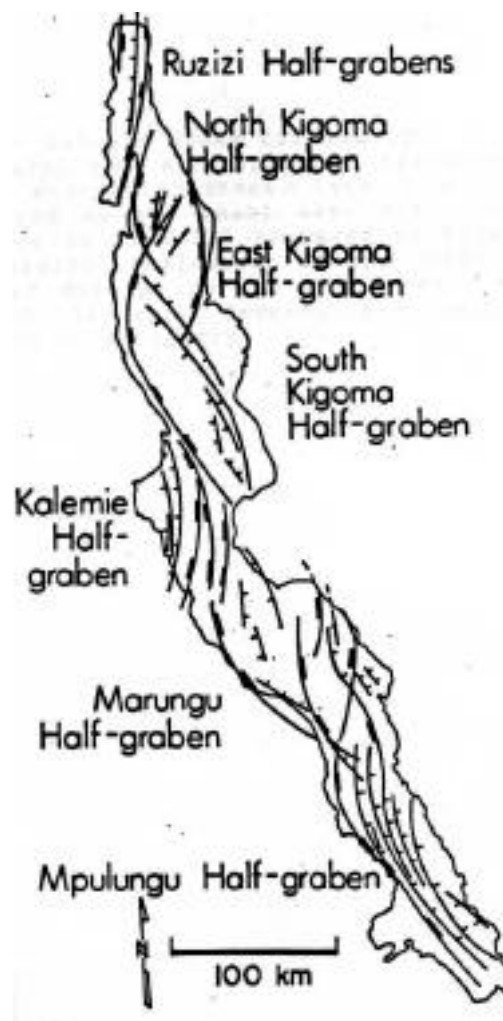


## *Lake Sedimentation and structural relations*

Deforestation and subsequent rapid erosion are the most severe environmental problems facing Lake Tanganyika (Patterson & Mackin, (Ed.) 1998). Unfortunately continuing population pressure on marginal lands, poor land management systems, and an increasing amount of land abandonment are serving to aggravate the erosion. The large amount of forest clearing has lead to rapid headward erosion, stream incision, and gully formation. The problem is most severe in the north of the catchment area (Burundi), for example the River Ntahangwa has rates of soil erosion between 28-100 tonnes per hectare per year, nearly all of which is distributed into the lake (Cohen et al., 1993). Such expansive erosion has caused the creation of large deltas such as from the Ruzizi which has experienced an order of magnitude increase in it's rate of outbuilding prior to large-scale deforestation within it's watershed (Caljon, 1987).

A bathymetric survey was completed by a Belgian expedition in 1946-47 (Capart 1949). Results indicate that the lake is divided into three distinct basins with shoal regions (<500m) at the northern and southern ends of the lake, see Figure 2. over page. The northern basin (Kigoma basin) has a maximum depth of 1310m and is separated from the central (Kungwe basin) by a broad sill of 655m. The central Kungwe basin has a maximum depth of 885m and is separated from the southern basin (Kipili basin) by another sill with a depth of 700m. The Kipili basin is the deepest with a maximum depth of 1410m. These three basins are subdivided into a collection of seven strongly asymmetric sub basins which are all half-grabens. The total volume of the lake is ~18940km<sup>3</sup> (Edmond et al. 1993) and the lake is largely surrounded by mountains, the tallest of which occur on the western side with elevations in excess of 2000m at the northern end.

**Figure 2.** Morphological map of Tanganyika basin, (Burgess, 1985).



The half-graben units have typical widths and lengths of 40 and 110km respectively (Burgess, 1985), the spatial distribution and linking of which are very complex. However, the basic structural configuration can be summarised as a series of half grabens whose dip-directions tend to alternate along strike, the boundary between adjacent half grabens is an accommodation zone that is either high or low relief (Burgess, 1985). Thus within the lake basin there are several morphological elements such as border fault margins, littoral platforms, midlake structural highs and axial deep basins. The influence of such structural form on the drainage pattern and hydrology of the lacustrine area is strong (Tiercelin et al., 1992).

Tiercelin et al. (1992), also note that sedimentation of fault margin areas include colluvial rockfalls, piedmont deposits, downslope bars, fan deltas, hydrothermal salts, and mineralisation. Sedimentation related to littoral platforms is characterised by fan and lateral littoral deltas as well as by prograding deltas. Characteristic of most, but not all Tanganyika deltas are high-density underflows generated by cold, mineral and sediment rich rivers. These are usually associated with submerged canyon and channel systems which have deeply incised platforms and slopes that can usually support underflow for many kilometres, but are confined by the structural grain of the midlake highs (Tiercelin et al., 1992). Lake Tanganyika's vast age (9-12 ma) and sizeable catchment area has produced huge amounts of sediment, with more than 4km depth in the deepest parts of the lake basins (Rosendahl et al., 1986).

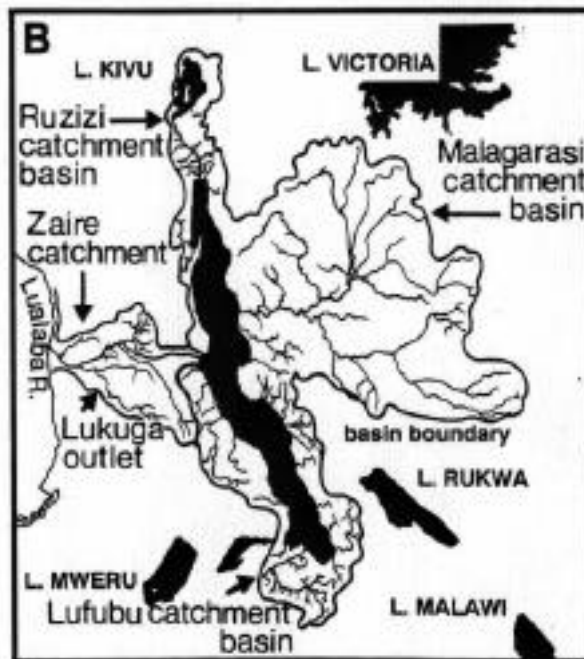
The lake level varies annually by less than one metre, which is explained by the following hydrologic balance. The estimated total discharge into the lake is  $18.2\text{km}^3 \text{ yr}^{-1}$ , precipitation is  $29\text{km}^3 \text{ yr}^{-1}$ , and evaporation  $43\text{km}^3 \text{ yr}^{-1}$ . The only outflow from Lake Tanganyika (which drains some 250,000km of surrounding countryside) is the Lukuga River which averages  $4.2\text{km}^3 \text{ yr}^{-1}$  (Edmond et al. 1993). This represents an outflow of only ~9% of the input, the rest is removed by evaporation (Edmond et al. 1993).

Edmond et al. (1993) also note that three rivers entering the lake are responsible for 58% of the total inflow, and therefore the majority of sediment input into the lake; the Malagarasi, Ruzizi, and Lufubu, the behaviour of which is strongly influenced by the dynamics of rainfall input, see Figure 3. Due to the sheer size and volume of Lake Tanganyika it is expected that the incoming river water and sediment load are mixed rapidly with the surrounding waters with the greatest suspended sediment concentration near to the large river mouths (Huttula, 1997). There are three different types of inflow from rivers into the lake and these depend on the density difference (a function of temperature and salinity) between the river and lake water. Logically if the river water is less dense than the lake water then the river water will most likely flow as a surface current; overflow, and if the river water is more dense than the lake water then the river water will sink; underflow. However conductivity (salinity) generally increases over depth (Lake Tanganyika Research project (LTR), FAO-FINNIDA, personal communication, 1999) and temperature decreases, therefore if river water is more dense than the surface waters of the lake but not more dense than the bottom waters of the lake then interflow will occur and the river water will equilibrate itself with lake water of the same density. Surface temperatures of the lake fluctuate between  $23.9^\circ\text{C}$  in early August at the Southern end up to  $28^\circ\text{C}$  at the end of the rainy season in March / April (Hutchinson, 1975). The lake was also found to have a weak thermal stratification, with seasonal mixing events

extending not much deeper than 150m. Temperatures below this remain constant at 23.1°C (Beauchamp, 1939).

Modes of introduction of the water borne sediments are of great importance to sedimentation studies since they will influence which areas and depths of the lake are affected by such inputs, however this has a direct bearing on which lake ecosystems are affected. And as yet, little is known about the modes of river inflow into Lake Tanganyika (Paterson & Makin, (Ed.) 1998).

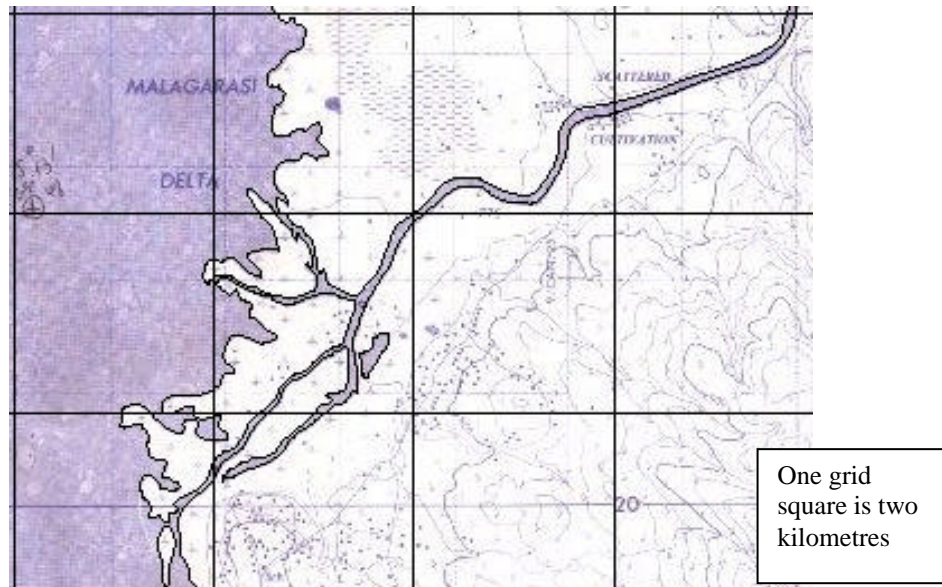
**Figure 3.** Drainage pattern of lake Tanganyika, (Tiercelin et al., 1992).



## ***The Malagarasi River Delta***

The largest tributary to the basin is over 475km long and together with its tributaries drains some 130,000km<sup>2</sup> the bulk of which receives 800-1200mm per year of rainfall which is mainly confined to the wet season of October-April (Patterson, 1998). The Malagarasi stretches from the Burundi and Tanzania mountainous border country through extensive swamp-lands before flowing through reaches characterised by rapids and waterfalls in the Misito escarpment, see Figure above. The river then bifurcates 5km from its mouth to form 4 major branches which span across the extensively prograding delta see Figure 4. The Malagarasi inlet region features a large plateau, which extends over 40km in the north-south direction and 15km in the east-west direction and lies in the South Kigoma Basin. Here channels up to 75m deep are incised into the older rift sediments, the largest of which is believed to have been formed during the last low stand in lake level 13,000 years ago, which is 600m below present levels (Hecky & Degens, 1973). The river discharge has been monitored by a NORCONSULT study for the period 1975-80 (NORCONSULT, 1982) the maximum monthly discharge was obtained as 430m<sup>3</sup>s<sup>-1</sup> in April and May, the mean monthly discharge at the end of the dry season (September) is one tenth of the wet season value at around 50m<sup>3</sup>s<sup>-1</sup>.

**Figure 4.** Map of the Malagarasi Delta, Surveys & Mapping Division Ministry of Lands, Housing and Urban Development, Government of the United Republic of Tanzania.



## ***The Ruzizi River Delta***

The Ruzizi River delta is the largest axial drainage system in the Tanganyika basin and is believed to have been in existence since the Plio-Pleistocene (Stoffers & Hecky, 1978), however rainfall stations are few but it is likely to be similar to that of Tanzania with around 800-1200mm per year or perhaps even more in the mountainous areas to the north. The Ruzizi flows down from the northern volcanic area of lake Kivu in a 150km course through the Kivu-Ruzizi graben. The river develops into a meandering channel draining a wide floodplain which bifurcates roughly 10km from it's mouth forming two channels, the Grande Ruzizi (responsible for the main sedimentation area) to the east, and Petite Ruzizi to the west which spread across the extensively prograding delta. The Ruzizi waters are notoriously rich in dissolved minerals due to the volcanic influence of the Kivu region (Tiercelin & Mondegeur, 1991), and also suspended sediment due to expansive erosion, as a result waters enter Lake Tanganyika as a dense underflow. Sediments vary from the organic rich mud's of the lagoon to the west of the Grande Ruzizi mouth to the quartzo-feldspathic and micaceous sands of the platform that extends 30m into the lake at a depth of roughly two metres (Tiercelin et al., 1992). Submerged valleys also exist just to the west of the present Petite Ruzizi River, thus transporting and depositing sediment deep into the Bujumbura sub-basin, see Figures 5 and 6 below (Tiercelin et al., 1992).

**Figure 5.** Rift axial margin drainage & littoral platform of Ruzizi, (Tiercelin et al.,1992.)

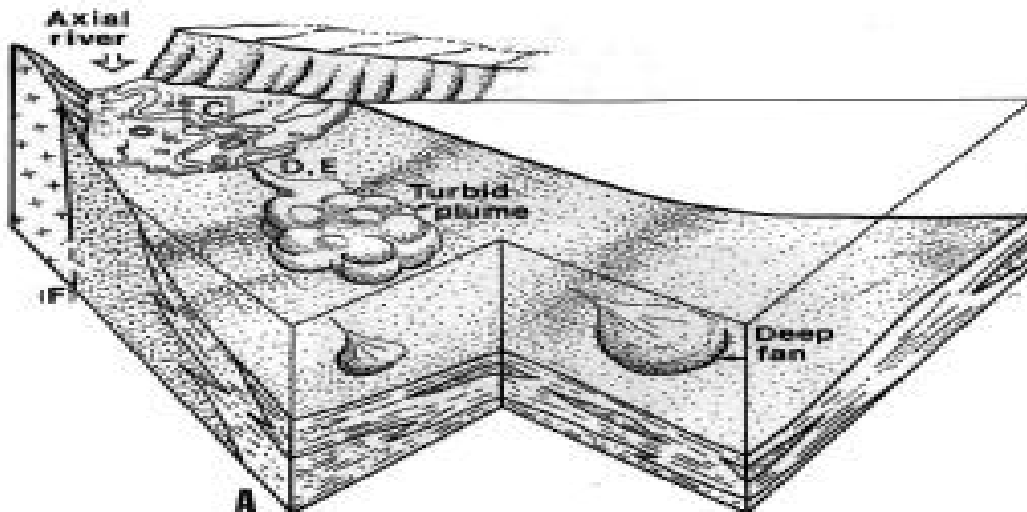
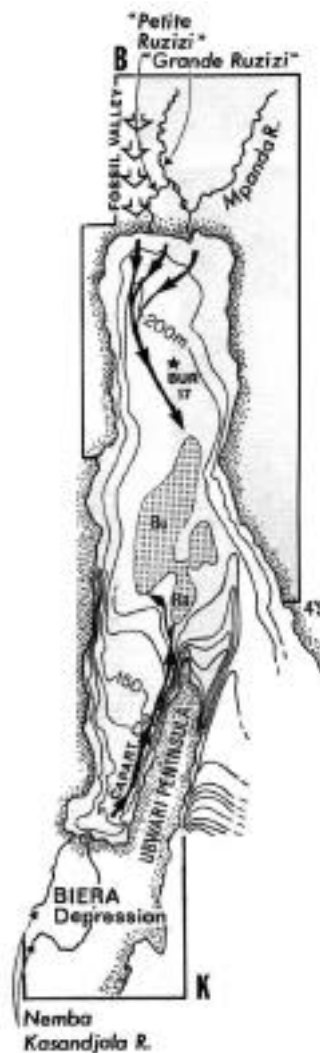


**Figure 6.** Bathymetric map of the Bujumbura sub-basin showing the Bujumbura (Bu) and Baraka (Ba) central depressions and the Ruzizi channel system. (Tiercelin et al., 1992.).



### ***Sediment Yield***

In conjunction with NRI and LTBP, King's College have produced a regional scale (1-8km pixel size) erosion model of the Lake Tanganyika catchment and surrounding area on a daily to dekadal timestep (Drake et al., 1999). One of the aims was to investigate the routing of erosion in order to estimate actual sediment inputs to the lake. The routing program is based on the notion that topography controls the drainage direction within each cell on the basis of steepest descent. The erosion model only considers soil detachment by overland flow and doesn't account for the deposition of sediments, therefore a delivery ratio is used to simulate deposition. The delivery ratio argues that steep headwater zones are the main sediment producing zones of a catchment and that as slope decreases so does sediment production, thus the delivery ratio decreases with increasing catchment size. This is a relationship that is further supported by Milliman & Syvitsky (1992), who suggested that in areas of thermal extension of the crust sediment loss varied with the size of the

basin. Results indicated yields decreasing from  $100\text{t}/\text{km}^2 \text{y}^{-1}$  in  $500\text{km}^2$  basins to yields of  $30\text{t}/\text{km}^2 \text{y}^{-1}$  in basins with an area of over a million square kilometres. Therefore it seems that short rivers that lead into the lake without passing through significant swamplands or large deltas may have a large part to play in the sedimentation of Lake Tanganyika.

The routing program was applied for the month of March 1996, see Figure 7, over page. Routing indicates that the total amount of sediment reaching the lake in March 1996 was around  $1.6 \times 10^6$  tonnes, while sediment deposited in the catchment was around  $2.4 \times 10^6$  tonnes. The most sensitive areas appear to be in the northern catchment area of Burundi and Rwanda, here the Ruzizi River is estimated to provide 63.6% of the sediment yield for the lake during the month of March 1996, and it is therefore likely to have a large effect on local biodiversity.

The drainage area of the Malagarasi appears to have much less sediment yield than would seem normal from its size and this has been linked to a deficiency in the model which was parameterised using data from small catchments, and therefore has difficulty dealing with large rivers and gently sloping floodplains. It is likely that results from this current project may highlight whether or not the Malagarasi transports a significant amount of sediment into the lake.

Sedimentation rates derived from sediment core analysis (see Figure 8, Tiercelin & Mondegeur, 1991) generally concur with the modelling and also indicate higher sedimentation rates in the north (max. rate  $\text{ca}4700\text{mm}/1000\text{y}^{-1}$ ) than the south (max. rate  $<1500\text{mm}/1000\text{y}^{-1}$ ) while rates from the centre of the lake are even lower (max rate  $<500\text{mm}/1000\text{y}^{-1}$ ). Thus it would seem that the Ruzizi is the dominant source of sediments in Lake Tanganyika, while sediments from the Malagarasi "appear to have become largely trapped in its delta system" (Tiercelin & Mondegeur, 1991) as well as being deposited in various upstream swamplands.

**Figure 7.** Total sediment transported from up stream ( $\times 1000 \text{ t km}^2$ ) during March 1996, Northern Lake Tanganyika (Drake et al., 1999).

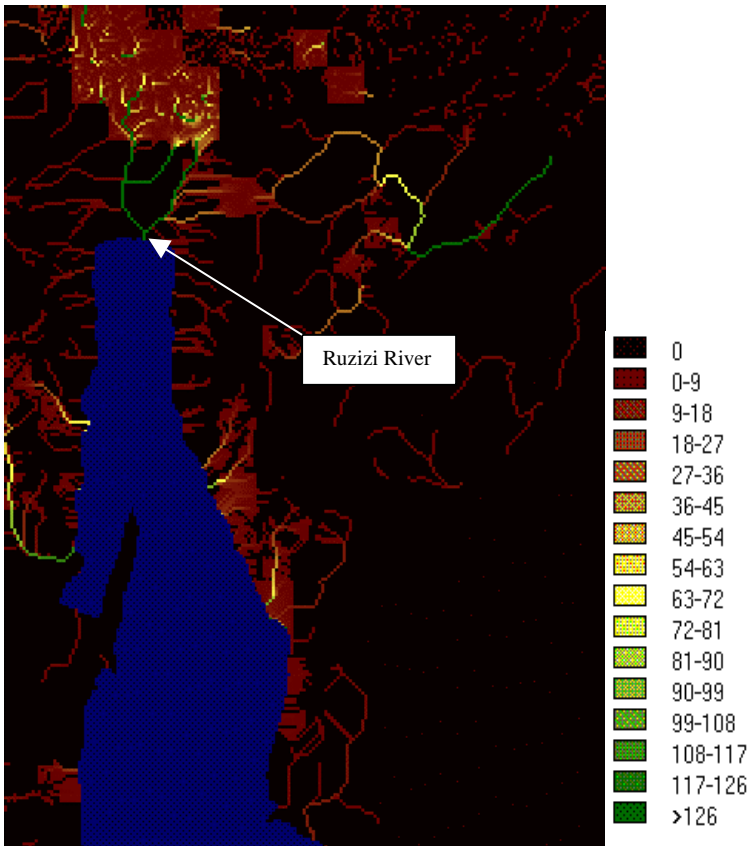


**Figure 8.** Sediment Core data from Tiercelin & Mondegeur, scanned in from Patterson & Mackin (Ed.) (1998).

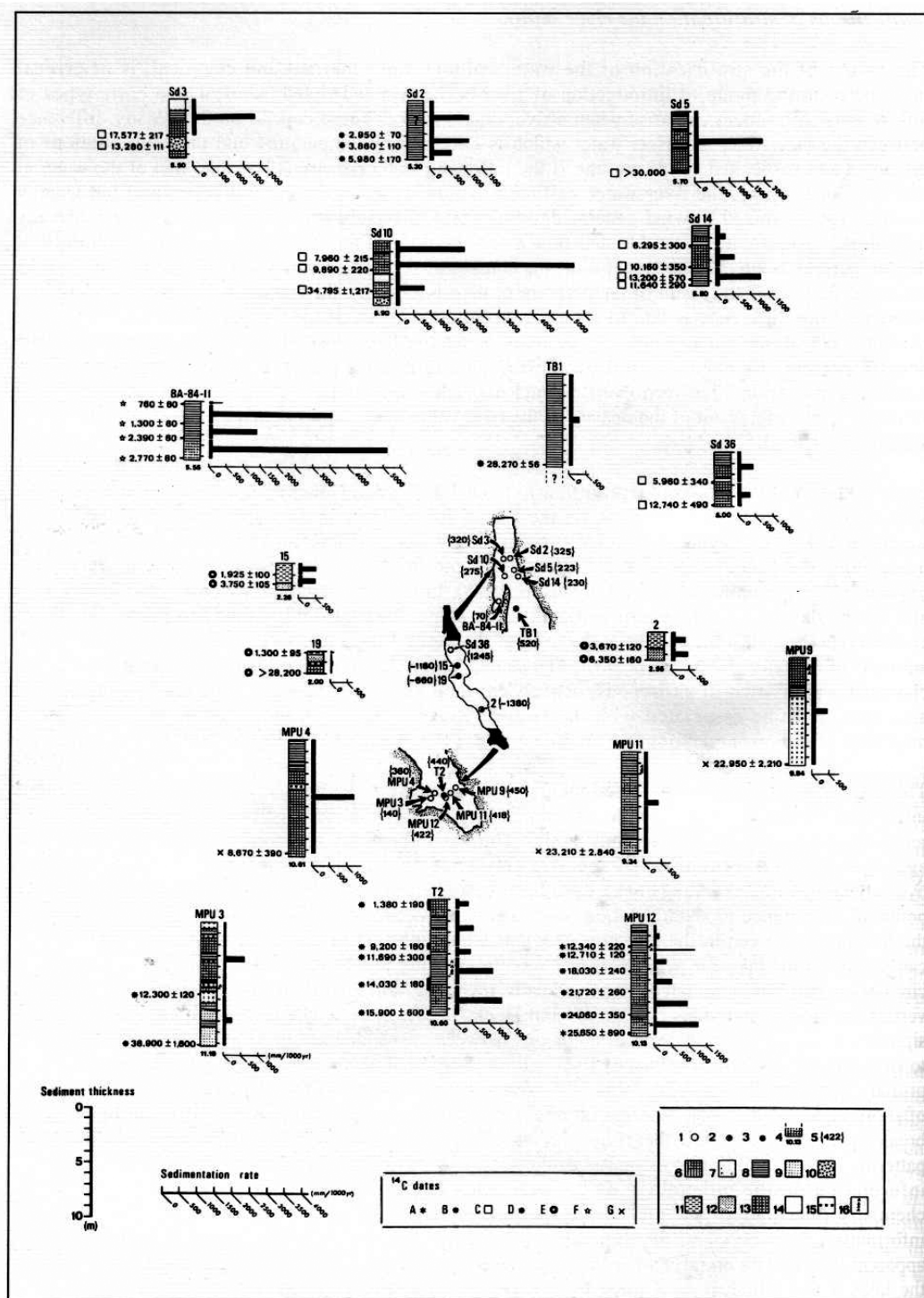
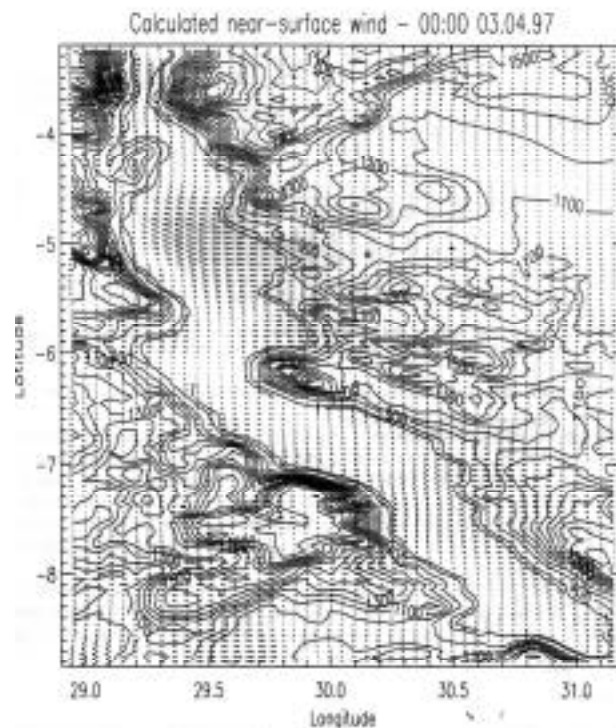


**Figure 2.3** A review of <sup>14</sup>C dating on Lake Tanganyika sediments and corresponding sedimentation rates. 1–3, coring sites; 4, maximum length of cores (m); 5, water depth at coring site (metres below lake level); 6, homogeneous mud; 7, flaky mud; 8, laminated mud; 9, silt and silty clay; 10, coarse sand and gravel; 11 carbonate-rich facies; 12, kaolinite-rich facies; 13, smectite-rich facies; 14, 'Argile Beige', nontronite layer; 16, pyroclastics. (Source: Tiercelin and Mondegeur, 1991.)

## ***Lake Circulation***

It seems that near surface currents in the lake are wind driven (Huttula, 1997) and therefore follow prevailing patterns such as those shown in Figure 9, below for 4th March 1997. More interestingly there is a periodic oscillation in the thermocline that was first discovered by Coulter in 1963. The thermocline extends to ~400m and is seen to vary with an internal wave motion whereby the thermocline depth fluctuates with a frequency of 26.3 days in the dry season and 33 days during the wet season, this is due to forcing by prevailing wind patterns (Huttula, 1997). During the dry season there are prominent south-easterly trade winds that cause upwelling of the cool nutrient rich hypolimnetic waters in the south. The thermocline tilts downwards towards the north, and typically varies by 20-30m between ends. Diurnal variations of surface winds between the lake/land breeze system have been shown to highly dominate the short scale surface current pattern especially in shallow areas such as the Malagarasi and Ruzizi areas Huttula (1997).

**Figure 9.** Calculated near surface wind over lake Tanganyika region, March 1997. Isolines show orography in metres above mean sea level, (Huttula (Ed.) 1997).



### ***Impacts of excess sediment loading***

Increased sedimentation rates of recent years are having a detrimental effect on the lake, the list below summarises the effects listed by recent studies.

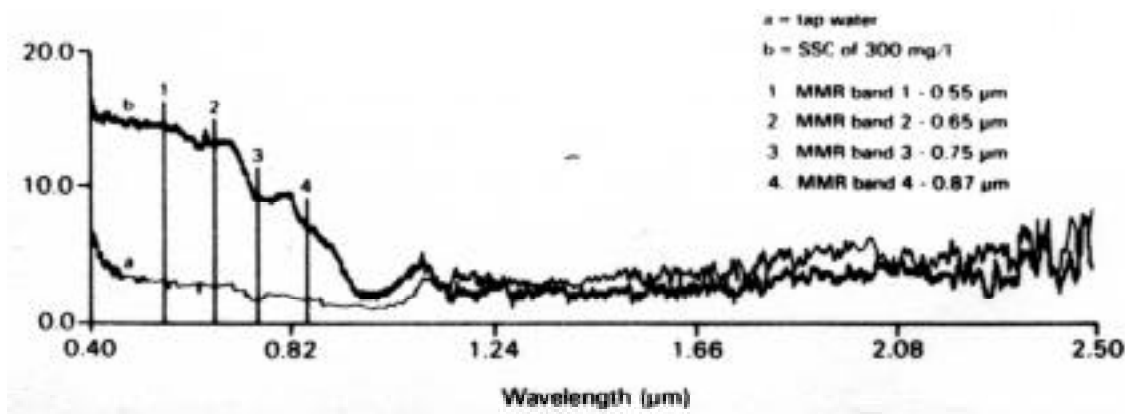
1. The large volumes of sediment entering the normally clear littoral and sub littoral environments of Lake Tanganyika have been shown to cause a large decrease in the lake's species richness, Cohen et al. (1993) illustrated this with survey results indicating a 35-65% decrease in species richness in sediment plume effected areas of Lake Tanganyika.
2. Suspended sediment affects filter feeding organisms by interfering with their feeding apparatuses, habitat complexity is also reduced by the infilling of crevices and overhangs which would otherwise support specialised biota (Cohen et al. 1993).
3. Large sediment loadings decrease the nutritional value of detritus (Graham, 1990).
4. Sediments have been shown to act as both nutrient and contaminant sinks, this can potentially alter the nutrient dynamics of the entire water body (Cohen et al. 1993).
5. Sediments can abrade the body of aquatic organisms and cause physical damage (Cohen et al. 1993).
6. As suspended sediment concentration increases light penetration into the water body decreases and this reduces photosynthetic rates (Grobelaar, 1985). This effects the algal cover which is the basis of the littoral food webs, and fish spawning sites.

### ***Monitoring of suspended sediments***

It is generally accepted that information on contemporary sedimentation processes in Lake Tanganyika is very limited (Patterson & Mackin, (Ed.) 1998). In situ measurements of sedimentation are limited in the temporal and spatial domains because of the cost and sheer logistical endeavour that would be required to consistently sample a large enough area of the lake. Satellite remote sensing provides an alternative means for obtaining relatively low cost simultaneous information on surface water conditions offering a complete sample of the spatial population (Harrington et al. 1992).

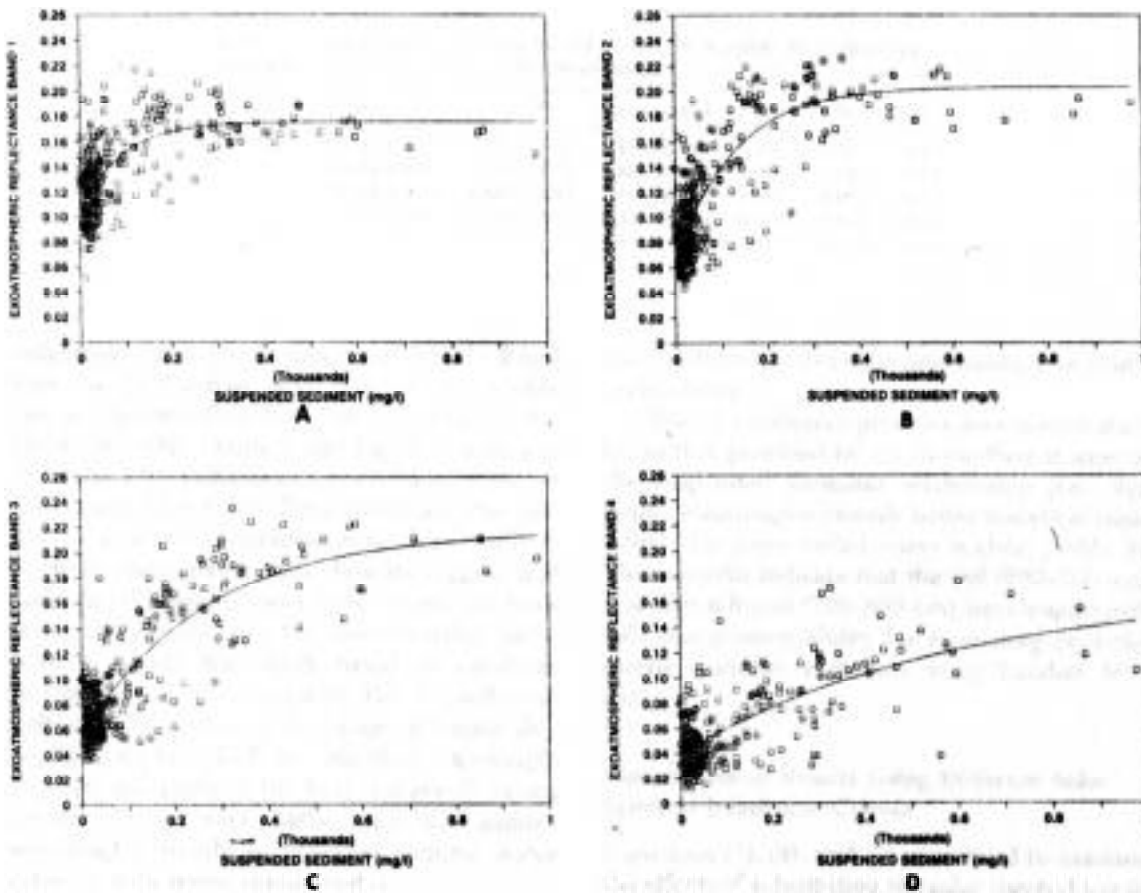
The absorption of radiation by water molecules increases greatly between the wavelengths of 480-700nm (Chen et al., 1991) and can be seen in Figure 10, below. The interaction of suspended matter in the upper water column alters the absorption and scattering characteristics of water, thus significantly increasing reflectance in the visible bands with larger concentrations of suspended matter.

**Figure 10**, Percentage reflectance of tap water and water with a suspended sediment concentration of 300mg/l, (Novo et al., 1989).



Many studies have found positive linear relationships between specific sediment types and reflectance, see Figure 11 from Harrington et al., (1992) which shows a series of scatterplots with best fit curves for Landsat TM bands 1-4. They found highest  $R^2$  values in the NIR wavelength of Landsat TM (700-800nm), with an  $R^2$  value of 0.716, this is in line with previous research conclusions such as those from Ritchie et al. (1976).

**Figure 11.** Scatterplots and best fit curves for the relationships between exoatmospheric reflectance and SSC (Harrington et al., 1992).



However the form of relationships such as those seen in the figure above appear to be very variable between studies (Chen et al., 1991). The reason for this is due to the sensitivity of the relationship to various factors; these include the physical and optical properties of the particular sediment, such as mineralogy and colour (McKim et al., 1984, Witte et al., 1982). Also sensor viewing geometry, and solar zenith angle have been identified as largely influential (Novo et al. 1989), as well as the specific SSC range, particle size and sensor wavelength (Chen et al., 1991; Novo et al., 1991; Holyer, 1978, Moore, 1977).

Upon successfully deriving such relationships many studies have then tried to estimate SSC/TSM quantitatively and have, according to Novo et al. (1991), "had only modest performances in inland water studies". Such studies include Ritchie et al. (1975) studying SSC in North Mississippi Reservoir's; Johnson, (1975) using aircraft multispectral data; Scherz & Van Domelen, (1975) monitoring the US Great Lakes using Landsat and aircraft imagery; Ritchie et al. (1976) again studying North American reservoirs, Munday & Alfoldi, (1979) who tested diffuse reflectance

models for aquatic suspended solids, and Tassan & Sturm, (1986) who used the Coastal Zone Colour Scanner (CZCS) data for coastal regions.

Inadequate sampling and methodology are also responsible for the difficulty in reaching quantitative SSC/TSM estimates from remotely sensed data. The following list notes such issues (Curran et al. 1987).

**1. Aerial variability in SSC.** The two most important sources of error in the measurement of SSC are the use of an inadequate number of sample points to represent each ground resolution element, and the use of an inadequate number of ground resolution elements to represent each class of SSC. It is practically impossible to gain an adequate sample size from such large spatial areas as used in remote sensing investigations. For example, Hay 1979 indicates that;

**"to determine the accuracy of a five class classification of SSC, a flotilla of 25 boats would be required during the hour of satellite overpass to record not only the five samples that are needed to represent the spatial variability of the SSC within each ground resolution element, but also the 50 ground resolution elements that are needed to represent the spatial variability of each class."**

**2. Vertical variability in SSC.** There will most probably be error when relating SSC measured below the surface to spectral reflectance which occurs at or near to the water surface (Curran et al. 1987).

**3. Temporal variability in SSC.** Large errors of location can occur when trying to align the simultaneously sampled lake and remote sensing data (Curran et al. 1987).

**4. Atmospheric signal.** Based on data presented by Moore (1977), atmospheric scattering accounts for over 95% of the signal measured by a satellite sensor over clear deep water. The offset must be removed to isolate the SSC/TSM signal.

Such hardships plus difficulties in producing water leaving radiance measurements adequate at a precision with current radiometers have meant that laboratory studies on the spectral properties of water are a long way behind those undertaken on vegetation and soil (Bowker et al., 1985). Nevertheless with a situation such as Lake Tanganyika the potential of remote sensing for just qualitative analysis, let alone quantitative analysis is vast. With some space-borne instruments, daily

monitoring of near surface SSC/TSM should be potentially possible thus offering the sedimentologist a new and very adaptable data source that provides a level of coverage vastly superior to ground collection methods.

## Specific Aims:

1. To assess the possibility of using satellite imagery and remote sensing techniques in the detection and monitoring of near-surface sediment plumes in Lake Tanganyika.
2. To evaluate the advantages and disadvantages of the ATSR-2 and AVHRR sensors used in the study and suggest which is of most use in a monitoring role.
3. To suggest reasons why particular sediment plume patterns are occurring through the use of primary and secondary data sources.
4. To highlight relationships and methods that will build towards a more quantitative evaluation of sediment plumes from space-borne satellite remote sensing systems.

# Methodology

## ***Satellite Data Pre-processing and Analysis***

Satellite data for the project is taken from the ATSR-2 sensor on-board the ESA ERS-2 satellite, and also the AVHRR sensor on-board the NOAA-14 satellite. ATSR-2 data was ordered through NERC and obtained from the Rutherford Appleton Laboratories. AVHRR data was obtained from NRI's LARST station situated in Kigoma, Tanzania. AVHRR and ATSR-2 were chosen because their coarse resolution and good temporal return periods mean that large areas could be monitored at a relatively frequent time interval, the sensors also include visible through to thermal wavebands that will allow visible and thermal monitoring of suspended material plus a wide variety of atmospheric and cloud correction techniques.

The images were taken from January 1997 to April 1997, and then from November 97 to April 1998, basically coverage of two wet seasons. Before data was ordered quick-look views were used to identify cloud free days, this resulted in 33 usable days for ATSR-2 data. AVHRR imagery was collected from the LARST station in Kigoma and was selected on the basis of it being relatively cloud free.

Satellite analysis and pre-processing was undertaken using the ENVI (v3.0) image processing package.

## ***ATSR-2/AVHRR Data Pre-processing***

ATSR-2 data was received in a gridded brightness temperature/reflectance format, thus containing gridded, calibrated brightness temperature and reflectance images across seven spectral bands shown in Table 1. AVHRR was received in it's block file format and was subsequently interpreted by the NRI NOM software, which converted the block file into a format that could be used by the ENVI image processing system.

**Table 1.** ATSR-2 and AVHRR spectral bands.

<b>Band</b>	<b>ATSR-2 Wavelength (<math>\mu\text{m}</math>)</b>	<b>Bandwidth</b>	<b>AVHRR Wavelength (<math>\mu\text{m}</math>)</b>	<b>Bandwidth</b>
1	0.55	20nm	0.58	1 $\mu\text{m}$
2	0.67	20nm	0.72	3.8 $\mu\text{m}$
3	0.87	20nm	3.55	3.8 $\mu\text{m}$
4	1.6	0.3 $\mu\text{m}$	10.3	1 $\mu\text{m}$
5	3.7	0.3 $\mu\text{m}$	11.5	1 $\mu\text{m}$
6	10.8	1 $\mu\text{m}$		
7	12.0	1 $\mu\text{m}$		

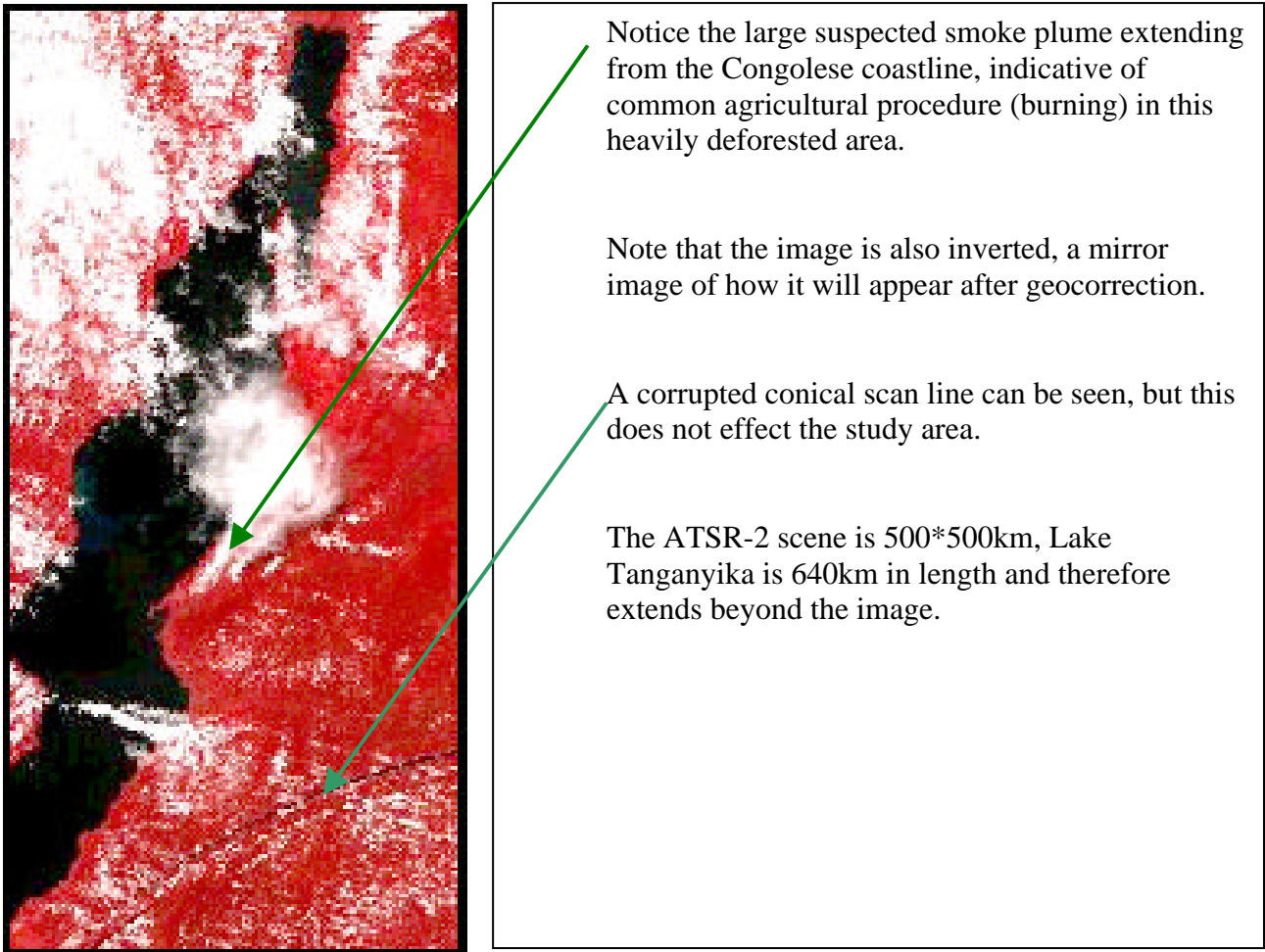
ATSR-2 provides a 500x500km, 1km resolution image with a return period of roughly three days, AVHRR has 1.1km resolution with a maximum image width of 2700km, although some of the images were resampled to various sizes before received for analysis. Before the images could be analysed there were certain data pre-processing steps that needed completing.

## ***Data Pre-processing,***

### ***1. Geocorrection.***

ATSR-2 images were manually geocorrected using a DEM of the area as the base image, a first degree polynomial warp was applied using nearest neighbour resampling. Ground control points were located around the lake shore and RMS errors were kept below 0.55 for this area. Figure 12, shows an uncorrected ATSR-2 image subset of the Lake Tanganyika area, note that the ATSR-2 scene is smaller than that of the lake.

**Figure 12.** A histogram stretched Raw ATSR-2 false colour image subset of the Lake Tanganyika area, 27/04/98.



AVHRR imagery was geocorrected automatically by the NOM software.

## ***2. Conversion to Reflectance/Brightness Temperature.***

The ATSR-2 visible bands (1-4) are in "normalised sensor counts" and thus require conversion into top-of-atmosphere fractional-reflectance units. This requires only linear scaling by a single conversion factor (one-per-channel). These conversion factors have been derived using data from the on-board visible calibration system (VISCAL) of ATSR-2, the calibration coefficients were found at the ATSR-2 web site ([http://www.atstr.rl.ac.uk/html/calibration\\_table.html](http://www.atstr.rl.ac.uk/html/calibration_table.html)). Thermal brightness temperatures were already calibrated. An example of a reflectance calibrated and geocorrected ATSR-2 image can be seen in Figure 13.

**Figure 13.** A histogram stretched, reflectance and geo-corrected ATSR-2 false colour image of the Lake Tanganyika area, 27/04/98.

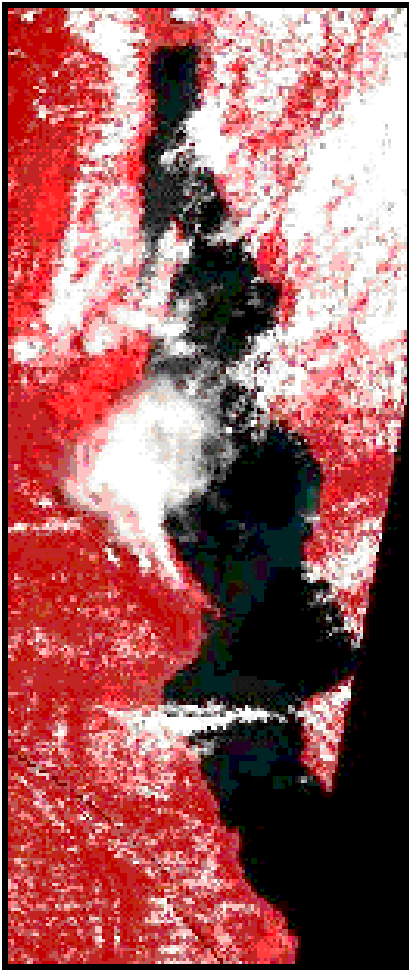


Image has been geo-corrected to a lat/long grid projection, hence the diagonal edge on the eastern boarder.

The reflectance calibration has also been applied to each visible band.

AVHRR imagery was automatically converted to reflectance/brightness temperature by the NOM software.

### ***3. Sun angle correction.***

The following correction was used to correct for the effect of the solar zenith angle in both ATSR-2 and AVHRR imagery (Stumph, 1992):

$$\mathbf{band\ reflectance/cos\theta}$$

Where;  $\theta$  is solar zenith angle.

Solar zenith angle is provided by the ATSR-2 and AVHRR image header. An example of a corrected ATSR-2 image can be seen in Figure 14.

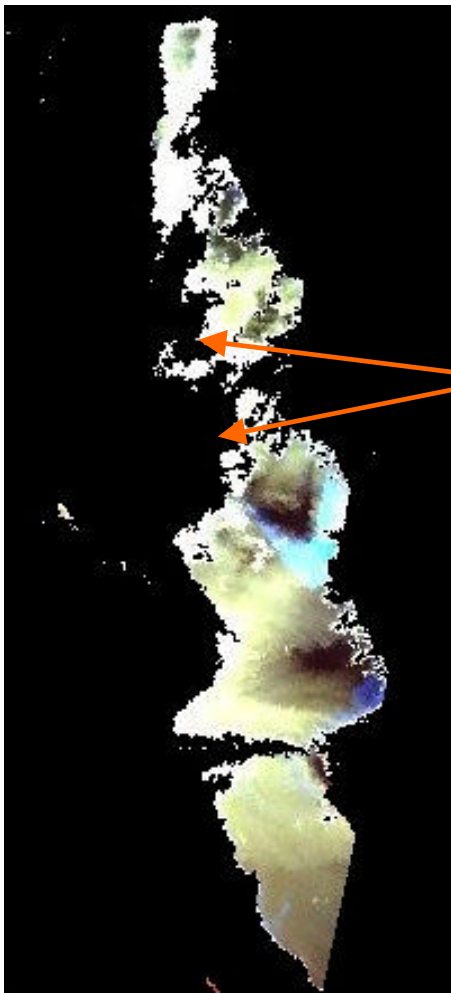
**Figure 14.** A histogram stretched, reflectance, geo-corrected, and sun angle corrected ATSR-2 false colour image of the Lake Tanganyika area, 27/04/98.



#### ***4. Land/water masking.***

Since this study is observing the lake it is of benefit to mask out all other areas, this was achieved using a band 4 shortwave infrared ( $1.6\mu\text{m}$ ) threshold for ATSR-2 and band 2 NIR ( $0.72\mu\text{m}$ ), this works because theoretically deep clear water should absorb heavily in the NIR wavelength, land and cloud have much greater reflectance and are therefore easily distinguishable from a water body. The threshold was determined empirically and was generally between 0.01 and 0.1 (= albedo, i.e. reflectance divided by 100) depending on the level of cloud/haze of the particular ATSR-2 scene. Any pixel found to be greater than the threshold value for reflectance was assumed to be cloud and was assigned a value of zero, any pixel that was less than the threshold was assumed to be water or haze/high cloud, and was assigned a value of one. A mask image was then produced which largely covered land areas, effects were still present due to the occurrence of cloud and haze, but these will be masked out by further cloud masking techniques. Figure 15 is an example of an image after the land mask has been applied.

**Figure 15.** A histogram stretched, reflectance, geo-corrected, sun angle corrected, and land masked ATSR-2 false colour image of the Lake Tanganyika area, 27/04/98.



As can be seen from the image the NIR threshold also removes some of the more reflective cloud.

The variation in reflectance of the lake is much more noticeable now that the largest source of variance (the land, and major clouds) has been removed.

As a result it is possible to identify suspected near-surface sediment plumes.

However there is still a great deal of variation due to cloud and atmospheric effects. These will be removed in the final two steps.

### **5. Cloud masking techniques.**

It was especially important in this study to obtain accurate estimates of the surface properties of the lake since small deviations in reflectance will represent significant amounts of suspended matter, therefore the methods which identified cloud-free and cloud-filled pixels needed to be as reliable as possible. After testing many different cloud detection techniques **two** were chosen for use in the study. These were found to provide the best performance under the given conditions.

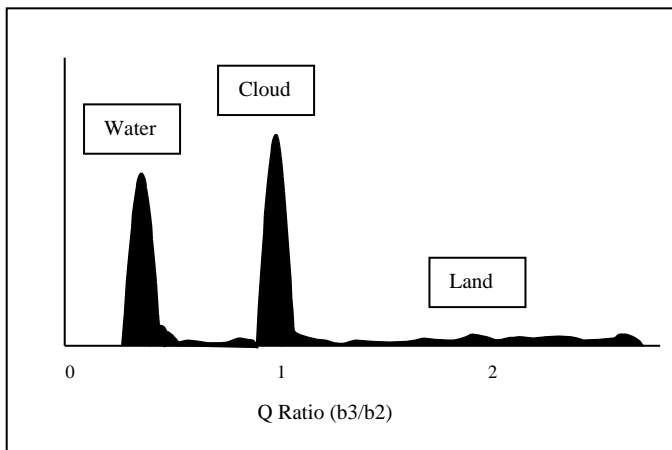
**i. Saunders & Kriebel, (1988).** The first is a simple brightness temperature threshold which uses the approximate twelve micron channel of ATSR-2/AVHRR. This channel is used because clouds have a greater optical depth at these wavelengths (Olesen & Grassl, 1985). Radiation emitted by cloud tops are by their very nature cold due to their altitude, therefore a temperature threshold between 283-289k, depending on the particular image, was used. Thresholds are much easier to determine over large water bodies since the water surface temperature varies only six degrees Celsius over the year. A pixel was identified as being cloud-filled if the brightness temperature was

less than the given threshold and was given a value of zero. If a pixel had a value equal to or greater than the threshold then it was assumed to be cloud-free and was assigned a value of one. A mask image was then produced.

**ii. Saunders & Kriebel, (1988).** The second test uses a ratio between NIR and Red reflectance's, in this case known as the Q ratio (NIR/Red). The Q ratio is close to unity over clouds since the reflectance of clouds only decreases slightly at NIR wavelengths. Over land the Q ratio is greater than unity due to reflectance increasing in the longer wavelengths, and over water it is less than unity due to the greater NIR absorption and enhanced backscattering at the shorter wavelengths due to molecular and aerosol scattering, see Figure 16. Therefore a simple histogram analysis of the Q ratio can be used to identify cloud-free peaks over land (greater than unity) and water (less than unity). Since we are interested only in removing clouds from a large water body a threshold below unity can be set so that all pixels other than those representing water are given a value of zero, and those representing water are given a value of one. A mask image is then produced.

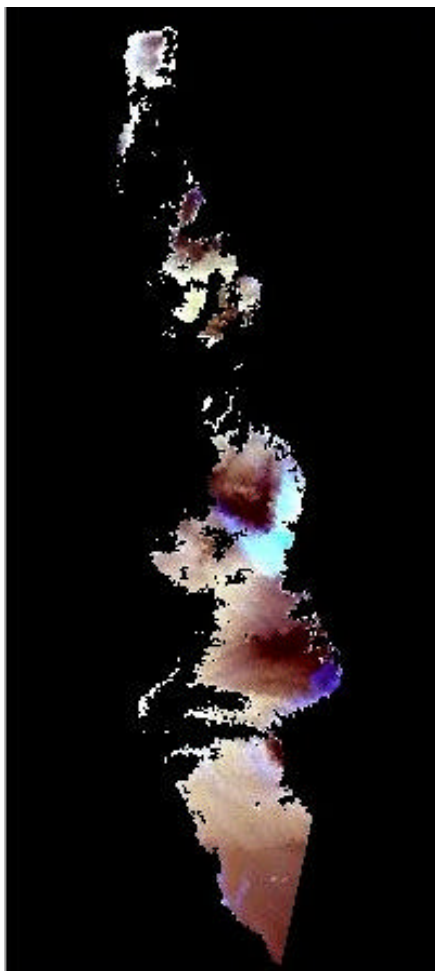
The result of the cloud screening procedures can be seen in Figure 17.

**Figure 16.** Histogram of Q ratio image.



If the histogram analysis offers no well defined peak for areas of cloud then over water a threshold of 0.75 was used (Saunders & Kriebel, 1988).

**Figure 17.** A histogram stretched, reflectance, geo-corrected, sun angle corrected, land and cloud masked ATSR-2 false colour image of the Lake Tanganyika area, 27/04/98.



The image has now had almost all of the cloud effects removed.

As a result the observed variation in reflectance over the image is a fraction of what it was before any of the masking procedures were initiated. This results in an even clearer view of the variation in the lake that is caused by suspended sediment when applying a standard linear stretch to the data.

Plumes can now be clearly seen, but there are still considerable atmospheric noise caused by Rayleigh and aerosol effects.

## ***6. Atmospheric Correction***

The main problem that must be faced when analysing remotely sensed data of water bodies is that of the atmosphere. Clouds aside, it is quoted that only around 20% of the radiant energy of water bodies arriving at the AVHRR sensor channel 1 (Red) is a signal from the earth's surface, the majority is due to atmospheric effects, and in AVHRR channel 2 (NIR) over 95% of the signal is due to the atmosphere (Wooster, 1998). There are many different types of atmospheric correction ranging from the simple to the incredibly complex. The size and scope of this project demanded a correction that could be applied quickly and with significant positive impact. Preference was given to a relatively simple but familiar methodology described by Stumph (1992), which has been well described and used under a wide range of operating conditions. The correction technique includes processing to remove the effects of changes in the down-welling solar irradiance caused by; aerosols, Rayleigh scattering, and glint.

The first step was to obtain the atmospheric transmittances for the ATSR-2 and AVHRR Red and NIR channels. Rayleigh and gaseous absorption optical depths were needed to attempt this and for ATSR-2 these were provided by the Rutherford Appleton Laboratories, and for AVHRR were obtained from Stumph (1992). Atmospheric transmittance calculations use Rayleigh optical depth ( $\tau_r$ ) and gaseous absorption optical depth ( $\tau_g$ ) in the calculation of total atmospheric transmission from earth to sun and from earth to sensor.

Equation 1.

$$T_0 = \exp [(-\tau_r/2) + \tau_g/\cos \theta_0]$$

$$T_1 = \exp [(-\tau_r/2) + \tau_g/\cos \theta_1]$$

Where:

- $T_0$  atmospheric transmission from earth to sun
- $T_1$  atmospheric transmission from earth to sensor
- $\tau_r$  Rayleigh optical depth
- $\tau_g$  gaseous absorption optical depth
- $\theta_0$  solar zenith angle
- $\theta_1$  satellite view angle

Next the radiance corrected for Rayleigh and gaseous effects can be calculated, note that for small areas (<200km across) it is not necessary to calculate the Rayleigh component as it is not expected to change significantly in the Red and NIR wavelengths, therefore single values of  $T_0$  and  $T_1$  can be calculated using mean values of  $\theta_0$  and  $\theta_1$  that are representative of the region of interest.

Equation 2.

$$R_c' = [(A(\theta_1)/(\theta_1 T_0(\theta_1)) - (A(\theta_2)/(T_1(\theta_2) T_0(\theta_2)))]$$

Where:

- $R_c'$  albedo corrected for Rayleigh and gaseous effects
- $A(\theta_1)$  the albedo measured at the sensor in the Red band
- $A(\theta_2)$  the albedo measured at the sensor in the NIR band

Because the study area is relatively small it is not necessary to calculate the Rayleigh component as it is not expected to change significantly in the Red and NIR wavelengths, therefore this component

can be treated as a bias. This is achieved by taking the minimum value for  $R_c'$  that corresponds to the value for the clearest water. This value is called  $R_{bias}$ .

The atmospherically corrected radiance ( $R_d$ ) is thus described by:

Equation 3.

$$R_d = R_c' - R_{bias}$$

The end result here is an image that has passed through the six steps of geocorrection, reflectance calibration, sun angle correction, land masking, cloud screening, and finally atmospheric correction, an example of such an image can be seen below in Figure 18.

**Figure 18.** A histogram stretched, reflectance, geo-corrected, sun angle corrected, land and cloud masked, and atmospherically corrected ATSR-2 colour image of the Lake Tanganyika area, 27/04/98.



The image shown here is now fully corrected through all of the previously explained 6 steps.

The atmospheric correction takes the NIR and Red band to provide a single channel output that has been displayed using a red/white colour table.

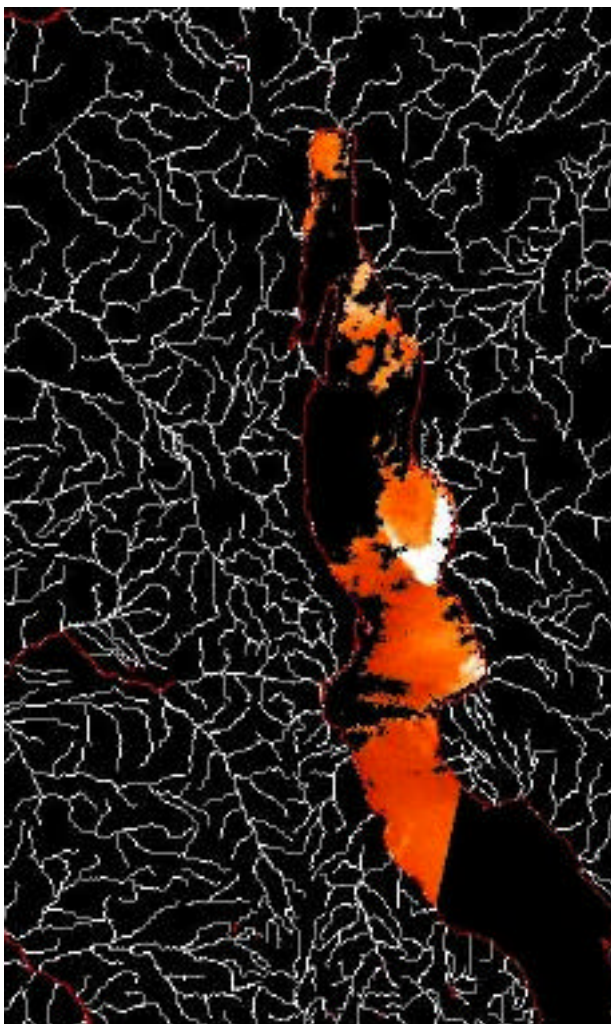
Dark red indicates low reflectance and hence low suspended matter, lighter colours of orange and white indicate higher reflectance and greater suspended matter concentration. Black areas are masked out due to the presence of cloud or land.

The finished product should be representative of the reflectance from the lake surface and therefore is a function of the amount of suspended sediment. All that remains to be done is the application of the following equation (Prangma & Roozkrans, 1989), which describes the quantitative relationship between atmospherically corrected water column radiance and the concentration of total suspended matter in the lake surface. The adjustable parameters (a & b) must be calibrated using field data.

Equation 4. 
$$\text{Log(TSM)} = a \log(R_d) + b$$

However the implications of correctly calibrating the adjustable parameters for the whole of Lake Tanganyika is beyond the scope of the study, for the most part the adjustable parameters are left out and only a qualitative estimate is provided by the imagery. This point will be discussed in greater detail later. Finally to add clarity a vector file of rivers and a lake outline is overlaid, plumes can now be matched up with known river mouths, see Figure 19, below.

**Figure 19.** A histogram stretched fully corrected image with rivers and lake outline vector files.



Sediment plumes can now be clearly linked with known rivers.

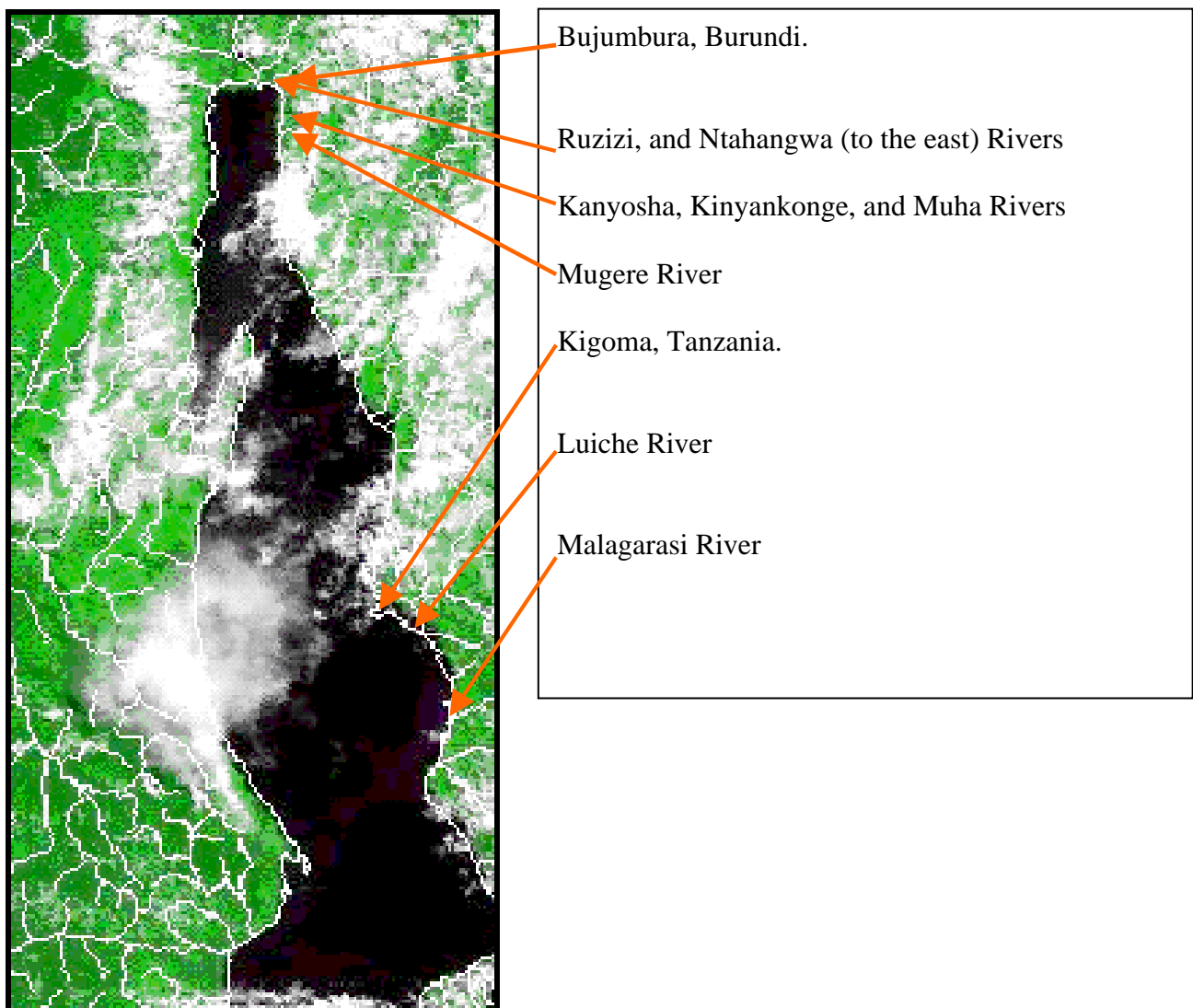
### ***Image Interpretation***

The image processing techniques described above were then applied to images that showed evidence of displaying plumes, in the end this resulted in eight ATSR-2 and four AVHRR images. The qualitative images were then observed and plume behaviour was described, and partially explained by additional secondary, and field collected data. The various attributes of both sensors were also taken into consideration in an evaluation of the effectiveness of each sensor.

### ***Fieldwork Techniques and Data Collection***

Fieldwork took place over a three week period from July 17th until August 7th, 1999. Two weeks of the stay were spent in Bujumbura, Burundi at the northern end of the lake, the remaining week was spent in Kigoma, Tanzania. The image below indicates the study locations and the main rivers that were sampled.

**Figure 20.** False colour ATSR-2 image of the study with an overlay of the main rivers



### ***Data Collection***

Data was collected using a 5m fibreglass boat with a 40HP engine, except for the Luiche river sampling day when a 2m inflatable Zodiac boat with 15HP engine was used. In total there were 5 sampling trips on the lake, these were as follows:

Table 2. Date and nature of sampling trips on Lake Tanganyika.

<b>Date</b>	<b>Nature of sampling mission</b>
20/07/99	Sampled the Ntakangwa river with the Pollution Special study team, limited time due to weather conditions. But travelled by road and sampled Ruzizi and Ntakangwa upstream. Data collected: TSM, and sediment grab samples.
22/07/99	Sampled Ruzizi Delta and Ntakangwa river mouth with Sedimentation Special Study Team. Data collected: TSM, radiometer, and sediment grab samples.
26/07/99	Sampled 4km offshore from Ruzizi Delta in a 1km study area, took 2km transect towards Ntakangwa river, and took samples from the Ruzizi Delta. Data collected: TSM, sediment grab samples, and radiometer data, but the data logger failed so the recordings were lost.
30/07/99	Sampled the Luiche river with Nyanza students, 3km transect from 500m upriver into lake. Data collected: TSM, and sediment grab samples.
03/08/99	Sampled the Malagarasi River/Delta, took 10km transect from 5km upriver into lake. Data collected: TSM, sediment grab samples, and radiometer data.

Sampling had to be conducted so as to fit in with the sampling times of the Pollution and Sedimentation Special Studies schedule, and when in Kigoma (sampling the Luiche and Malagarasi Rivers) sampling was arranged along with the requirements of the Nyanza Project. The boats were kindly skippered by LTBP staff: Jean-Marie Tumba, and Robert Wakafumbe, and on the Luiche trip by Nyanza Project instructor Mark Woodworth.

### ***Equipment and Technique***

#### ***The Grab Sampling***

A Ponar Grab Sampler was used in the collection of lake/river/delta bottom sediment. Sediment collected by this method was supposed to be used in a spectral analysis that would have sought to identify a laboratory relationship between TSM and reflectance, once back in the UK. However time constraints meant that this was not able to be undertaken.

### ***The Radiometer Recordings***

A four channel Skye Instruments radiometer was used to take spectral measurements of the lake surface water under different TSM concentrations. Before measurements of the surface reflectance were taken at each sample site a measurement of the solar irradiance was first taken to ensure calibration procedure was maintained. Recordings of lake surface reflectance were taken facing the sun, from a height of one metre at nadir position in order to avoid angular effects. Care was also taken so as not to cause any shadowing on the water's surface, it is also noted that the texture of the water surface will vary considerably with the amount of wind present, and this is likely to affect reflectance measurements.

A notable exception is that of the Malagarasi radiometer data which had to be collected whilst avoiding sun glint from the choppy waters therefore it was not possible to face the sun at all times. However, irradiance was measured before commencing each different sample site recordings, therefore this should reduce the associated error.

A Skye Instruments data hog was used to store the radiometer data. The data hog was pre-set to record every 30 seconds, after the initial solar irradiance recording three more measurements of the lake/river surface were taken. At each sampling site the sampling time period was recorded so as to aid future identification of the data after retrieval.

The radiometer data was calibrated using a reflectance panel of known reflectance under a range of solar exposure.

### ***Suspended Sediment data collection***

Total Suspended Matter (TSM) in this study was taken as the difference in dry weight between a filter paper of 0.75 $\mu$ m grade, before and after filtering a 100ml sample of lake water. Results are provided in mg $l^{-1}$  units, therefore the result of a 100ml filter sample is multiplied by ten. Lake/river water was taken from the top 15cm of water and was collected in 300ml sample bottles so that if an error occurred with the filtration there was always enough lake water left for at least one more sample. The sampling site was clearly marked on each bottle, and before filling the sample bottle it was flushed out with lake/river water to remove any substances left in the bottle after the cleaning procedure. Sample bottles were then stowed and transported back to the lab for analysis.

The lab equipment used were as follows:

- Mettler AE240 Analytical Dual Range Balance (in Bujumbura labs)
- AND HR-120 Balance (in Kigoma labs)
- Whatman GF/F (50 class) 90mm diameter Hardened Circles
- 500ml butner jar with rubber tube and hand pump
- Ceramic funnel
- 250ml measuring cylinder

Filter papers were pre-weighed and subsequently used for the filtration of 100ml samples. During filtration air was sucked out of the butner jar using the hand pump. After filtration the samples were placed on a drying tray and put in an oven to dry for at least 12 hours. However the oven was simply used to store the samples in a dust/breeze free environment, it was not used to actually heat the samples because the temperature range only began at 50°C which is too hot for the drying of filter papers. After the drying period the filter papers were re-weighed and the results recorded.

It is duly noted that the filter sample size of 100ml is likely to be inaccurate at low sediment concentrations, however because of the manual pumping technique if larger sediment concentrations are encountered then filtering of a sample over 100ml becomes a very difficult task, therefore in the interests of consistency all filtered samples were 100ml.

### ***GPS Recordings***

At each sample point the geographical co-ordinates were recorded using a Garmin GPS III Plus instrument which is accurate to 15m.

### ***Data collection procedures at sample sites***

A note-like brief summary of all fieldwork undertaken is now presented.

#### **LTBP Bujumbura, Burundi, 20th July, 1999. Sampling trip to Ntakangwa River.**

The first sampling trip was supposed to reach the Ntakangwa, Ruzizi, and Giteza areas, however large waves prevented travel to Ruzizi or Giteza, therefore limited data was collected. This sampling trip was carried out by the Pollution Special Study team.

Once at the Ntakangwa river mouth 7 bottles were collected from across the river (from the surface 10cm) 10m upstream. River width here is 16m, with a depth of 30cm. The radiometer was out of

action and therefore no measurements were taken. After finishing the Ntahangwa sampling continued upstream where rivers are accessible by vehicle. Samples were then taken from the Ntahangwa river 1050m upstream where 4 samples from the middle of the flow were taken, at 10cm depth. River width is ~5m and mean depth is 30cm. The Ruzizi river was also sampled at Gatumba; the main bridge on the road to Uvira, where 4 sample bottles were taken at 10cm depth from the middle of the river (width 50m). It is stressed that data taken on this day was intended to characterise river sediment levels, check laboratory methodology, and validate data with that taken by the Pollution Special Study team.

**LTBP Bujumbura, Burundi, 22nd July, 1999. Ruzizi Delta sample.**

Sampling was performed on this day along with the Sedimentation Special Study. Sampling began at the mouth of the Grande Ruzizi tributary here the mouth is 70m wide and a shallow delta/plateau extends 30m beyond the shoreline due south. A line transect was taken across the Ruzizi mouth approximately 10m north from the shoreline (40m from the end of the plateau, i.e. upriver). The Ponar grab sampler was used to collect sediment samples every 10 metres. Time restrictions meant that no radiometer samples were taken here.

The Ntahangwa river was also sampled, here radiometer data and water samples from 10cm depth were taken 10m upstream of the mouth, measurements were taken at 3m intervals across the river.

**LTBP Bujumbura, Burundi, 26th July, 1999. Ruzizi, Ntahangwa, and Lake sample.**

Sampling was conducted without any of the Special Study teams, therefore the personnel included the author and the boatsman. Sampling began with a random grab sample of the Ruzizi delta/plateau. Twelve samples were taken, along with four water samples which were taken to characterise the TSM for that time period. Sampling continued 4km south of the river mouth in the open lake where a 1km<sup>2</sup> area was randomly sampled with a total of 23 bottles collected for TSM analysis. Next a 2km line transect was taken 3km due south of the Ntahangwa river mouth heading Northwest (towards the Ntahangwa mouth), a total of 20 water bottles taken (1 every 10 m), again for TSM analysis. Also manage to briefly sample the Ntahangwa river and collect 6 grab samples across the mouth (3m intervals). Radiometer data was recorded but later it was found that the data logger failed, so all recordings were lost.

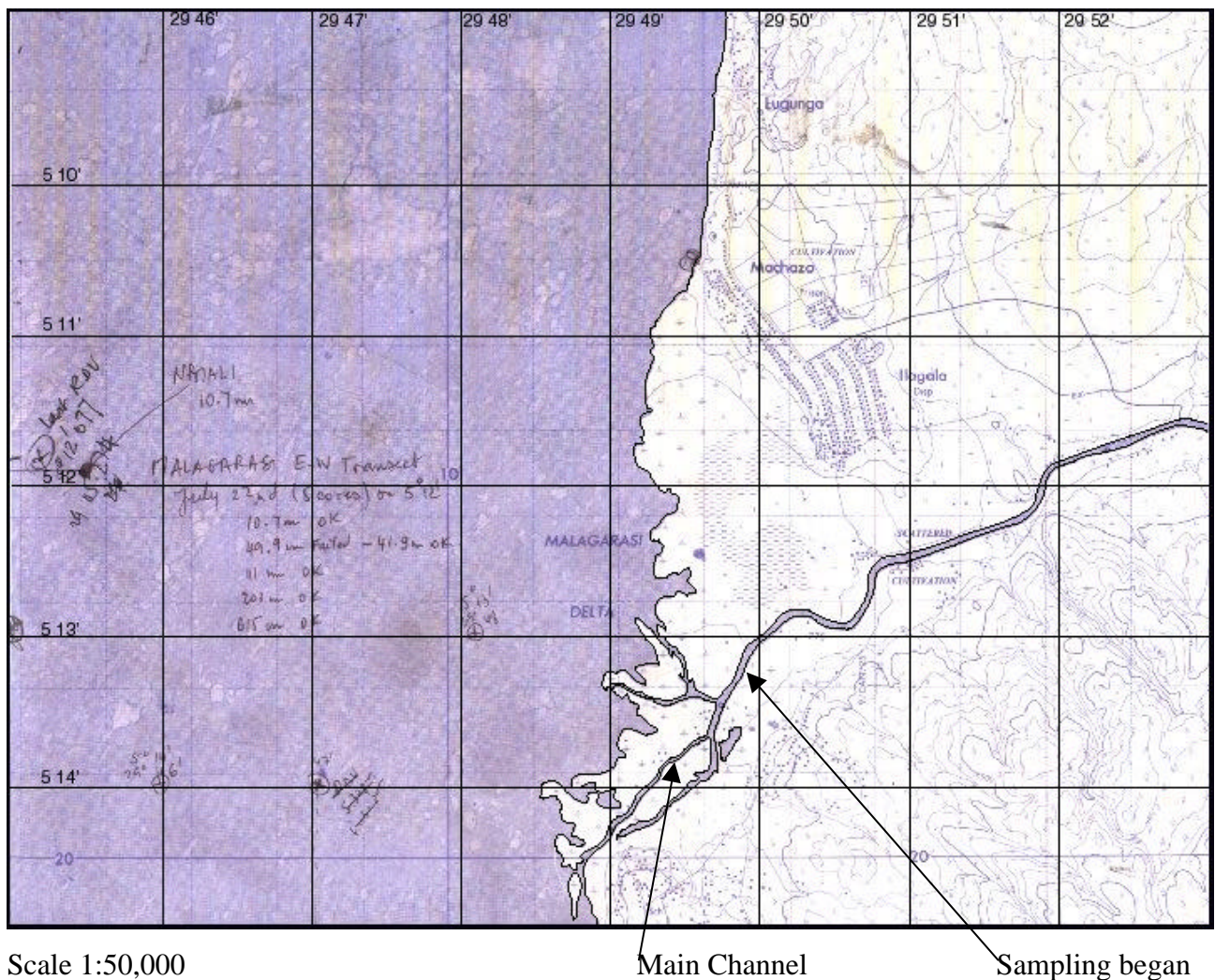
**LTBP Kigoma, Tanzania, 30th July, 1999. Luiche River sample.**

Took a small inflatable along with a Nyanza project student and instructor down to the Luiche River. Sampled using the grab sampler and also suspended sediment bottles, 10 sites (sampling every 100m) extending from inside the mouth of the Luiche. Unfortunately the grab sampler was only operative for 4 grabs, after this the bottom was too hard to obtain samples and also too deep as we travelled over a kilometre into the lake.

**LTBP Kigoma, Tanzania, 3rd August, 1999. Malagarasi Delta/River sample.**

Travelled in the large fibreglass boat to the Malagarasi Delta/River where a 10km transect was taken commencing 5km upstream, see Figure 21.

**Figure 21.** Map of the Malagarasi Delta, Nyanza Project, 1999. (Surveys & Mapping Division, Ministry of Lands, Housing and Urban Development. Government of the United Republic of Tanzania).



Sampling began 500m upstream of the first junction in the main river channel, and continued in the main channel and out into the lake/delta. Samples were taken every 500m according to the GPS. Variables measured at each sample point were water bottles (for TSM analysis), sediment grab samples, and radiometer data.

### ***Secondary Data Sources***

River and Lake data for Bujumbura area was kindly provided by Tharcisse Songore of the Sedimentation Special Study team (LTBP, 1999), Gabrielle Hakizimana of the Pollution Special Study team (LTBP, 1999), and for the Malagarasi River/Delta data was provided by the Director of the Tanzania Fisheries Research Institute (TAFIRI) Mr. Deonatus Chitamwebwa. Additional river data included the rivers Kinyankonge, Kanyosha, Mugere, and Muha, all 4 rivers flow into the lake within 20km south of Bujumbura and can be seen in Figure 20.

### ***Field and secondary data analysis***

The field data of TSM was collated and analysed in Excel 97, simple averaged plots were produced of TSM levels over the study period as well as individual plots of transect results for the Malagarasi and Luiche rivers. Reflectance data from the radiometer was used in a regression analysis with the corresponding TSM results for the transect of the Malagarasi and Luiche Rivers.

The secondary river/lake data consisted of temperature, conductivity and some discharge and SSC data. Again analysis was conducted in Excel and plots were produced of the aforementioned variables. A calculation of density was conducted using the equation of Chen & Milliero (1977)(see equation below) provided already in Excel format by Graeme Patterson (Personal Communication, 1999). Density was calculated for lake and river water over different time periods in order to analyse the proportion of sinking/floating plumes for each river.

Equation 5.

$$d^p = d^o / (1 - P/K)$$

$$d^o \text{ (g cm}^{-3}\text{)} = 0.9998395 + 6.7914 \times 10^{-5}t - 9.0894 \times 10^{-6}t^2 + 0.0171 \times 10^{-7}t^3 - 1.2846 \times 10^{-9}t^4 + 1.1592 \times 10^{-11}t^5 - 5.0125 \times 10^{-14}t^6 + (8.221 \times 10^{-4} + 3.87 \times 10^{-6}t + 4.99 \times 10^{-8}t^2)S(\%)$$

$$\begin{aligned}
K(\text{bar}) = & 19652.17 + 148.376t - 2.329t^2 \\
& - 1.3963 \times 10^{-2}t^3 - 5.90 \times 10^{-5}t^4 \\
& + (3.2918 - 1.719 \times 10^{-3}t + 1.684 \times 10^{-4}t^2)P \\
& + (-0.8985 + 2.428 \times 10^{-2}t + 1.114 \times 10^{-2}P) S(\text{‰})
\end{aligned}$$

Where:  $d^P$  and  $d^O$  are the densities of lake water at the applied pressures  $P$  and  $O$  (sea level), respectively,  $t$  is the temperature in  $^{\circ}\text{C}$ ,  $S(\text{‰})$  is the salinity.

$$S(\text{‰}) = 0.9951437g_T$$

Where  $g_T$  is the total grams of dissolved salt in one kg of lake water, usually this increases with depth.

# Results

## *Satellite Imagery Analysis*

Eight ATSR-2 and four AVHRR images were prepared using the steps outlined in the methodology and are displayed in chronological order over the next few pages. It is important to note the date of each image and the type of image as it is the aim not only to observe plume patterns but also the differences between the two sensors. ATSR-2 images have a much smaller scene size than AVHRR (512x512km compared to in excess of 2000x2000km), and therefore never cover the whole of Lake Tanganyika in one image, AVHRR images are large enough to include Lakes Malawi and Victoria as well as the Indian Ocean coastline, thus the AVHRR images also yield results for these areas of water too.

The order of the images is listed below in Table 3:

<i>Satellite Image date</i>	<i>Sensor type</i>	<i>Figure number</i>
22nd March, 1997.	ATSR-2	Figure 22
22nd January, 1998.	ATSR-2	Figure 23
26th February, 1998.	ATSR-2	Figure 24
1st March, 1998.	ATSR-2	Figure 25
4th March, 1998.	ATSR-2	Figure 26
20th March, 1998.	ATSR-2	Figure 27
6th April, 1998.	AVHRR (NOAA-14)	Figure 28
14th April, 1998.	AVHRR (NOAA-14)	Figure 29
23rd April, 1998.	AVHRR (NOAA-14)	Figure 30
24th April, 1998.	ATSR-2	Figure 31
27th April, 1998.	ATSR-2	Figure 32
18th May, 1998.	AVHRR (NOAA-14)	Figure 33

It should be noted that each image has been contrast stretched, apparent qualitative sediment levels cannot therefore be compared between images. This is also why the lake area in some images appears a lighter shade of orange, the images have been stretched in order to best display the given sediment plumes around river mouths, not to enable inter-image comparison of ambient near-surface sediment in the vast body of lake waters. Areas of black on the image have been cloud/land masked.

Figure 22. 22nd March, 1997. ATSR-2

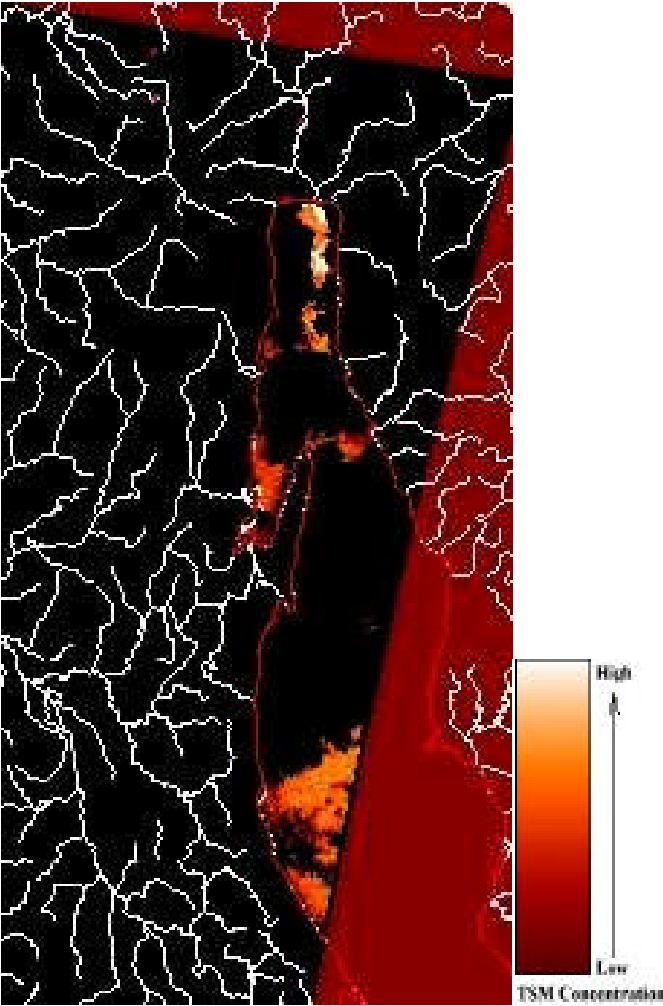


Figure 23. 22nd January, 1998. ATSR-2

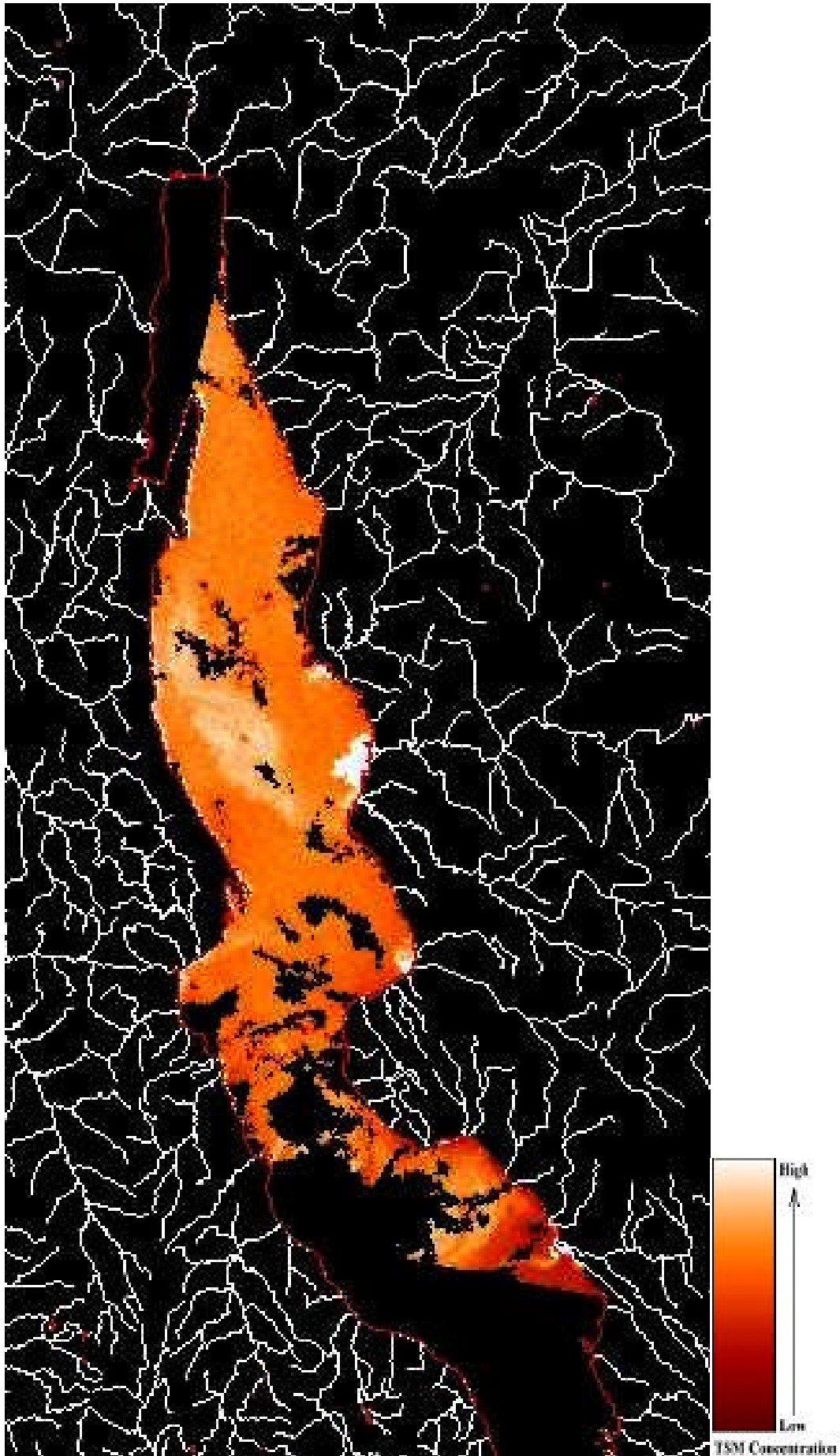


Figure 24. 26th February, 1998. ATSR-2

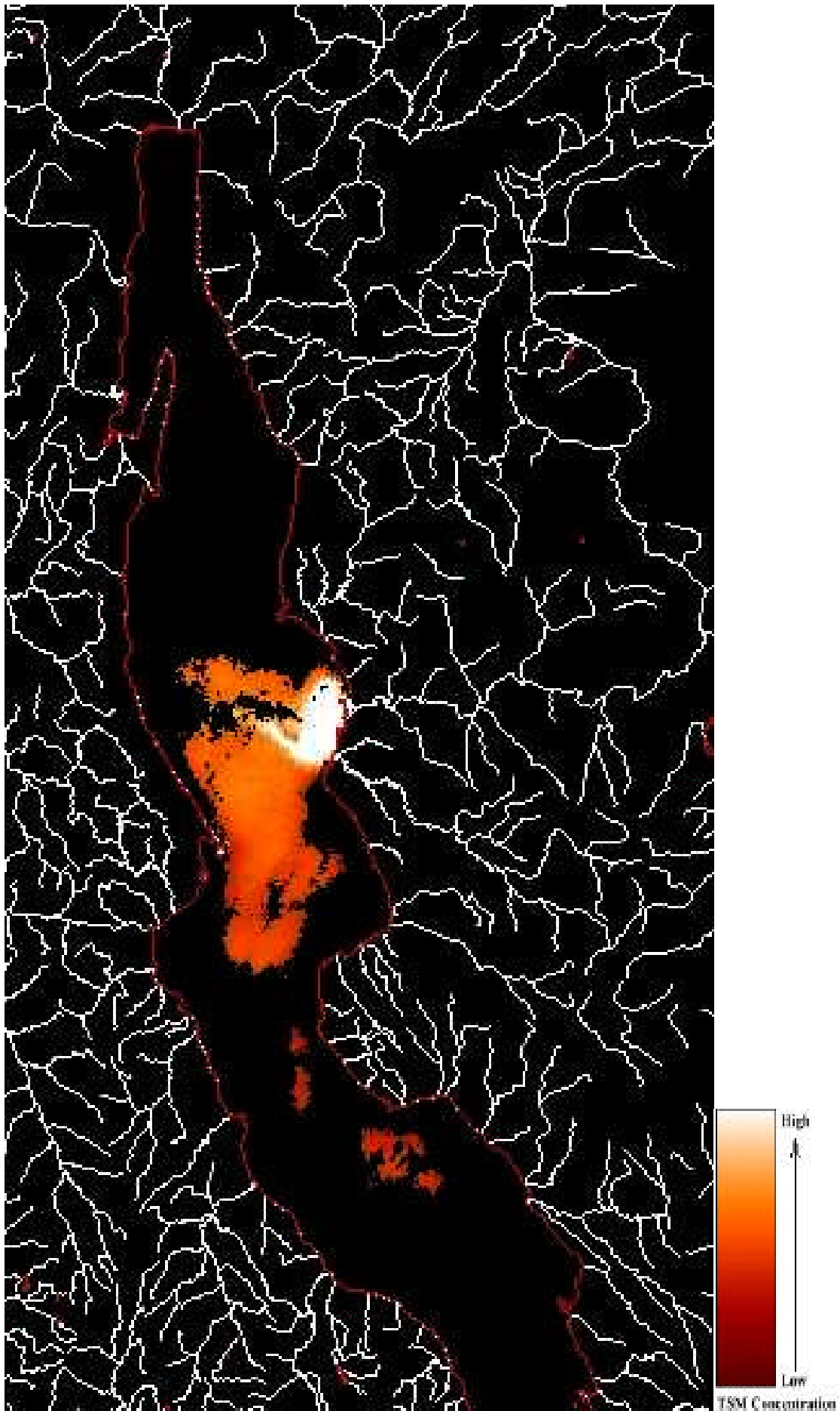


Figure 25. 1st March, 1998. ATSR-2

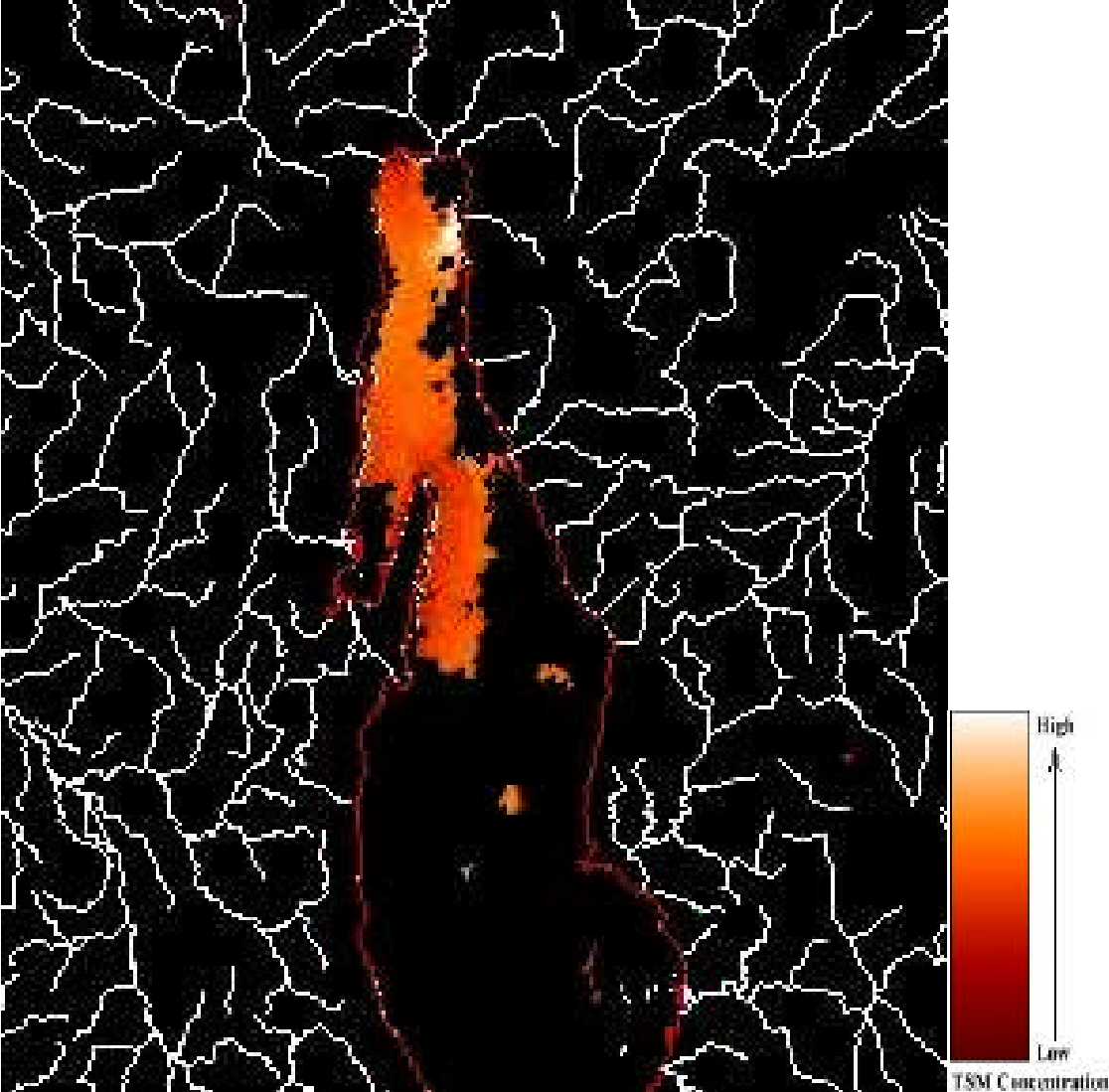


Figure 26. 4th March, 1998. ATSR-2

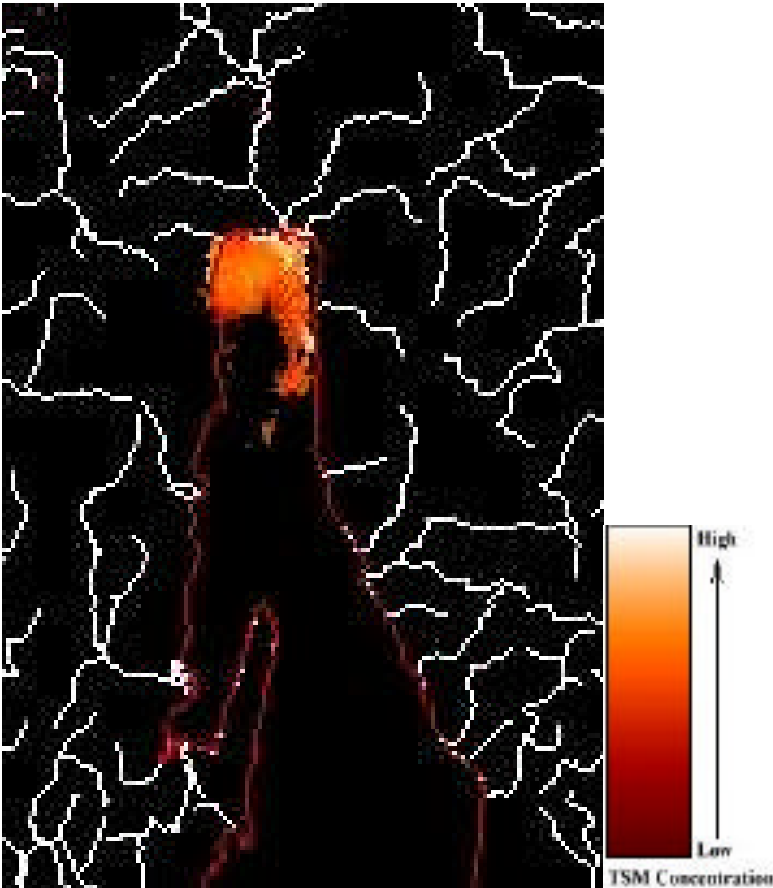


Figure 27. 20th March, 1998. ATSR-2

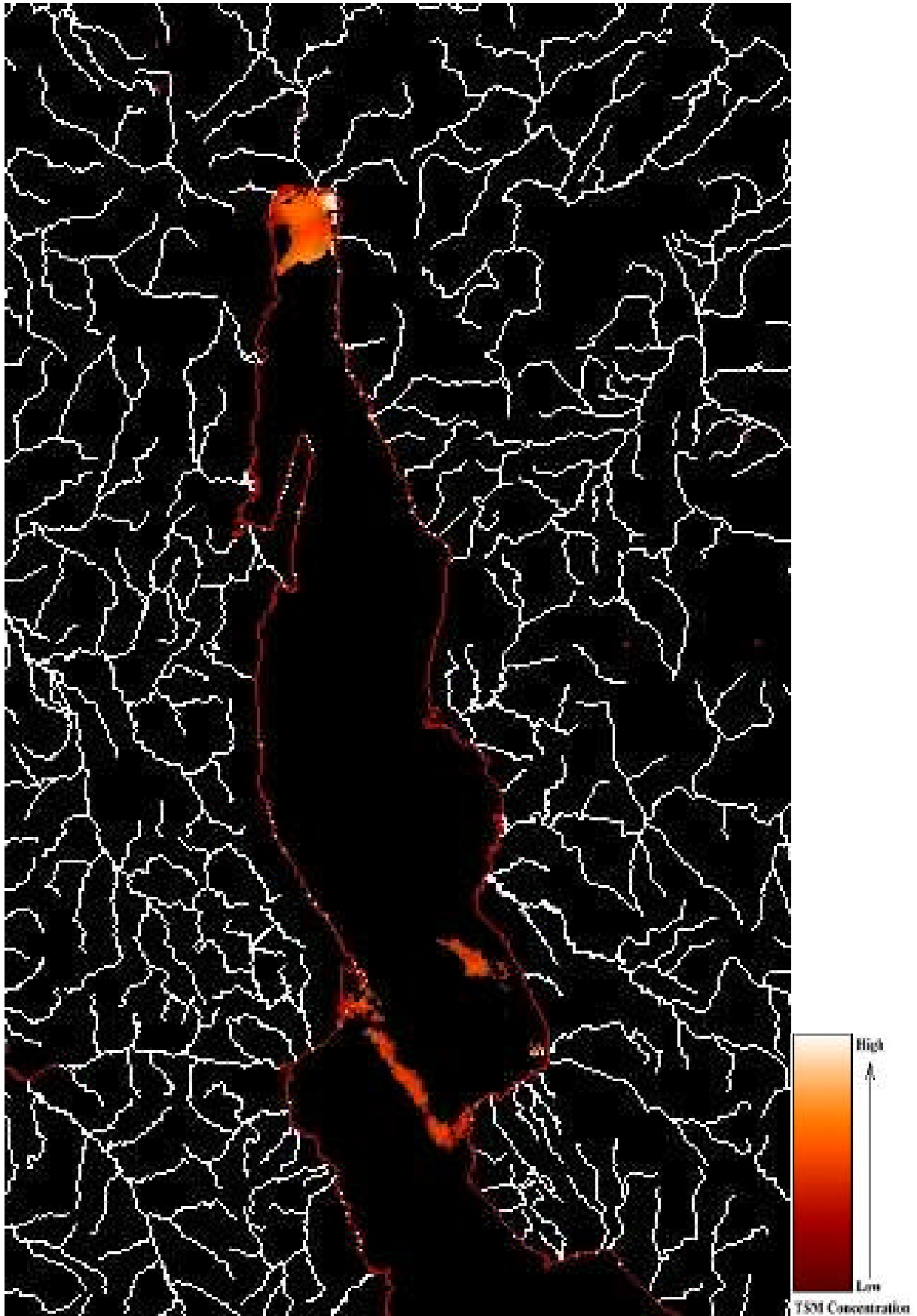


Figure 28. 6th April, 1998. AVHRR (NOAA-14)

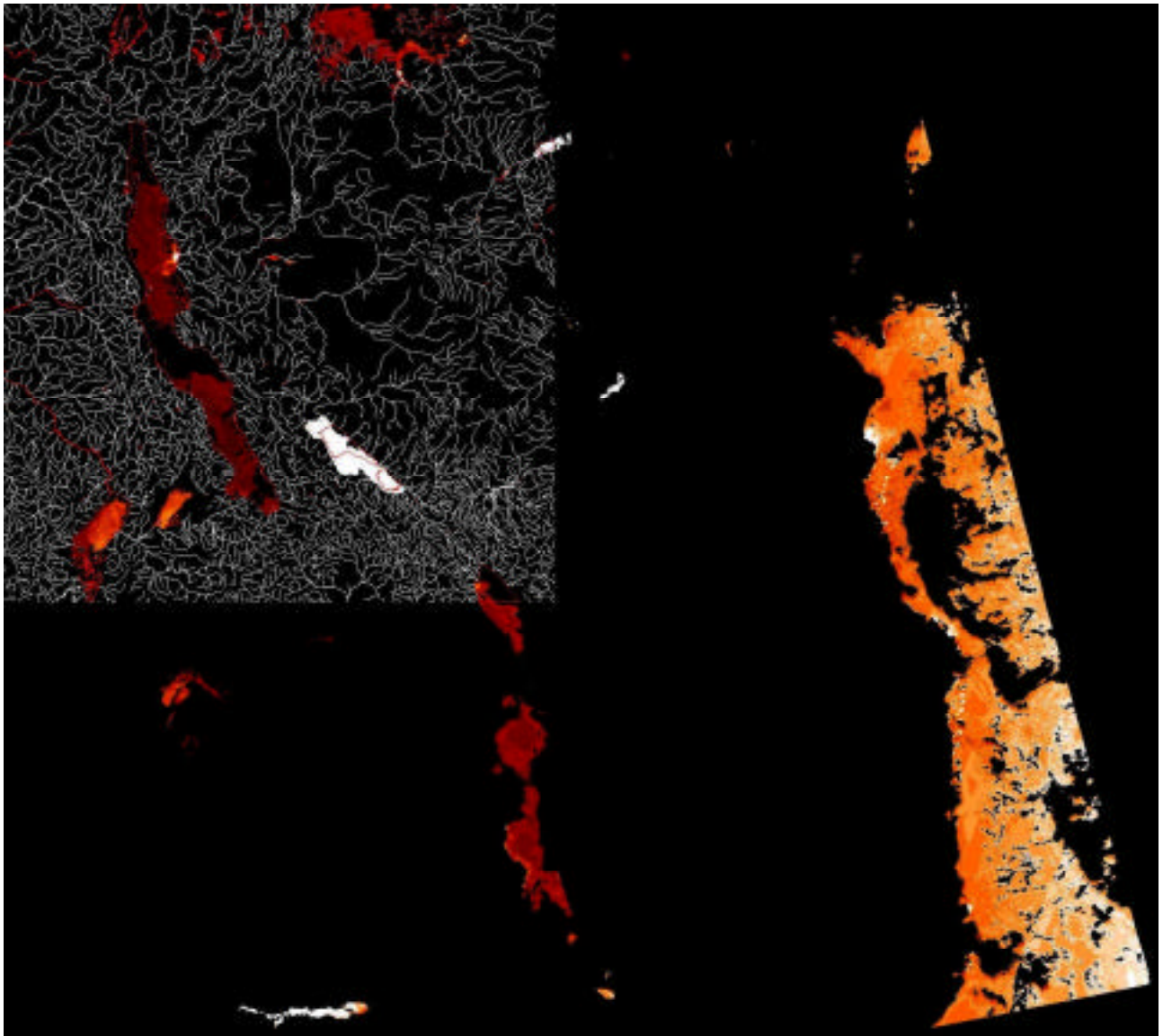


Figure 29. 14th April, 1998. AVHRR (NOAA-14)

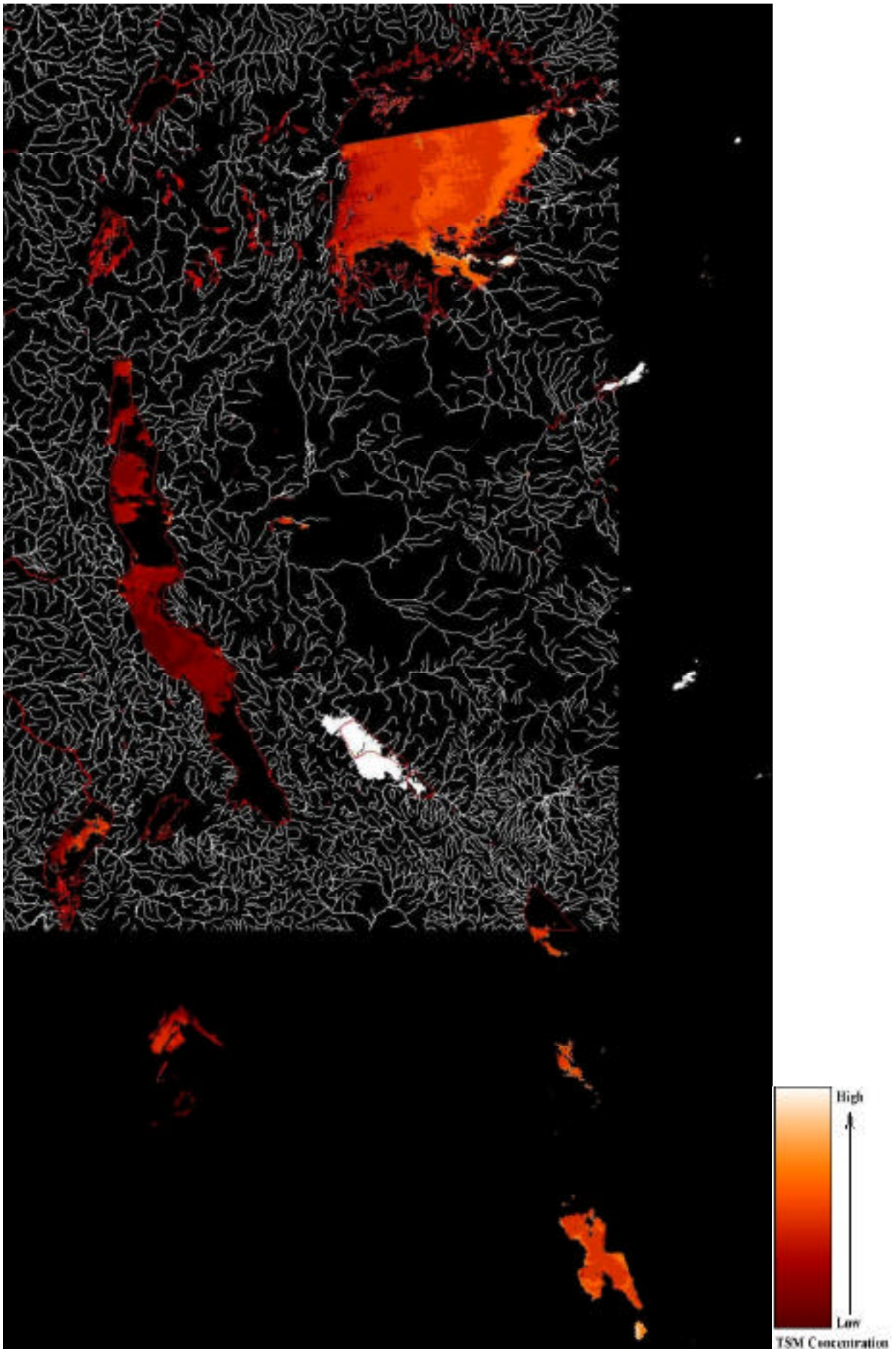


Figure 30. 23rd April, 1998. AVHRR (NOAA-14)

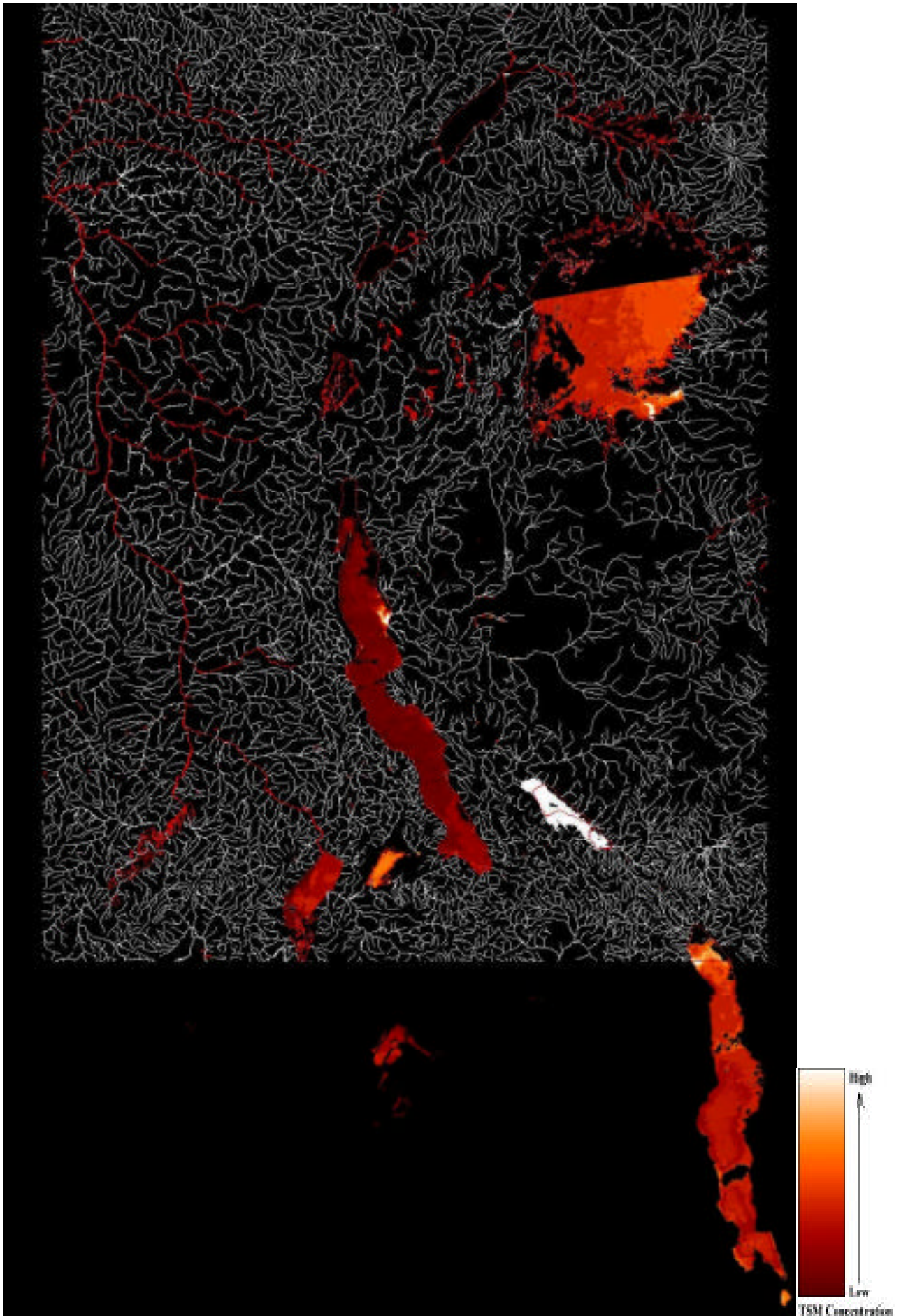


Figure 31. 24th April, 1998. ATSR-2

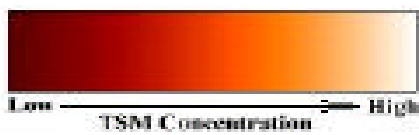
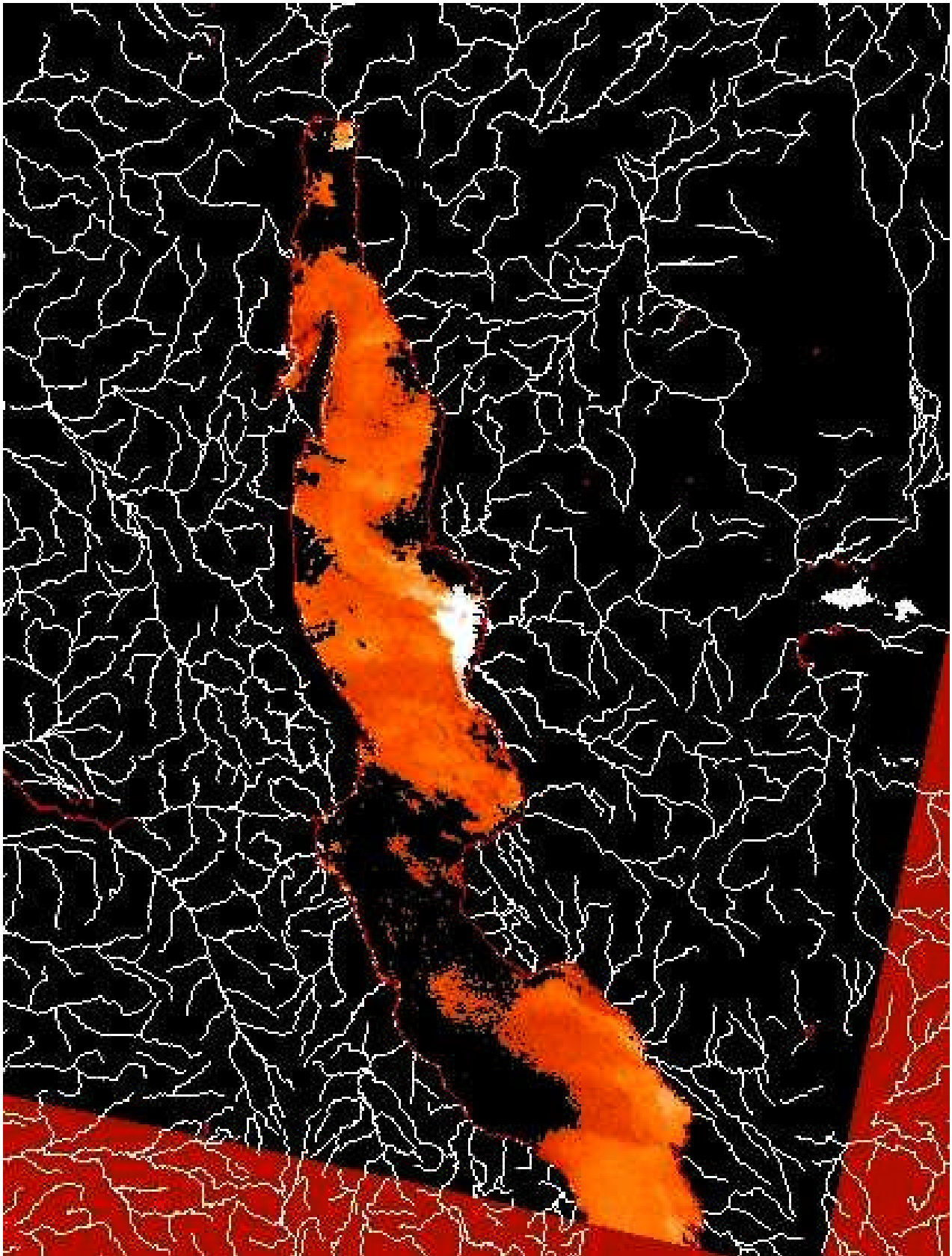


Figure 32. 27th April, 1998.

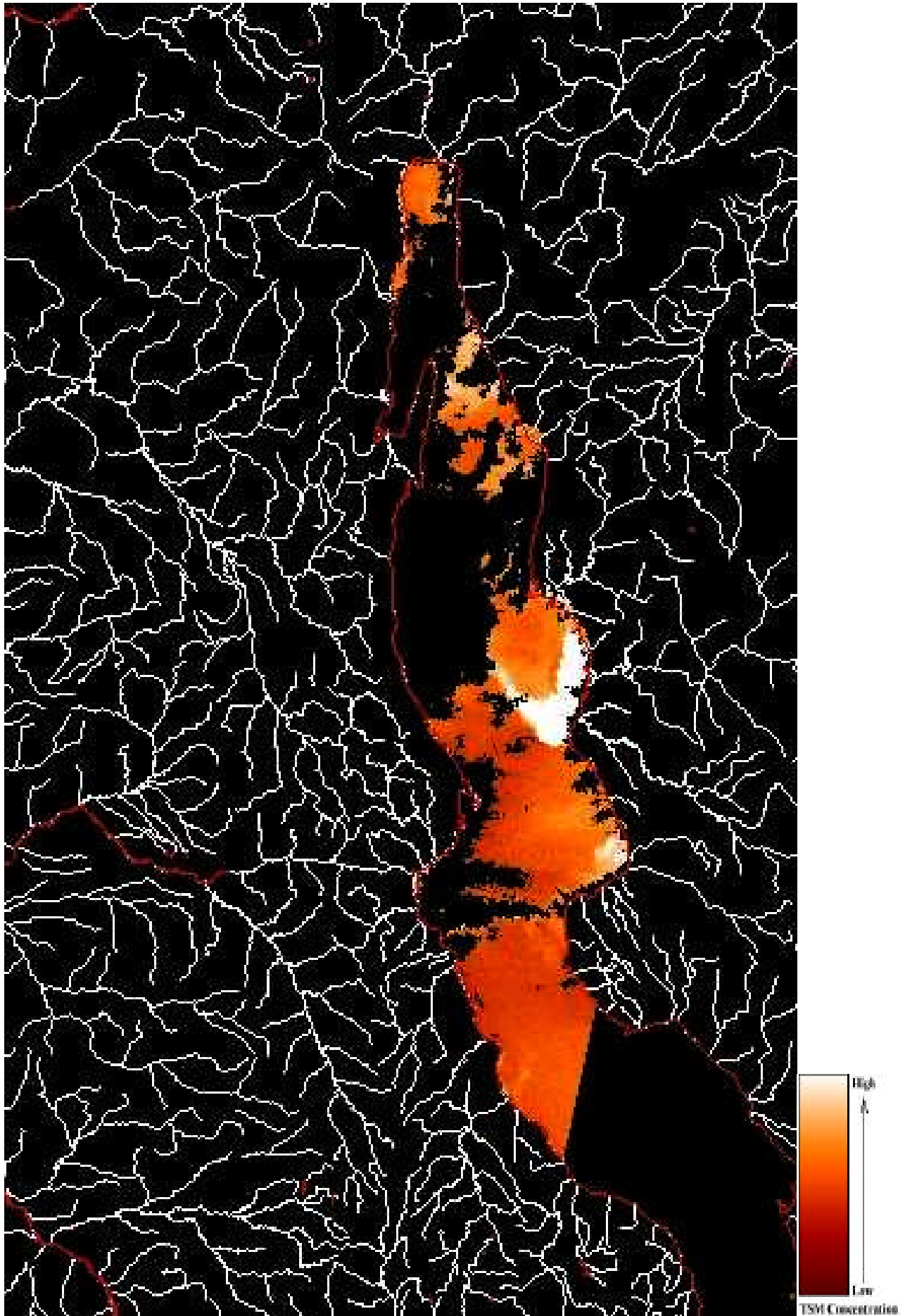
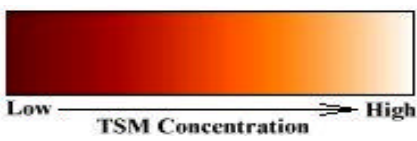
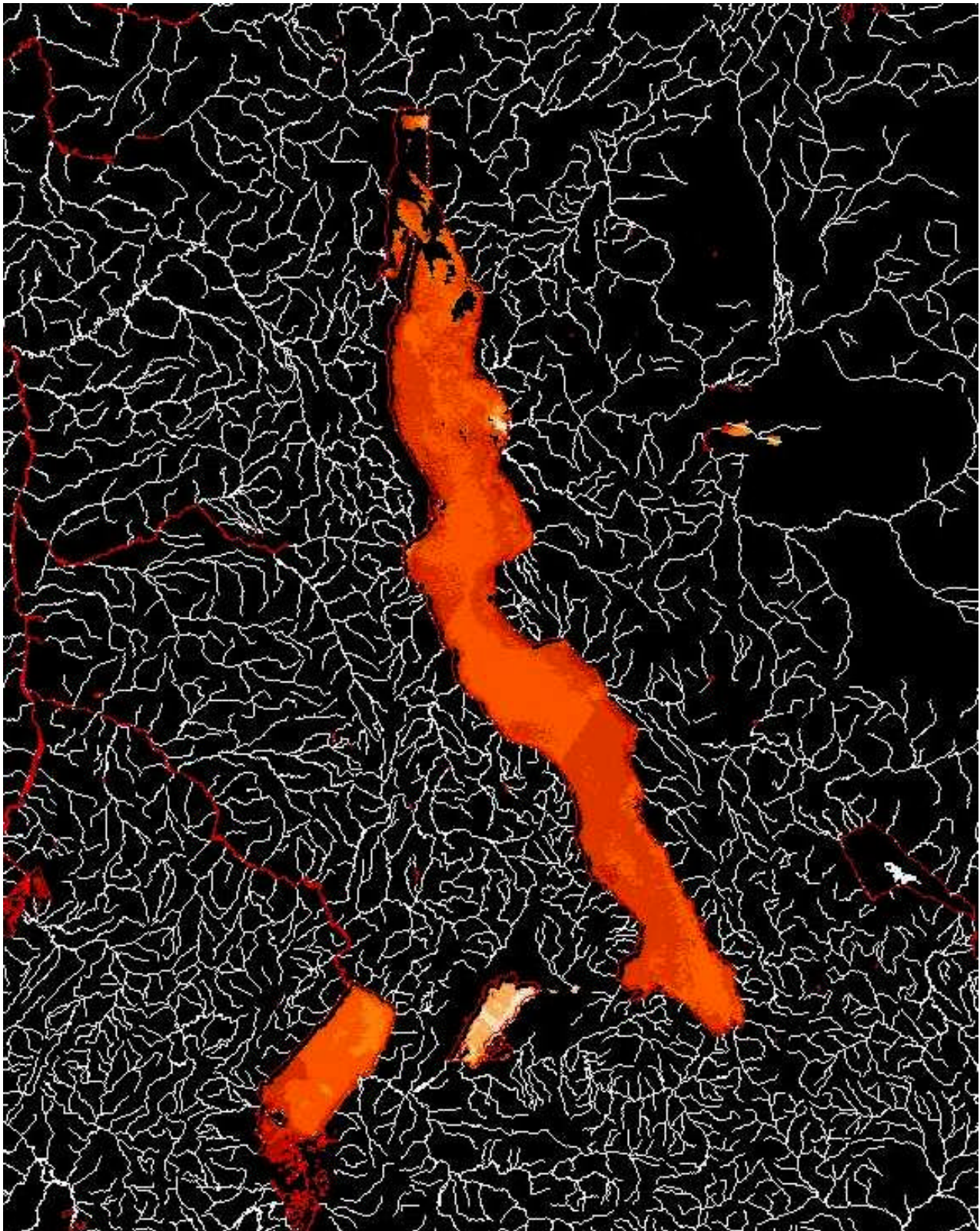


Figure 33. 18th May, 1998. AVHRR (NOAA-14)



## River/Lake interaction

### Lake density analysis

The Secondary data taken from the LTBP Pollution Special Study, and Sedimentation Special Study teams included temperature and conductivity and was consequently used to calculate the lake and river density (Chen, T.C. & F.J.. Millero, 1977). The data begins in August 1998, and continues with up to 4 recordings per month until July 1999. Figure 34, shows seasonal average lake temperatures (taken from LTBP Sediment and Pollution teams) plotted with seasonal minimum and maximum temperatures as reported by Hutchinson (1975), this external data source was used to more confidently characterise the extreme maximum and minimum temperature of the lake. The dry season was taken as extending from May to October and the wet season from November to April. Figure 35, shows the fluctuation in conductivity for the Burundian rivers over the temporal monitoring period, data is not continuous and the recording varies from one sample up to four samples per month per sample location therefore data points are plotted, not lines. Figure 36, shows the conductivity for the Malagarasi as it covers a different temporal period. The two figures also include average lake conductivity for the wet and dry season (the solid lines) which was calculated from the lake data. Average lake and river conductivity can be seen in Figure 37, except here there are no seasonal means for conductivity since it has little seasonal variation.

**Figure 34.** Seasonal average temperatures. Data source; Pollution Special Study team.

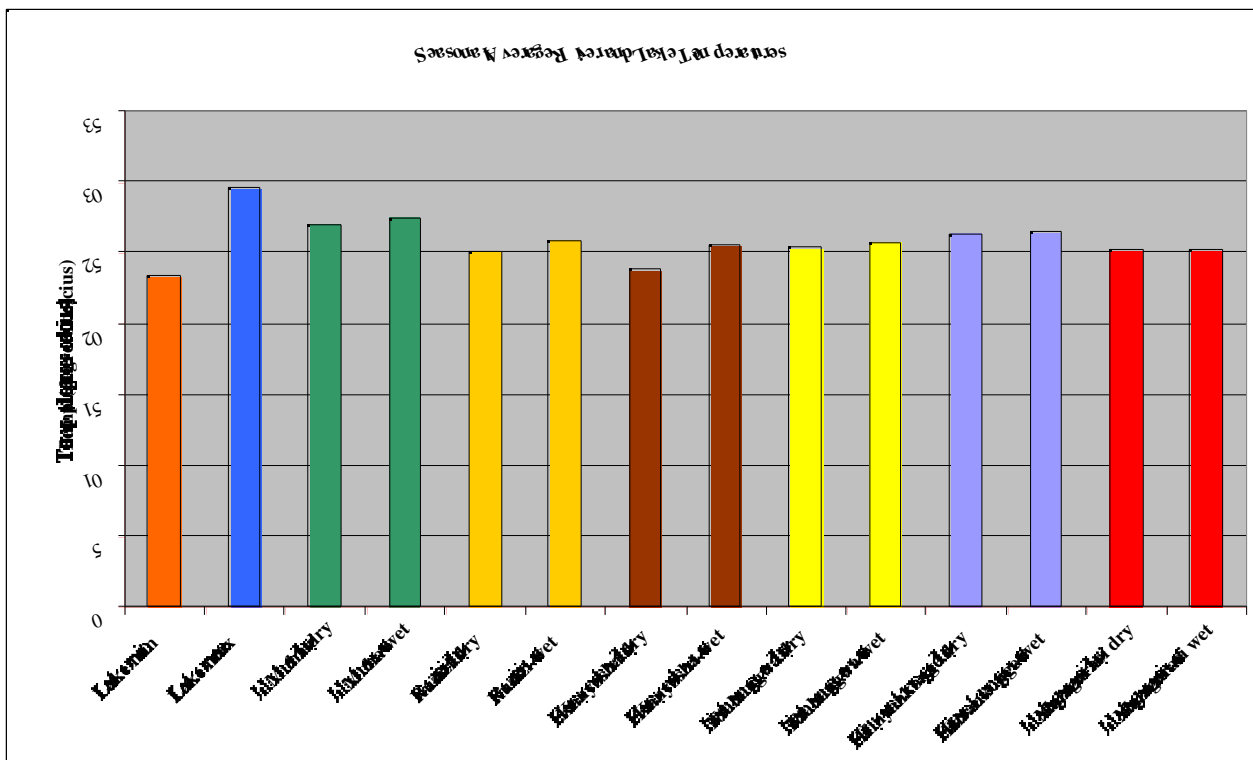


**Figure 35.** Conductivity data plot for all rivers. Data source; Pollution Special Study team.

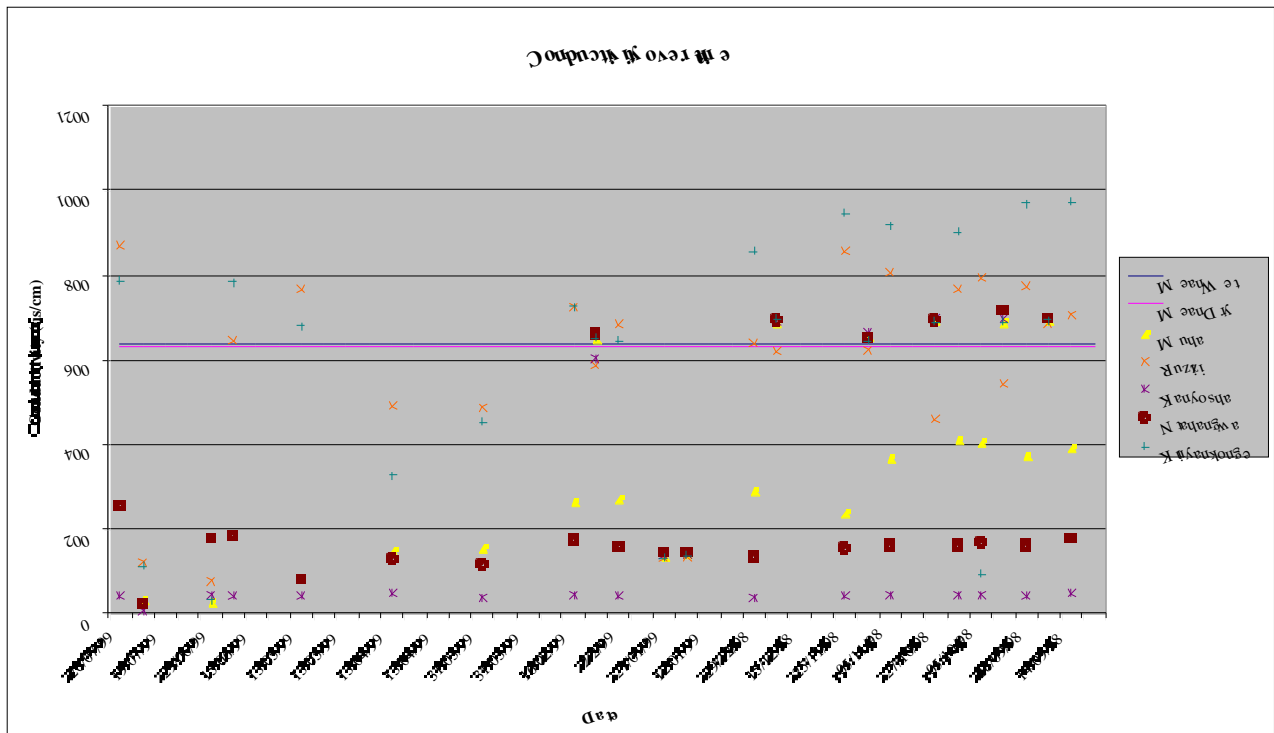


**Figure 36.** Malagarasi conductivity data. Data source; Pollution Special Study team.

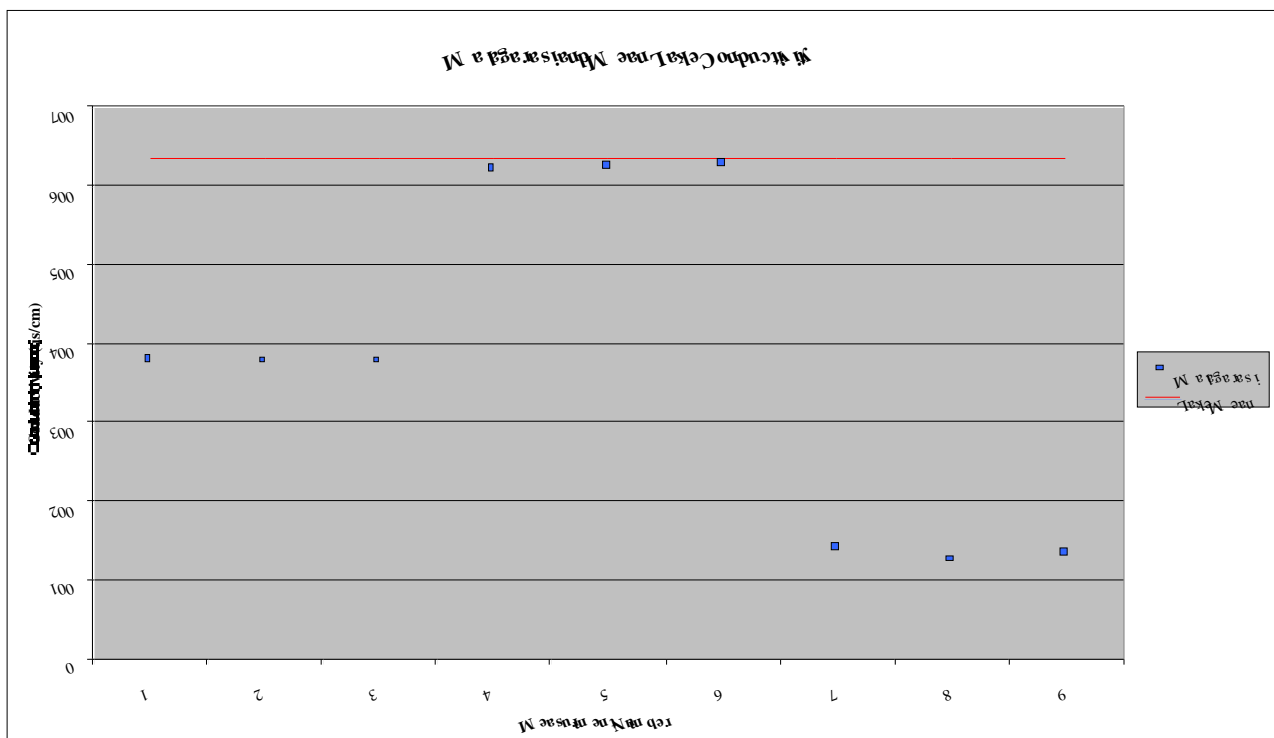
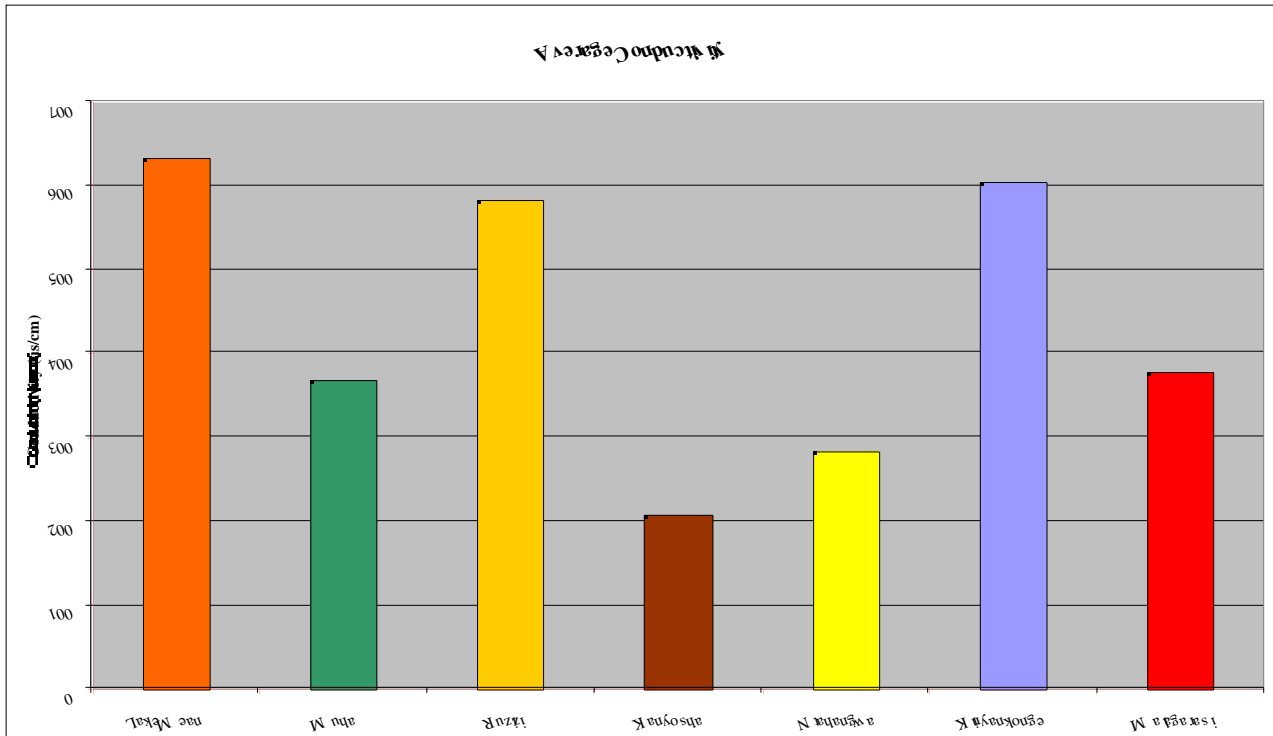


**Figure 37.** Average Conductivity plot. Data from; Pollution Special Study team.



Density is calculated from temperature and conductivity, the equation (Chen and Milliero, 1977) was found to be very sensitive to temperature. Figure 38, shows Burundian river density plotted over time, and Figure 39, shows Malagarasi River data, the two graphs also include the dry and wet season extreme densities calculated using the maximum (wet season) and minimum (dry season) temperatures reported by Hutchinson (1975). The sensitivity of temperature in the density equation was another reason why Hutchinson's data were taken, we therefore have an upper and lower boundary for the lake density. Again because the monitoring is not continuous and there aren't always the same amount of data points per month the data is plotted as points with no adjoining lines. Figure 40, shows average density for the rivers and lake.

**Figure 38.** Density data plot for the lake and rivers. Calculated from Pollution Special Study data.

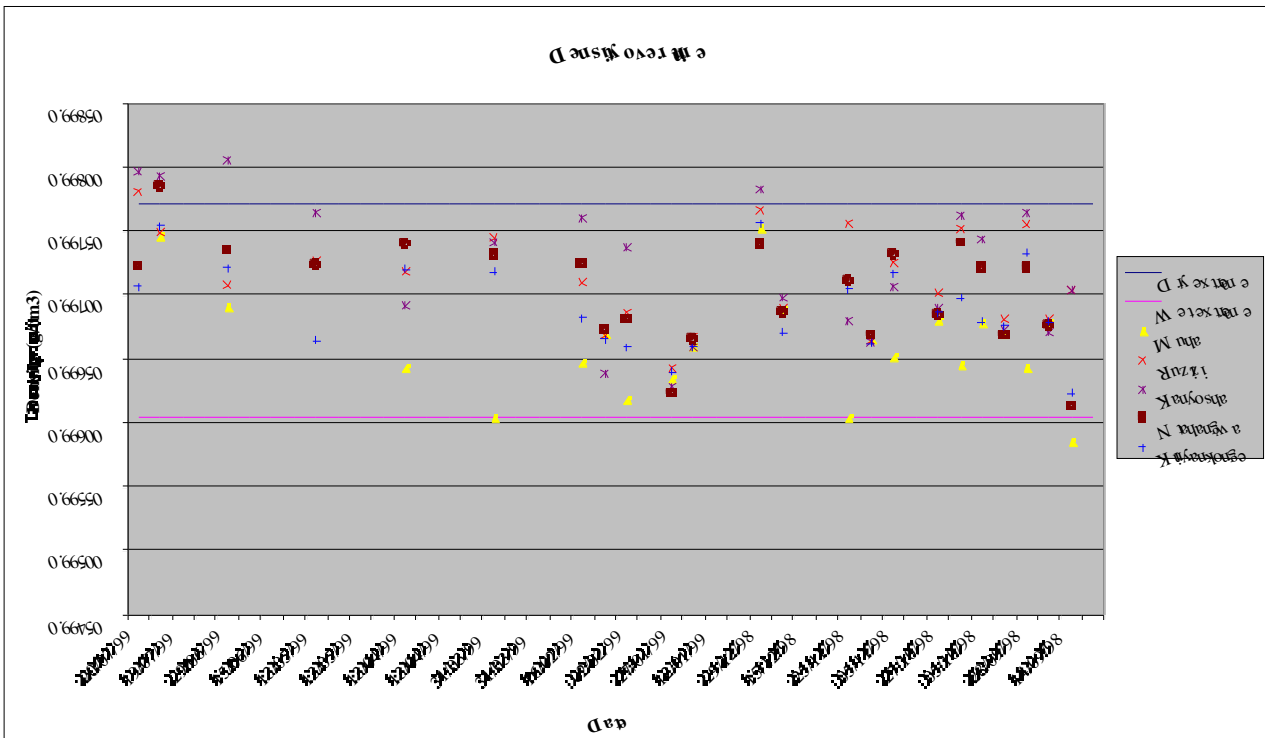


**Figure 39.** Malagarasi River density data, calculated from Pollution Special Study data.

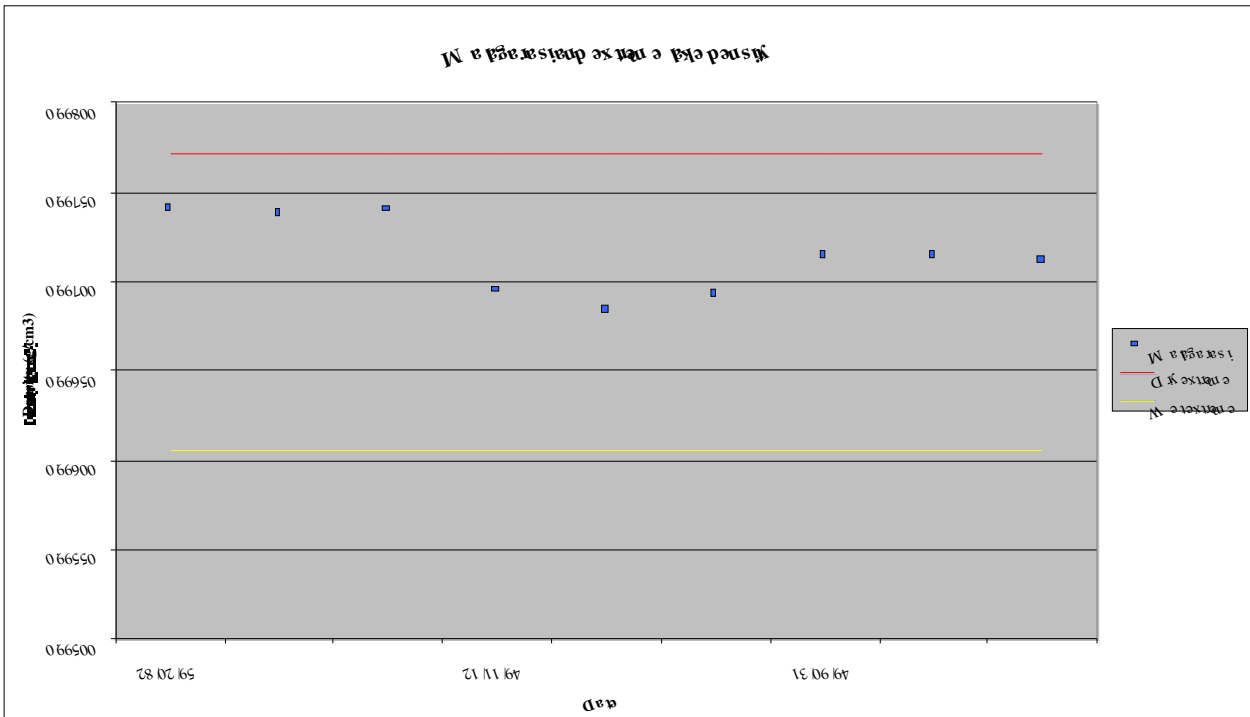
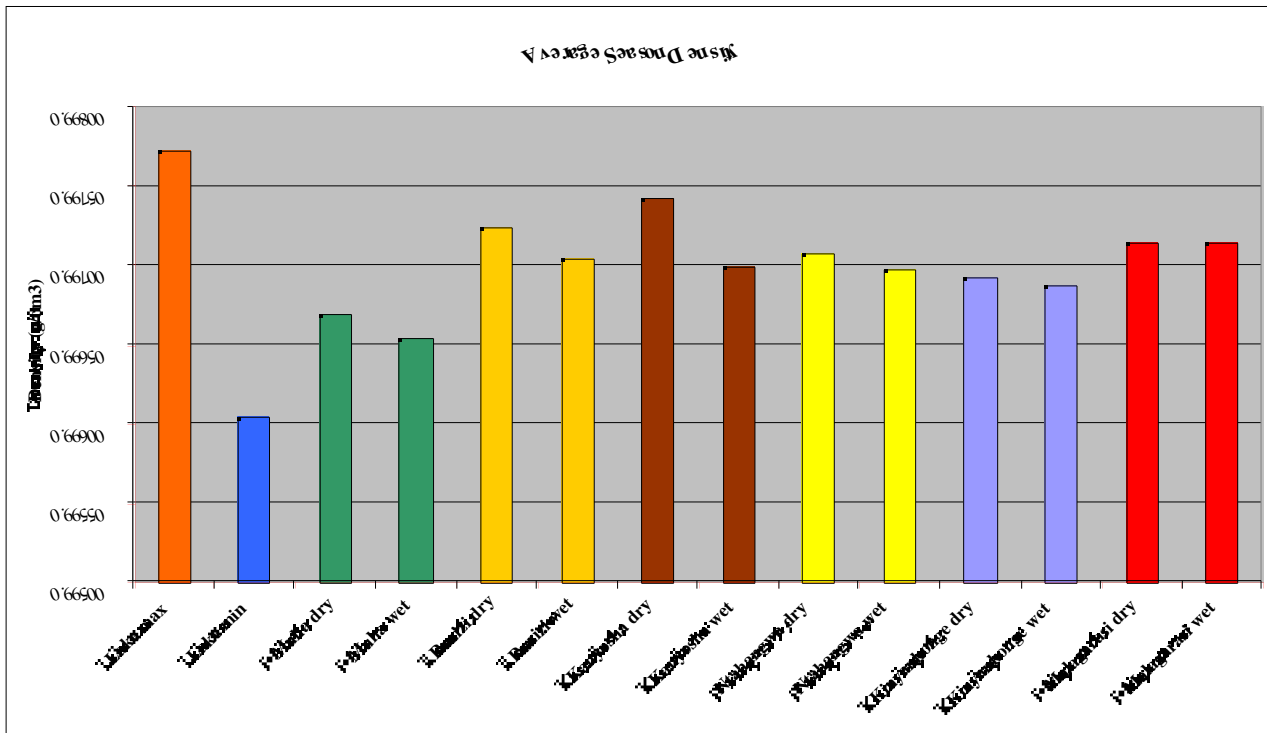


**Figure 40.** Average lake and river density, calculated from Pollution Special Study data.

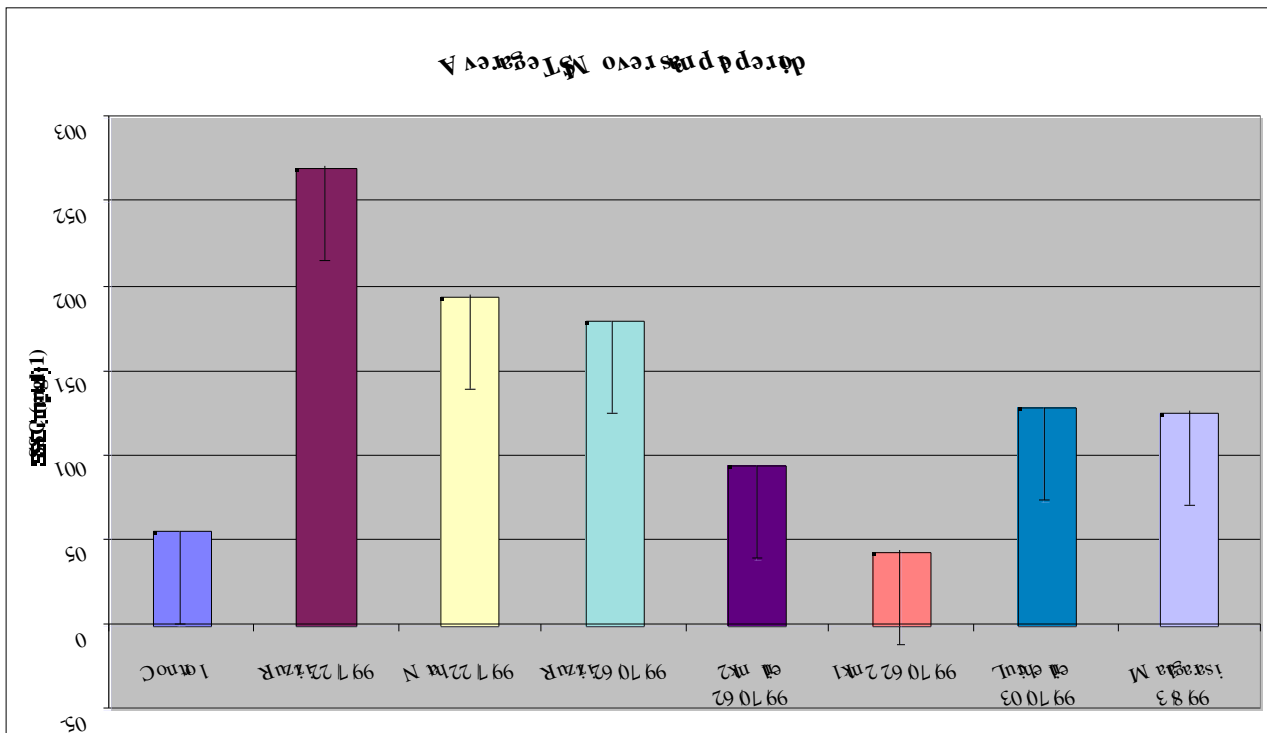


### ***Lake/River TSM analysis***

Figure 41, shows sample TSM data for the fieldwork dates, TSM is plotted as daily averages from each sample site. The data includes a control column which was derived by filtering distilled water samples which should in theory contain no suspended matter. This method was employed to test the accuracy of the lab equipment and technique, the result after weighing ten filter papers was an average TSM of 55.04mg<sup>-1</sup>, with a minimum of 44.1, a maximum of 61.2, and a standard deviation of 5.3. This average error is used to provide the error bars on each of the other columns thus indicating the possible amount of error in the TSM results.

Analysis of Figure 41 indicates that the Ruzizi was transporting the most sediment during the monitoring period, and that the Ntshangwa is also a significant contributor during the temporal period. The Malagarasi and Luiche Rivers have average TSM lower than those of the two previously mentioned rivers but have significantly more TSM than that of the lake itself.

**Figure 41.** Average TSM concentration for each sample point during each temporal monitoring period.



The Luiche and Malagarasi rivers were sampled using a line transect technique in order to try and illustrate the change in TSM from high concentration (upriver) through to a lower concentration as samples are taken further away from the river mouth into the lake. Figures 42, and 43, show TSM starting upriver and continuing into the lake, at each sampling point one TSM sample was taken. Also at each data point radiometer measurements (apart from the points noted in the methodology) were taken in order to characterise the decrease in reflectance as TSM decreases along the transect, results for each of the three bands indicate a general lowering of reflectance in all three bands over the transect, with all three bands behaving consistently with theory; that is green reflecting more highly than the red band due to decreased water absorption, and the NIR band typically absorbing, in most cases over 90% of incoming radiation.

Figure 42. Luiche River line sample of TSM.

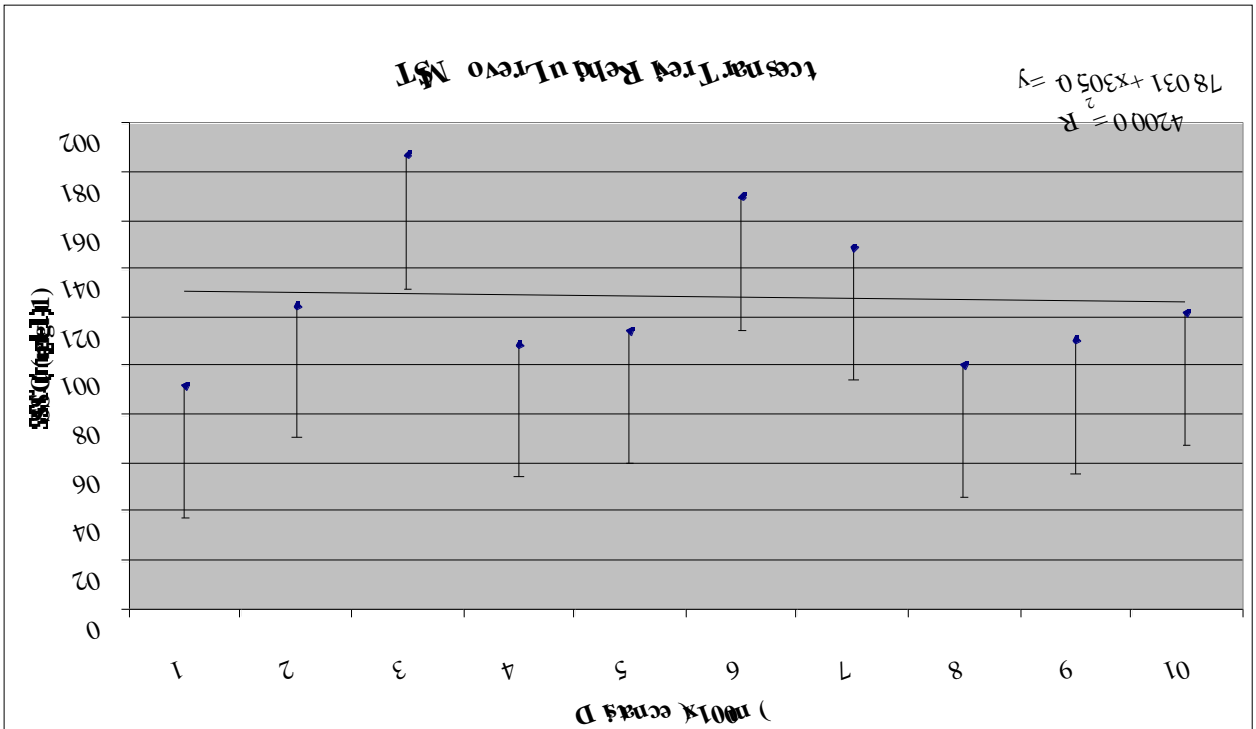
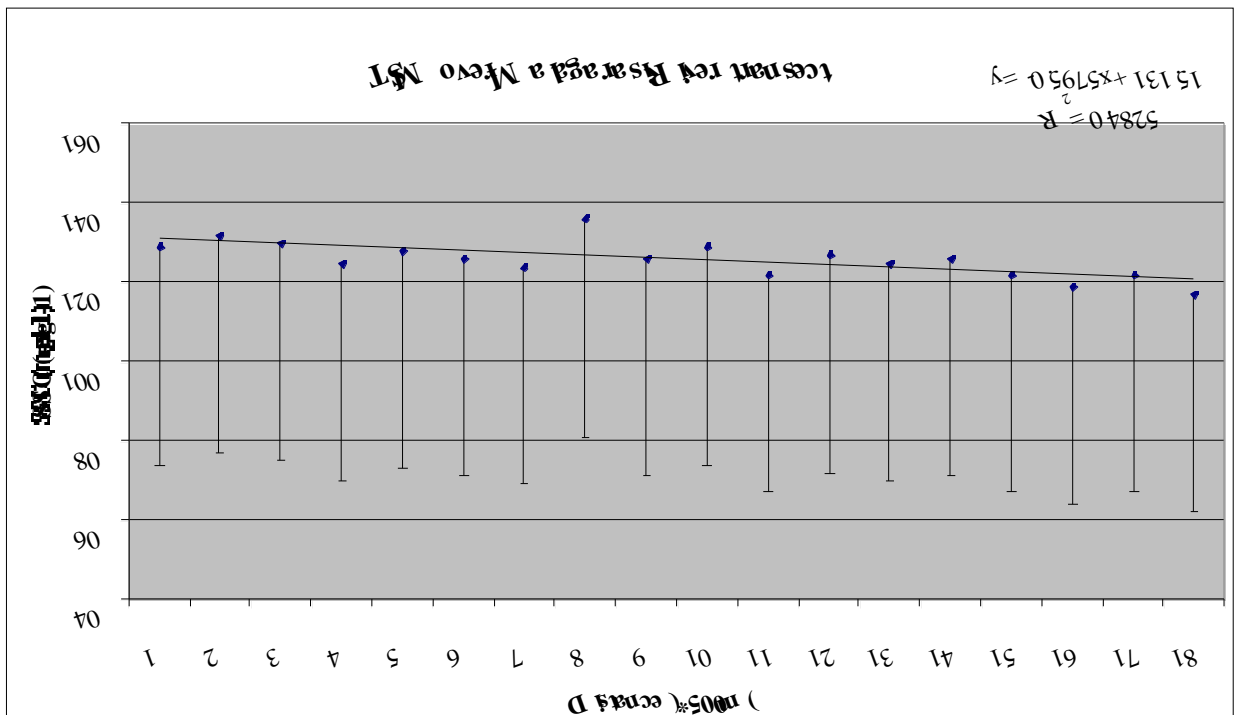
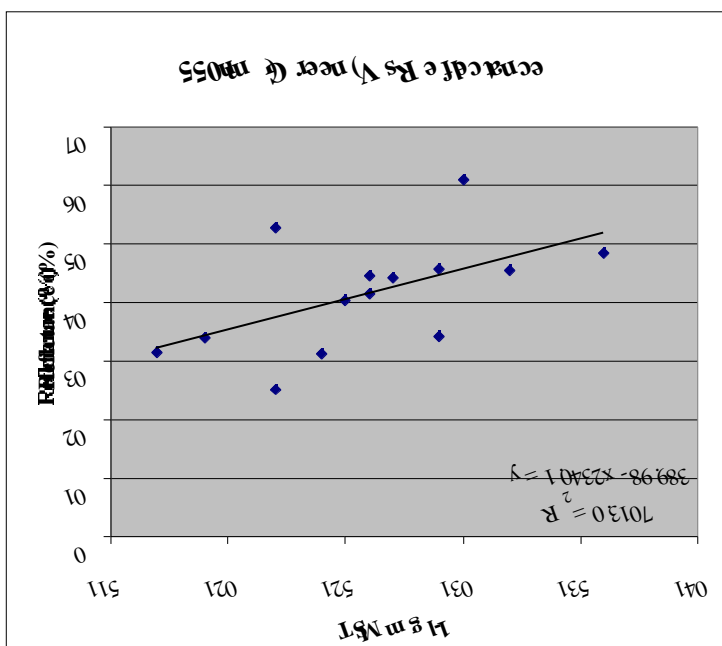


Figure 43. Malagarasi River line sample of TSM.



What is interesting is the next three scatterplots (Figures 44, 45, & 46) with regression lines that all indicate statistically significant positive "relationships" between reflectance and TSM at the 95% confidence level ( $R^2$  values of 0.31 [0.55 if the two reflectance's over 50% are removed] at the green band, 0.52 at the red band, and 0.66 at the NIR band), and that results are similar to those of Harrington et al. (1992). It should be noted that conditions for collecting radiometer data were far from ideal with significant influence from sun-glint and surface waves, much better  $R^2$  values can be obtained through laboratory analysis, but unfortunately the limited time period of the study did not allow for this.

**Figure 44.** Green Band reflectance and TSM concentration.



**Figure 45.** Red Band reflectance and TSM concentration.

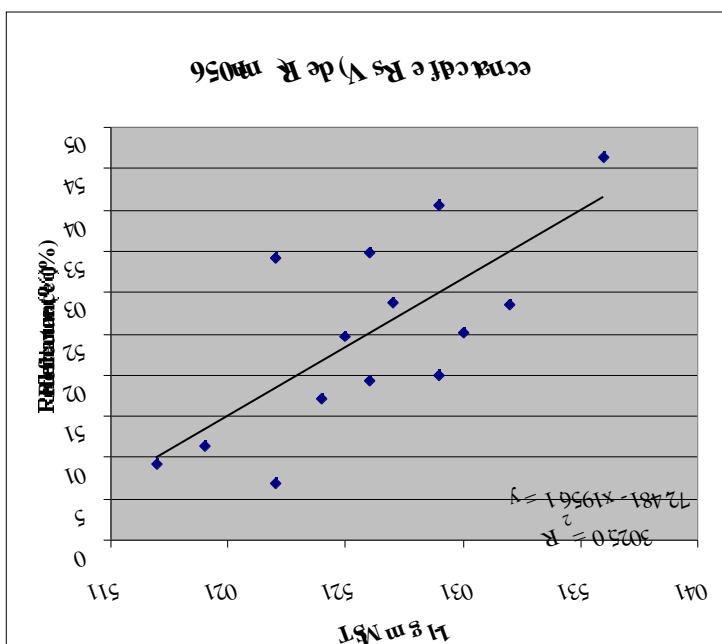
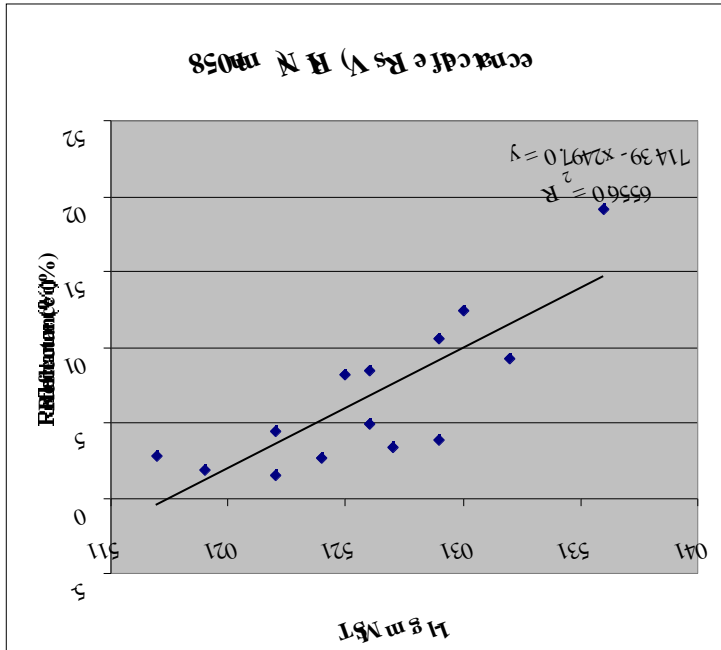


**Figure 46.** NIR Band reflectance and TSM concentration.



Secondary data taken of TSM and discharge from the Sedimentation Special Study was also analysed for the Ruzizi and Ntampangwa rivers, results are shown in Figures 47, and 48, sampling commences November 1998, and runs until June 1999. For each date there is one TSM sample.

Figures 47, and 48, represent the total of the secondary SSC and discharge data for the Ntampangwa and Ruzizi Rivers and indicate maximum SSC levels in excess of 2000mg<sup>l</sup><sup>-1</sup> during the wet season, which is clearly a huge figure indicating massive soil erosion. There also appears to be a positive correlation between TSM level and discharge in the two graphs which is most likely brought about by higher levels of erosion (and hence TSM concentrations) during times of high discharge (which is ultimately caused by increases in rainfall). Correlation results show r values of 0.72 and 0.4 for the Ntampangwa and Ruzizi Rivers respectively, with only the Ntampangwa r value being significant at the 95% confidence limit. This is clearly not a large enough data set to ascertain confident relationships between TSM and discharge, neither is it enough to define a causal relationship, but it would seem logical that an increase in discharge is the causal factor responsible for an increase in TSM.

**Figure 47.** Ntshangwa River SSC and discharge. Data from; Sedimentation Special Study team.

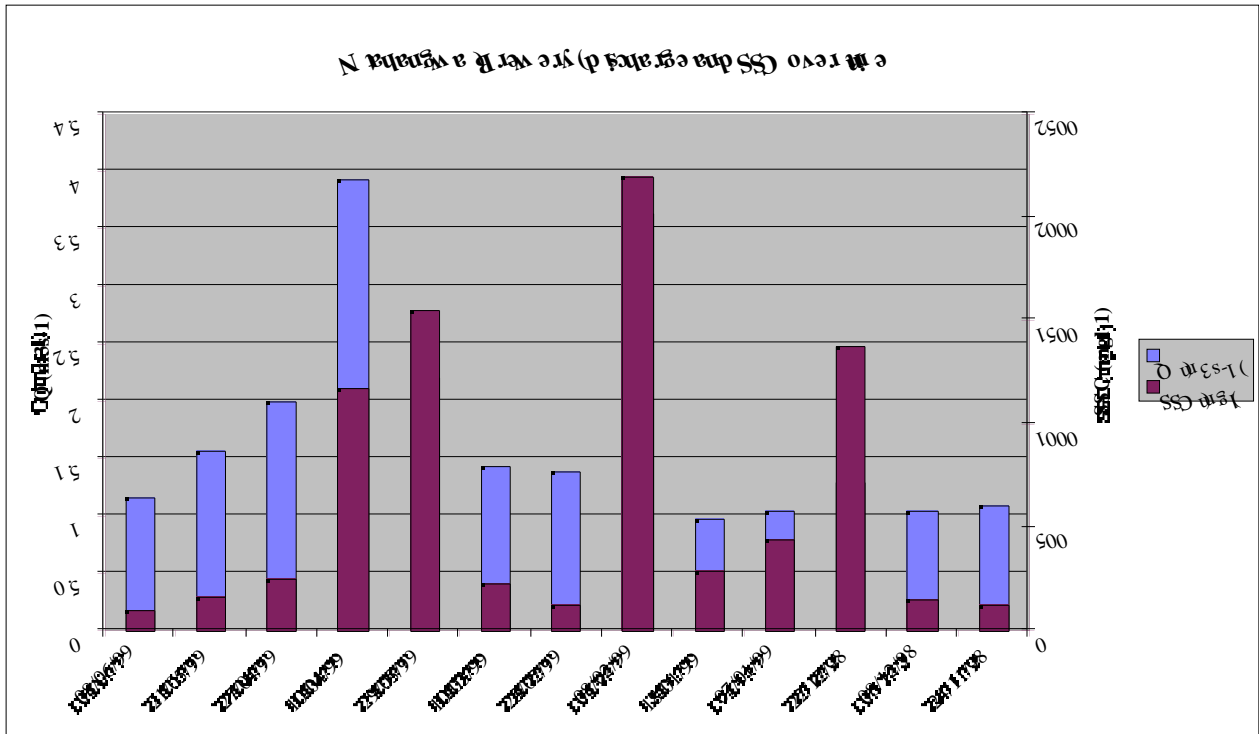
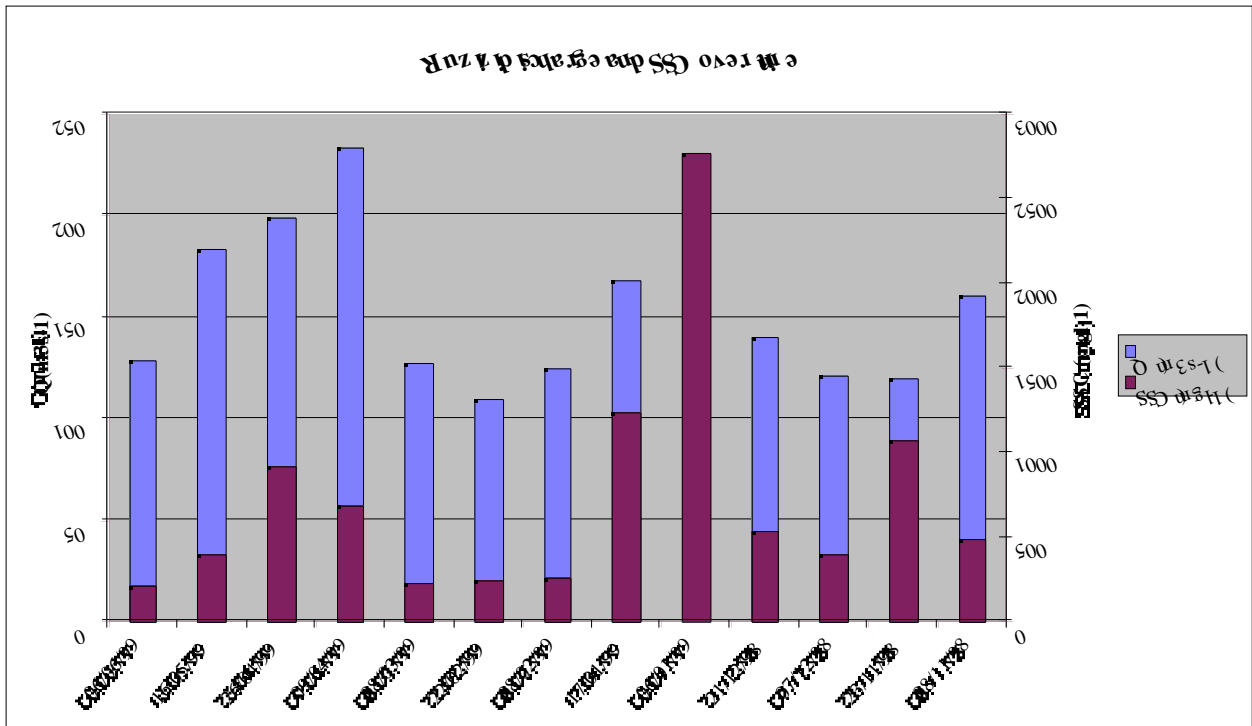


**Figure 48.** Ruzizi River SSC and discharge. Data from; Sedimentation Special Study team.



# Discussion

## ***The fundamental relationship between TSM and reflectance***

Figures 44, 45, & 46 indicate statistically significant relationships (at 95% confidence limit) between TSM and reflectance in all three bands, the likely causal relationship is that the decrease in TSM is reducing reflectance. If this is correct then it is likely that the increases in reflectance detected from our satellite imagery indicate the same relationship and are therefore detecting sediment plumes. It is also probable that other parameters discussed in the literature review effect reflectance from the water surface, but where large increases in reflectance are located next to known river mouths it is likely that we are witnessing variance due to TSM fluctuations and are therefore observing a sediment plume.

Unfortunately radiometer data collection was limited due to mechanical failure and insufficient field collection time, and no simultaneous ground and satellite data were able to be obtained for comparison. Therefore it was not possible to investigate the relationship between ground reflectance and satellite reflectance so as to build upon a more quantitative result, but let it be said that this task is a large one and would require considerable time and resources.

## ***Satellite Imagery Interpretation - The patterns of observed plumes***

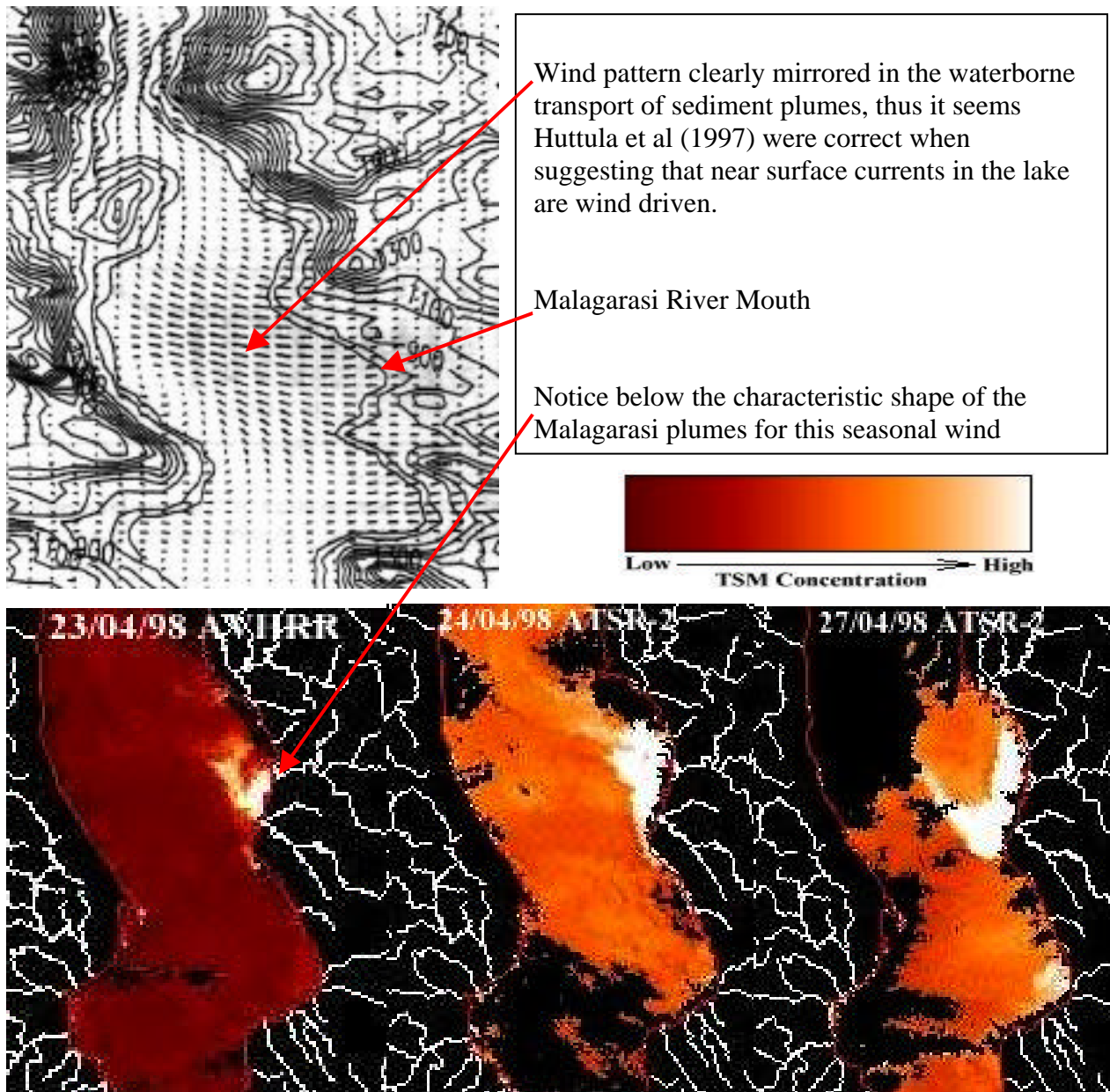
The image processing procedures applied to the satellite data have been successful in isolating water bodies, masking cloud, reducing the atmospheric effect, and highlighting the differences in reflectance and therefore the likely qualitative level of TSM in near-surface waters.

The following paragraphs will seek to identify and describe the spatial patterns of the detected near-surface sediment plumes.

Patterns that are displayed by the plumes of the Malagarasi River match closely the wind driven lake currents as modelled by Huttula et al. (1997) for March, model output can be seen below in Figure 49, which also includes Malagarasi plumes for 3 images dated 23rd, 24th, 27th April, 1998. It should be noted that due to the localised southerly current (Huttula et al., 1997) the river directly to the south of the Malagarasi (the Lugufu) may appear to be providing more sediment than it actually is. It seems likely that the southerly current usually moves Malagarasi plumes towards the outcrop (or point) from where there is no more wind shelter and the usual southerly winds dominate

the currents, therefore providing a plume that appears to be from the Lugufu (a much smaller river), but is mainly controlled by the Malagarasi.

**Figure 49.** Calculated near-surface wind over lake Tanganyika region (for 04/03/97). Isolines show orography in metres above sea-level. And satellite imagery from 23rd, 24th, & 27th April, 1998.

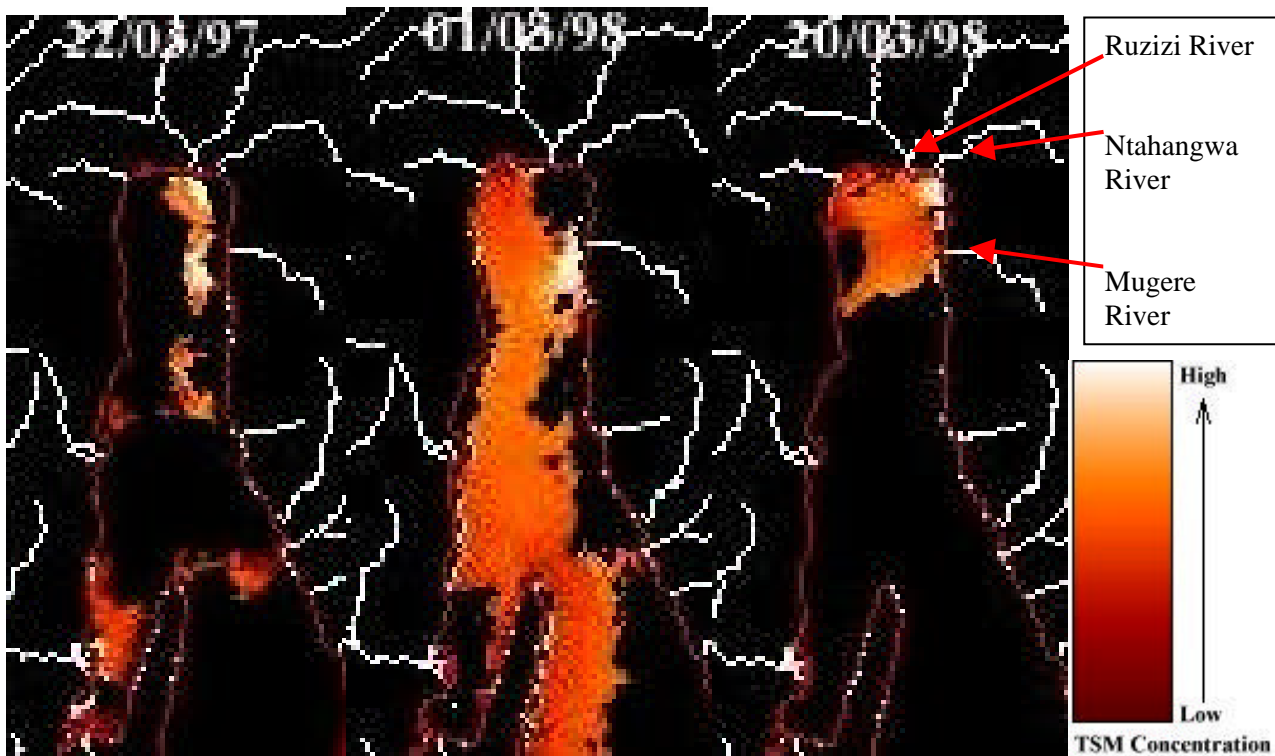


Other plumes in Lake Tanganyika are much less abundant than those of the Malagarasi, the image of 22nd January, 1998 (Figure 23) highlights a large plume from the Malagarasi which is carried almost completely across the lake to the Congolese side, it also matches the wind pattern discussed above. However there are a number of other plumes entering the lake on the Tanzanian (eastern)

side of the lake but these are not as large or extensive as the Malagarasi plume which appears to consistently cover tens, and even hundreds of kilometres.

The Northern end of the lake is captured in all but four of the twelve images and does on some dates indicate plumes emanating from the Ruzizi, Ntahangwa and Mugere rivers, see Figure 50, below.

**Figure 50.** Images of 22nd March, 1997; 1st March, 1998; and 20th March 1998.

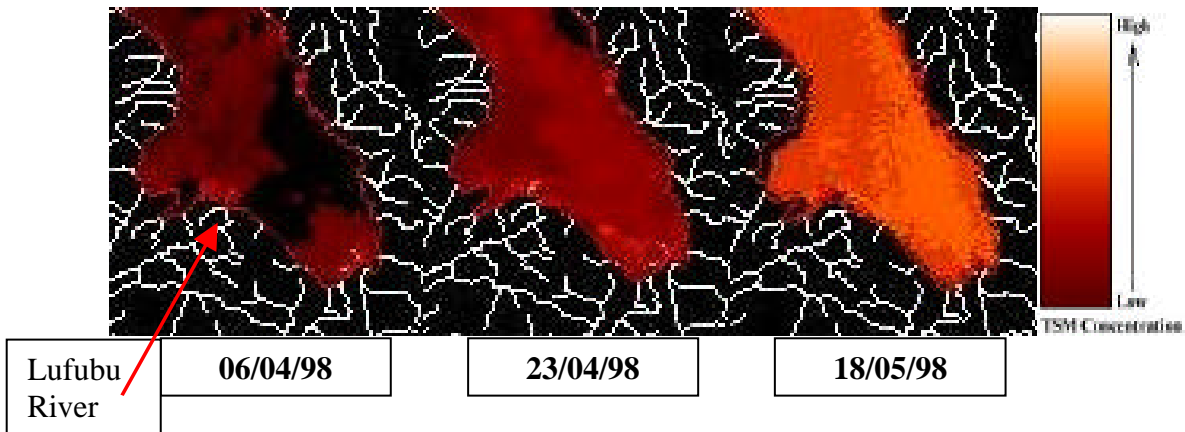


Plumes appear from the Ruzizi mouth on only two occasions over the monitoring period (22/03/97 & 4/03/98), whereas variation can be detected from the Mugere and/or Ntahangwa on five dates (22/03/98 [not displayed], 20/03/97 [Figure 27], 01/03/98 [Figure 25], 04/03/98 [Figure 26], 24/04/98 [Figure 31], and possibly 18/05/98 [Figure 33]).

It is interesting to note that the Ruzizi River doesn't have many large visible plumes, while modelling results estimated that the Ruzizi was responsible for a large amount of sediment input into the lake (Drake et al., 1999). The Ruzizi is noted by Edmond et al. (1993) along with the Malagarasi and Lufubu, as collectively providing 58% of the total inflow for the lake. It is also of consequence that the Malagarasi River is quoted by Tiercelin & Mondegeur (1991) as largely trapping sediment in its delta system as well as depositing heavily in upstream swamplands, clearly identifying many large plumes from this river is therefore somewhat interesting. Tiercelin & Mondegeur's statement is based on their study's sediment core analysis that indicated the central

basin to have a maximum sedimentation rate of  $<500\text{mm } 1000\text{y}^{-1}$ , which is very low when compared to that of the north with rates at a maximum of  $\sim 4700\text{mm } 1000\text{y}^{-1}$ , which incidentally is where the Ruzizi River flows into the lake. The Lufubu River at the very southern end of the lake, is only pictured in three of the images (06/04/, 23/04/98, and 18/05/98) and can be seen to provide little or no visible sediment plumes. Sedimentation rates for the south are indicated as having a maximum rate of  $<1500\text{mm } 1000\text{y}^{-1}$ .

**Figure 51.** Images of the Southern end of lake Tanganyika and the Lufubu River.



This study is concerned with the sediment dynamics of Lake Tanganyika, however the AVHRR data has provided imagery that has dimensions of  $2252.8 \times 2252.8\text{kms}$  and therefore provides whole/partial spectral coverage of Lakes Victoria and Malawi as well as the Indian Ocean coastline. These areas have been identified as having likely near-surface sediment plumes and can be seen in Figures 52 & 53, below. It should be noted that the atmospheric correction will not remain accurate for these areas because of the other areas having different sun and sensor zenith angles.

**Figure 52.** AVHRR image subsets of Lake Victoria and the northern end of Lake Malawi

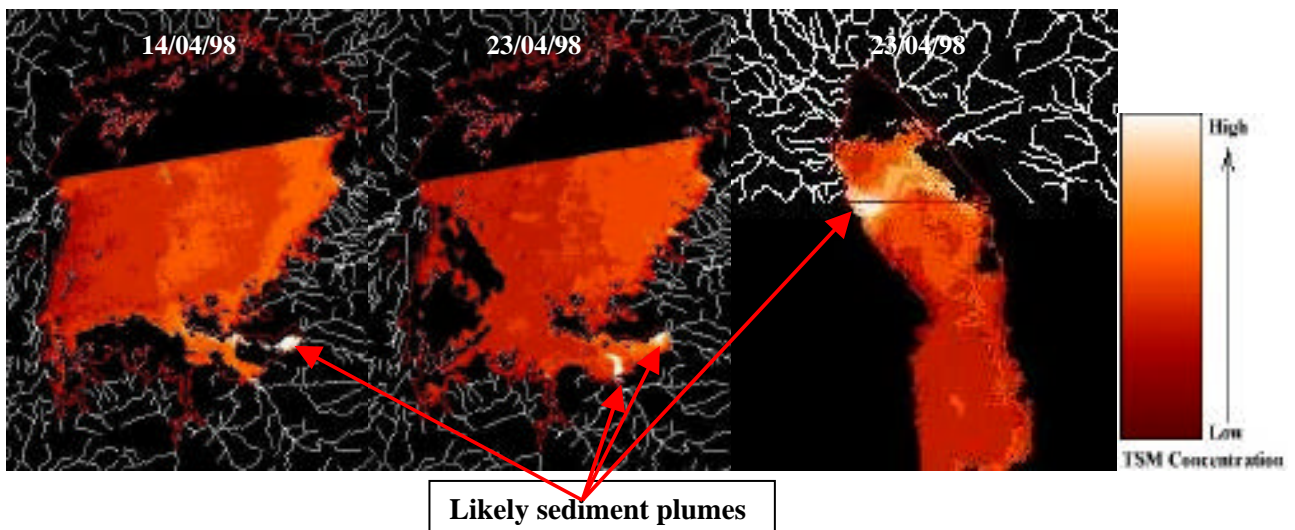
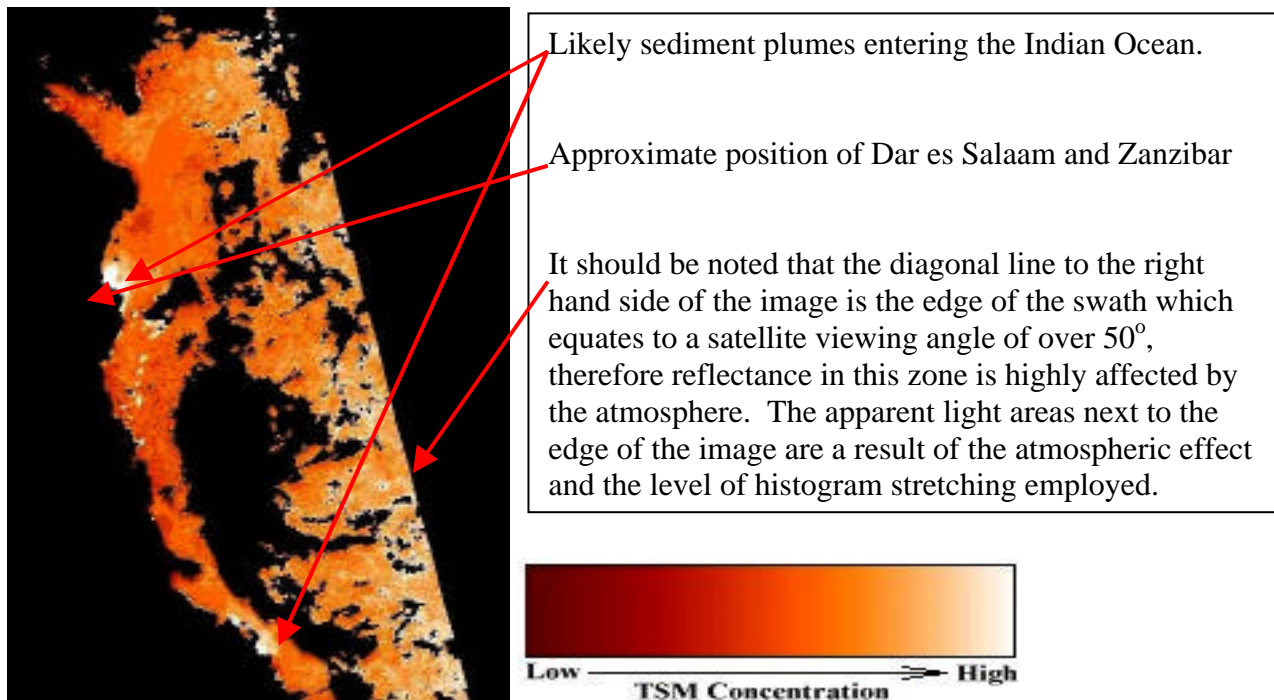


**Figure 53.** AVHRR image of the Tanzanian Indian Ocean coastline, 06/04/98.



Results such as these highlight the effectiveness and adaptability of the remote sensing analysis technique over both rivers and oceans. It also identifies the presence of suspected near-surface sediment plumes in two other major Rift Valley lakes, as well as the Indian Ocean. The Malawi plume appears to be very large, and the Lake Victoria plumes are visible in two of the three images analysed thus also suggesting the possibility that these areas are experiencing significant sediment input and hence the resulting ecological problems.

### ***Plume Analysis***

The main question that arises from the general description of the near-surface sediment plumes is why do we see such patterns? And why does the Ruzizi not provide more visible plumes, while the Malagarasi is producing huge plumes in a basin that is receiving relatively little sedimentation? The answers are to be found largely in the nature of the river water entering the lake and maybe to a certain extent in the general form of the lake floor.

The graphs of conductivity and temperature indicate that the Ruzizi and Kinyankonge rivers have the highest conductivity on average with the Malagarasi constituting over a third less. These conductivity's are all lower than the average lake conductivity, which unlike temperature varies only slightly between the wet and dry season. However if river conductivity over time is considered (Figure 35) we can see that there are a number of sample days where the Ruzizi, Kinyankonge, and Ntahangwa are significantly higher than the lake conductivity. If we also

consider lake temperature which can vary by as much as much as 6°C between the wet and dry season, and also that river temperatures too are very variable then the likely effect on sediment plume dynamics is complex. However, to consistently find a particular river (such as the Ruzizi) that has no near-surface plumes, even when we are confident that it must be transporting a great deal of sediment, would suggest that for the majority of the time the river water is more dense. Conversely when we observe a river which consistently deposits large sediment plumes (such as the Malagarasi), this would suggest that for the most part the river water is less dense than the lake water.

The density graphs (Figures 38, 39, & 40) mainly agree. Density plotted over time (Figures 38, & 39) indicate that under extreme conditions the majority of river input would sink during the wet season and float during the dry season, which is largely what we have observed from our wet season imagery. However it should be noted that the analysis did not extend into the dry season. It remains clear from the density data for the Malagarasi (Figure 39) that this river may also sink in the wet season and float in the dry, but the satellite data has clearly identified many large plumes. Clearly then the Malagarasi river water must be less dense than the lake water on a number of occasions in the wet season, and it is most likely the presence of an inadequate number of samples that is at fault here. For the Malagarasi there are only nine sets of temperature and conductivity measurements over three days sampling which is not enough to confidently characterise the temperature and salinity behaviour. The fact that the density equation has not been parameterised for the lake also has a bearing on the results.

Figures 54, 55, & 56 below include photo's taken of the Ruzizi River on 22nd July, 1999 on which date the Ruzizi was carrying a suspended sediment load in excess of 200mg l<sup>-1</sup> the sediment plume can clearly be seen to sink almost vertically down into the water column once it reaches the end of the submerged delta platform.

**Figure 54.** Southerly view out from the mouth of the Grande Ruzizi River, 22nd July, 1999.



**Figures 55, & 56** Close-up view of the sinking sediment plume, 22nd July, 1999.

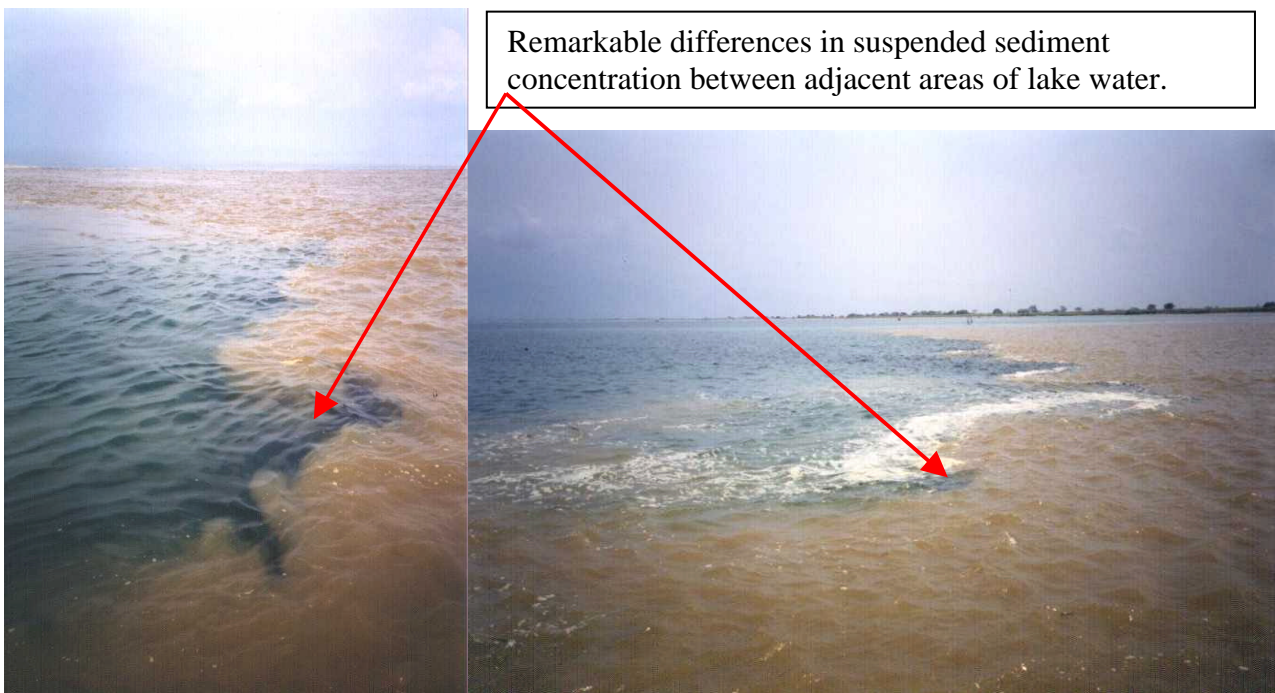


Figure 57, Shows the less turbid ( $125\text{mg l}^{-1}$  average) Malagarasi River on 3rd August, 1999 (looking south west outwards from the river mouth into the lake). The Malagarasi has a much less noticeable drop-off in TSM level than the Ntahangwa, in-fact on this particular day waters remained visibly turbid for many kilometres away from the mouth. This may also have something to do with the relatively shallow Malagarasi platform that exists up to 15km from the mouth of the river westwards, and 40km in the north south direction (Hecky & Degens, 1973).

**Figure 57.** Malagarasi River mouth (lakeward view), 3rd August, 1999.



The analysis of the Ruzizi data (although density data is somewhat inconclusive) for the most part agrees with the likelihood of the Ruzizi providing interflow or underflow, but either way providing sediment plumes that are significantly deep enough not to be identified by the satellite sensors. However there is still the disparity between Tiercelin & Mondegeur's study (1991) in which they suggested the reason for the  $^{14}\text{C}$  dating results being lower in the middle basin was that the sediment from the Malagarasi is largely trapped in its delta system, and other swamp systems upriver. Figure 8 shows data from Tiercelin & Mondegeur's study, sedimentation rates for the middle basin are represented by cores 15, 19, and 36 and can be seen to vary greatly from those of the North and South. However results from this current study would suggest that the Malagarasi does deposit significant amounts of suspended sediment into the lake, and these plumes are seen to remain at the near-surface for large distances before dispersing, so it is possible that the reason for there not being so much sedimentation in the middle basin is that the Malagarasi sediment is being transported up towards the north (under prevailing wind driven near-surface currents) and deposited/dispersed over a much wider area therefore creating less observable deposition in the middle basin.

### ***AVHRR and ATSR-2 Comparison***

AVHRR and ATSR-2 are very different sensors that have both been shown to be effective in identifying near-surface sediment plumes in large water bodies. ATSR-2 is a relatively new sensor that provides 512km wide, 1km resolution images with a return period of roughly three days and features an on-board automated visible band calibration system, and can provide water surface

temperatures to within 0.1k. It also takes two views of each ground surface pixel at nadir and at a forward view angle which allows very accurate, but complex atmospheric correction.

AVHRR however has a swath width of over 2000km with satellite zenith angles at the edges of the swath in excess of 50° off-nadir, the general relationship is that the further off-nadir measurements are taken the larger the path length of the radiation becomes through the atmosphere and therefore the greater the distortion of the pixel size and reflectance. The ATSR-2 scanner has a swath width of 512km and as a result does not experience such extreme problems with large satellite zenith angles as AVHRR, but this does however mean that it cannot provide daily coverage. Unfortunately for ATSR-2 the time of year that most sediment is input into the lake is obviously during the wet season which paradoxically is when the most cloud is present, and therefore when high temporal resolution monitoring is of utmost importance.

Although relatively few AVHRR images have been processed due to ATSR-2 providing the largest source of data for the study area and therefore receiving most attention in the analysis, it would seem that AVHRR provides the most efficient and effective results. One AVHRR image can provide a majority coverage of Lakes Victoria, Tanganyika, and Malawi (an ATSR-2 scene doesn't cover the entirety of Lake Tanganyika), not to mention the smaller lakes such as Kivu and Rukwa, and it can provide this at a daily temporal resolution, although some images are unusable due to the large off-nadir satellite view angles.

ATSR-2 has seven spectral bands ranging from green through to the thermal region whereas AVHRR has only five, this however did not prove to be a great hindrance in conducting the analysis for this project.

AVHRR is more widely available and cheaper to obtain than ATSR-2 imagery, it also has automated reflectance and geo-correction functions in most good quality image processing applications. However ATSR-2 has some advanced functions such as the dual view that make accurate atmospheric correction a possibility, but this was clearly beyond the scope of the project, it is also much more accurate at providing water surface temperatures than AVHRR, but again this is something that wasn't utilised in the project, although thermal analysis of plumes would be interesting further analysis. The smaller number of band wavelengths covered by AVHRR (five compared to seven for ATSR-2) did not prove troublesome, as the AVHRR bands are very similar to those of ATSR-2, and most of the published atmospheric and cloud correction procedures are designed for AVHRR. In the end it comes down to which sensor advantages suit the particular

project, in this case AVHRR was preferred, but that in no way reflects the doubtless capabilities of the ATSR-2 sensor.

# Conclusion

Scatter-plots of TSM and radiometer reflectance data yielded statistically significant positive relationships at the 95% confidence level under adverse field conditions, with  $R^2$  values of 0.31 (0.55 if the two reflectance's over 50% are removed) in the green band, 0.52 at the red band, and 0.66 at the NIR band. A similar relationship exists between satellite based remotely sensed data in similar bands, but the relationship was not able to be defined due to the lack of contiguous satellite data. However this relationship highlights the possibility for future quantitative estimation of TSM from remotely sensed imagery.

Large plumes have been successfully monitored over the data period in Lake Tanganyika, as well as suspected plumes in Lakes Victoria and Malawi and also the Indian Ocean. The effect of clouds and atmosphere serve to significantly limit the number of usable satellite images. It seems that the consistent presence of massive Malagarasi River plumes may indicate a greater level of sediment transport in to the lake than previously thought.

The Malagarasi River is quoted by Tiercelin & Mondegeur (1991) as largely trapping sediment in it's delta system as well as depositing heavily in upstream swamplands, a statement which is based on their study's sediment core analysis that indicated the central (Malagarasi) basin to have a maximum sedimentation rate of  $<500\text{mm } 1000\text{y}^{-1}$ , which is very low when compared to that of the northern (Ruzizi) basin with rates at a maximum of  $\sim 4700\text{mm } 1000\text{y}^{-1}$ . The presence of large buoyant wind driven plumes from the Malagarasi may therefore distribute sediment much more widely than rivers in the north such as the Ruzizi (whose plumes show evidence of consistently sinking). Therefore a lower than otherwise expected sedimentation rate taken near to the Malagarasi river mouth may not necessarily indicate that this river is largely trapping it's sediments upstream.

The observed plume patterns have been compared with the calculated buoyancy data for a number of sampled rivers and it has been suggested that a sediment plume will be successfully identified by remote sensing imagery if;

**1:** A river is transporting levels of suspended sediment high enough to significantly increase water leaving radiance.

**2:** A river is providing waters that are buoyant enough to be held in a near surface suspension.

The plume patterns displayed in the imagery have been seen to closely follow the seasonal near-surface winds described by Huttula et al. (1997), that are believed to be responsible for much of the top layer circulation in Lake Tanganyika.

Both AVHRR and ATSR-2 were shown to confidently identify sediment plumes, and although ATSR-2 has more bands and therefore more potential to provide a greater amount of information regarding the reflectance and thermal properties of the plumes, the capabilities of ATSR-2 were not fully utilised. Therefore in this study AVHRR data was found most suitable for the acquisition of cloud free imagery and therefore monitoring due to its increased temporal resolution and also superior spatial coverage compared to that of ATSR-2. It is also easier (and cheaper) to obtain, more widely used and as a result has a larger number of automated functions in image processing packages which further aids analysis.

## Criticisms/Further Work

The sheer spatial proportion and ecological significance of Lake Tanganyika are difficult to fathom, and there is still so much work that needs to be done here, this study certainly confirms that. In order to confidently identify or expand on any of the findings in this project, much more data needs to be collected and analysed than could be achieved during the three week fieldwork period. Field results should have encompassed a greater number of radiometer measurements, more reliable TSM estimation techniques, and the spectral response of the sediment should have been taken. It would also have been of considerable significance to have obtained satellite data for the study period, and to have visited during the wet season. A thermal analysis of the plumes as well as data from other sensor's such as SEAWIFS would also be a useful addition. Never-the-less results seemed to have contributed in some ways to a greater understanding of sediment interaction in the lake, and there can be no doubt as to the potential of this technique.

# Bibliography

**Albanakis, K.S., 1990.** Testing of a model for the simulation of a volume reflectance of water due to suspended sediment under controlled conditions, for various sediment types. *International Journal of Remote Sensing*, Vol.11, No.9, pp1533-1547.

**Beauchamp, R.S.A., 1939.** Hydrology of Lake Tanganyika. *Int. Rev. Gesamten Hydrobiol.* 39: 316-353. In: **Edmond, J.M., Stallard, R.F., Craig, H., Craig, V., Weiss, R.F., and Coulter, G.W., 1993.** Nutrient chemistry of the water column of Lake Tanganyika. *Limnology and Oceanography*, Vol.38, No.4, pp725-738.

**Burgess, C.F., 1985.** *The structural and stratigraphic evolution of Lake Tanganyika: a case study of continental rifting.* Unpublished MSc dissertation, Duke University, USA.

**Caljon, A., 1987.** A recently land locked brackish-water lagoon of Lake Tanganyika: physical and chemical characteristics. *Hydrobiologia*, 153, pp55-70.

**Capart, A., 1949.** Exploration Hydrobiologique du Lac Tanganyika: 1946-1947. *Result Sci.* V. 2. Fasc. 2. In: **Edmond, J.M., Stallard, R.F., Craig, H., Craig, V., Weiss, R.F., and Coulter, G.W., 1993.** Nutrient chemistry of the water column of Lake Tanganyika. *Limnology and Oceanography*, Vol.38, No.4, pp725-738.

**Chen, T.C., & Milliero, F.J., 1977.** The use and misuse of PVT properties for lake waters. *Nature*, Vol. 266, 707-708.

**Chen, Z., Hanson, J.D., and Curran, P.J., 1991.** The form of the relationship between suspended sediment concentration and spectral reflectance: it's implications for the use of Daedalus 1268 data. *International Journal of Remote Sensing*, Vol. 12, No. 1, 215-222.

**Cohen, A.S., Bills, R., Cocquyt, C.Z., Caljon, A.G., 1993.** The Impact of Sediment Pollution on Biodiversity in Lake Tanganyika. *Conservation Biology*, Vol.7, No.3.

**Coulter, G.W., 1963.** Hydrological changes in relation to biological production in southern Lake Tanganyika. *Limnology and Oceanography*, 8, 463-477.

- Curran, P.J., Hansom, J.D., Plummer, S.E., and Pedley, M.I., 1987.** Multispectral remote sensing of nearshore suspended sediments: a pilot study. *International Journal of Remote Sensing*, Vol.8, No.1, pp103-112.
- Drake, N., Wooster, M., Symeonakis, E., & Zhang, X., 1999.** *Lake Tanganyika Biodiversity Project Special Study on Sediment Discharge and its Consequences: Soil Erosion Modelling in the Lake Tanganyika Catchment.* Report for LTBP.
- Edmond, J.M., Stallard, R.F., Craig, H., Craig, V., Weiss, R.F., and Coulter, G.W., 1993.** Nutrient chemistry of the water column of Lake Tanganyika. *Limnology and Oceanography*, Vol.38, No.4, pp725-738.
- Graham, A., 1990.** Siltation of stone surface periphyton in rivers by clay sized particles from low concentrations in suspension. *Hydrobiologia*, 199, 107-115.
- Grobbelaar, J., 1985.** Phytoplankton productivity in turbid waters. *Journal of Plankton Research*, 7, 653-663.
- Harrington Jr, J.A., Schiebe, F.R., and Nix, J.F., 1992.** Remote Sensing of Lake Chicot, Arkansas: Monitoring Suspended Sediments, Turbidity, and Secchi Depth with Landsat MSS Data. *Remote Sensing of the Environment*, Vol.39, pp15-27.
- Hecky, R.E., & Degens, E.T., 1973.** Late Pleistocene-Holocene chemical stratigraphy and paleoclimatology in the Rift Valley Lakes of Central Africa. *Technical Report.* Woods Hole Oceanography Institution.
- Holyer, R.J., 1978.** Towards universal suspended sediment algorithms. *Remote Sensing of the Environment*, Vol.7, pp323-338.
- Hutchinson, G.E., 1975.** A Treatise on Limnology. Vol. 1, Part 1 - *Geography and Physics of Lakes.* Chichester, Wiley.

**Huttlua, T., (Ed.), 1997.** *Flow, Thermal Regime and Sediment Transport Studies in Lake Tanganyika*. Department of Applied Zoology and Veterinary Medicine, Kuopio University Publications C. Natural and Environmental Sciences 73.

**Johnson, R.W., 1975.** Quantitative suspended sediment mapping using aircraft multispectral data. *Proceedings of NASA Earth Resources Survey Symposium*, Houston, TX, pp2981-2998.

**Justice, C.O., and Townsend, J.R.G., 1981.** In: *Terrain Analysis and Remote Sensing*. Townsend, J.R.G., (Ed.), Allen and Unwin, London, pp38-58.

**Lake Tanganyika Biodiversity Project (LTBP) Home Page, 1999.** [www.ltbp.org](http://www.ltbp.org)

**LTBP Pollution Special Study, 1999.** Data collected under the guidance of Gabrielle Hakizimana for the project.

**LTBP Sedimentation Special Study, 1999.** Data collected under the guidance of Tharcisse Songore for the project.

**McKim, H.L., Merry, C.J., & Layman, R.W., 1984.** Water quality monitoring using an airborne spectroradiometer. *Photogrammetric Engineering and Remote Sensing*, 50, 353-360.

**Milliman, J.D., & Syvitsky, P.M., 1992.** Geomorphic/tectonic control of sediment discharge to the ocean: the importance of small mountainous rivers. *Journal of Geology*, 100: 525-544. In: **Patterson, G., and Mackin, J., (Ed.) 1998.** *The State of Biodiversity in lake Tanganyika - A Literature Review*. Chatham, UK: Natural Resources Institute.

**Moore, G.K., 1977.** Satellite surveillance of physical water quality characteristics. *Proceedings of the 12th International symposium on Remote Sensing of Environment*, University of Michigan, Ann Arbor, pp445-461.

**Munday, J.C., and Alfodi, T.T., 1979.** Landsat test of diffuse reflectance models for aquatic suspended solids measurement. *Remote Sensing of the Environment*, Vol.8, pp169-183.

**NORCONSULT, 1982.** *Kigoma water master plan*. Volume 7. Hydrology, Oslo.

**Novo, E.M.M., Hansom, J.D., and Curran, P.J., 1989.** The effect of viewing geometry and wavelength on the relationship between reflectance and suspended sediment concentration. *International Journal of Remote Sensing*, Vol.10, No.8, pp1357-1372.

**Novo, E.M.M., Steffen, C.A., and Braga, C.Z.F., 1991.** Results of a laboratory experiment relating spectral reflectance to total suspended solids. *Remote Sensing of the Environment*, Vol.36, pp67-72.

**Olesen, F.S. & Grassl, H., 1985.** Cloud detection and classification over oceans at night with NOAA-7. *International Journal of Remote Sensing*, Vol. 6, p1435.

**Patterson, G., and Mackin, J., (Ed.) 1998.** *The State of Biodiversity in lake Tanganyika - A Literature Review*. Chatham, UK: Natural Resources Institute.

**Prangma, G.J., & Roozkrans, J.N., 1989.** Using NOAA AVHRR imagery in assessing water quality parameters. *International Journal of Remote Sensing*, 1989, Vol. 10, Nos. 4 & 5, 811-818.

**Ritchie, J.C., Schiebe, F.R., and McHenry, J.R., 1976.** Remote sensing of suspended sediments in surface waters. *Photogrammetric Engineering and Remote Sensing*, Vol.42, pp1539-1545.

**Ritchie, J.C., Schiebe, F.R., Wilson, R.B., and May, J., 1975.** Sun angle, reflected solar radiation and suspended sediments in North Mississippi reservoirs. In: *Remote Sensing of Earth Resources*, Shahrokhi, F., Ed. Tullahoma, TN, University of Tennessee, pp. 555-564.

**Rosendahl, B.R., Reynolds, D.J., Lorber, P.M., Burgess, C.F., McGill, J., Scott, D., Lambiase, J-J., & Derksen, S.J., 1986.** Structural expressions of rifting: lessons from Lake Tanganyika, Africa. In: *Frostick, L.E., Renaut, R.W., Reid, I., & Tiercelin, J-J., (Eds.) Sedimentation in African Rifts*. Special Publication geol. Soc. London, 25, 29-43.

**Scherz, J.P., and Van Domelen, J.F., 1975.** Water quality indicators available from aircraft and Landsat images and their use in classifying lakes. *Proceedings of the 10th International Symposium on Remote Sensing of Environment*. University of Michigan, Ann Arbor, pp 447-460.

**Stoffers, P., & Hecky, R.E., 1978.** Late Pleistocene-Holocene evolution of the Kivu-Tanganyika basin. *Int. Assoc. of Sedimentol. Spec. Publ.*, 2, 43-55.

**Stumph, R.P., 1992.** Remote sensing of water clarity and suspended sediments in coastal waters. Presented at; *the First Thematic Conference on Remote Sensing for Marine and Coastal Environments*, New Orleans, USA.

**Nyanza Project, LTBP NSF, 1999.** *Malagarasi River Delta map; Surveys & Mapping Division, Ministry of Lands, Housing and Urban Development.* Government of the United Republic of Tanzania

**Tanzania Fisheries Research Institute (TAFIRI), 1999.** Data collected by the project, made available by the Director Mr. Deonatus Chitamwebwa.

**Tassan, S., and Sturm, B., 1986.** An algorithm for the retrieval of sediment content in turbid coastal waters from CZCS data. *International Journal of Remote Sensing*, Vol.7, pp643-655.

**Tiercelin, J-J., & Mondeguer, A., 1991.** The geology of the Tanganyika trough. Pp.7-48. In: **Coulter, G.W., (Ed.)** *Lake tanganyika and it's Life.* London: British Museum (Natural History)/Oxford University Press. In: **Patterson, G., and Mackin, J., (Ed.) 1998.** *The State of Biodiversity in lake Tanganyika - A Literature Review.* Chatham, UK: Natural Resources Institute.

**Tiercelin, J-J., Soreghan, M., Cohen, A.S., Lezzar, K-E., & Bouroullec, J-L., 1992.** Sedimentation in Large Rift Lakes: Example from the Middle Pleistocene - Modern Deposits of the Tanganyika Trough, East African Rift System. *Bull. Centres Rech. Explor.-Prod. Elf Aquitaine*, 16, 1, 83-111..

**Whitlock, C.H., Kuo, C.Y., and LeCroy, S.R., 1982.** Criteria for the use of regression analysis for remote sensing of sediment and pollutants. *Remote Sensing of the Environment*, Vol.12, pp151-168.

**Witte, W.G., Whitlock, C.H., Harriss, R.C., Usey, J.W., Poole, L.R., Houghton, L.R., Morris, W.D., & Gurganus, E.A., 1982.** Influence of dissolved organic materials on turbid water optical properties and remote sensing reflectance. *Journal of Geophysical Research*, 87, 443-446.

**Wooster, M.J., 1998.** Investigation into the possibilities for the remote derivation of suspended sediment distribution on Lake Malawi. *Unpublished Report.*

**Worthington, E.B., & Lowe-McConnell, R., 1994.** African Lakes Reviewed: Creation and Destruction of Biodiversity. *Environmental Conservation*, Vol. 21, No. 3.

**Zhang, X., 1999.** Soil loss, sediment deposit and yield estimates in Tanzania using remote sensing and GIS. *Unpublished report.*

